

1-1-1978

The tensile properties of compatible glassy polyblends based upon poly(2,6-dimethyl-1,4-phenylene oxide).

Lothar Walter Kleiner
University of Massachusetts Amherst

Follow this and additional works at: https://scholarworks.umass.edu/dissertations_1

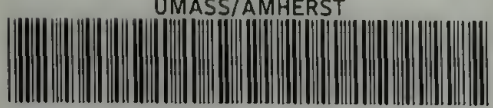
 Part of the [Polymer Science Commons](#)

Recommended Citation

Kleiner, Lothar Walter, "The tensile properties of compatible glassy polyblends based upon poly(2,6-dimethyl-1,4-phenylene oxide)." (1978). *Doctoral Dissertations 1896 - February 2014*. 632.
https://scholarworks.umass.edu/dissertations_1/632

This Open Access Dissertation is brought to you for free and open access by ScholarWorks@UMass Amherst. It has been accepted for inclusion in Doctoral Dissertations 1896 - February 2014 by an authorized administrator of ScholarWorks@UMass Amherst. For more information, please contact scholarworks@library.umass.edu.

UMASS/AMHERST



312066 0015 5635 5

THE TENSILE PROPERTIES OF COMPATIBLE
GLASSY POLYBLEND S BASED UPON
POLY (2,6-DIMETHYL-1,4-PHENYLENE OXIDE)

A Dissertation Presented

By

LOTHAR WALTER KLEINER

Submitted to the Graduate School of the
University of Massachusetts in partial fulfillment
of the requirements for the degree of

DOCTOR OF PHILOSOPHY

September 1978

Department of Polymer Science and Engineering

©

Lothar Walter Kleiner 1978

All Rights Reserved

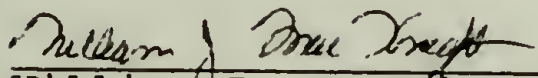
THE TENSILE PROPERTIES OF COMPATIBLE
GLASSY POLYBLEND S BASED UPON
POLY (2,6-DIMETHYL-1,4-PHENYLENE OXIDE)

A Dissertation Presented


By

LOTHAR WALTER KLEINER

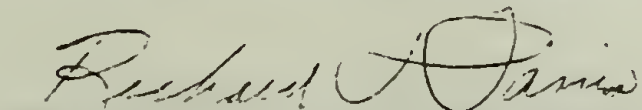
Approved as to style and content by:



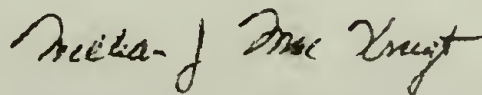
William J. MacKnight, Chairman of Committee



Frank E. Karasz, Member



Richard J. Farris, Member



William J. MacKnight, Department Head
Polymer Science and Engineering

DEDICATED
TO MY PARENTS

ACKNOWLEDGEMENTS

First, I wish to extend my gratitude to my thesis advisors, Professors William MacKnight and Frank Karasz, for their untiring theoretical and experimental assistance. Their helpful comments and encouragement were instrumental to the completion of this thesis. I also wish to thank Professor Richard Harris for agreeing to serve as a member of my thesis committee and for his many helpful suggestions relating to mechanical property measurement.

Next, I extend special thanks to Professor Isaac Sanchez for many illuminating discussions on lattice fluid theory, to Mr. Chester Napikoski for helping to modify the miniature injection molder, and to fellow students Joel Fried, Kenneth Rozkuszka, Fred Cummings, Peter Alexandrovich and Robert Cembrola for their assistance, encouragement, and friendship.

Finally, I wish to thank the faculty and students who made my stay at the University of Massachusetts a rewarding experience.

ABSTRACT

THE TENSILE PROPERTIES OF COMPATIBLE GLASSY POLYBLENDS BASED UPON POLY (2,6-DIMETHYL-1,4-PHENYLENE OXIDE)

(September 1978)

Lothar Walter Kleiner, B.S., Worcester Polytechnic Institute,
M.CHE., University of Delaware, M.S., Ph.D.,
University of Massachusetts

Directed by: Professors William J. MacKnight
and Frank E. Karasz

The mechanical behavior of compatible glassy polyblends based upon poly (2,6-dimethyl-1,4-phenylene oxide) (PPO) was investigated. In particular, the influence of composition, molecular weight, and molecular weight distribution upon the large deformation tensile properties was assessed. Various possible correlations between the experimentally determined moduli and theory are considered. Included are correlations with density, packing density, composite theory and lattice fluid theory. Similarities in behavior of the compatible glassy polyblends to the phenomenon known as "antiplasticization" is presented. The modeling of the properties of these polymer mixtures via Simplex lattice design is also detailed. Finally, attention is given to the development of compatibility criteria based upon the large deformation tensile property and density measurements.

It was shown that composite equations cannot adequately describe the mechanical behavior of compatible PPO based polyblends. However, it is possible to generate a second order Simplex equation which will closely model the modulus-compositional empirical trends. Furthermore, there are strong indications that the interaction term in the Simplex equation can serve as a useful gauge for compatibility and level of compatibility.

It was also shown that all the criteria for the phenomenon known as "antiplasticization" were fulfilled by all the compatible PPO based systems examined. For example, the high molecular weight "antiplasticizer", polystyrene (PS), when dissolved in PPO, decreases the glass transition temperature of the blend while raising the magnitude of the secant modulus and tensile strength above the value which would be predicted by the rule of mixtures.

Packing density was found to be useful for explaining antiplasticization and compatibility. It appears to be the key to understanding the moduli of glassy alloys. The density and packing density are the only equilibrium quantities which pass through a maximum similar to the modulus. These results suggest that compatibility might be handled without resorting to specific molecular interactions.

TABLE OF CONTENTS

	<u>Page</u>
<u>Acknowledgement</u>	v
<u>Abstract</u>	vi
<u>Chapter</u>	
I. Introduction	1
References	5
II. Theoretical & Experimental Background . .	6
A. Tensile Testing	6
B. Modes of Deformation	11
C. Antiplasticizers	32
D. Density	45
E. Thermal History	55
F. Modulus	57
G. Tensile Strength	74
H. Elongation at Yield & Break	78
I. Orientation	79
J. Modeling the Properties of Mixtures - Simplex Lattice Design	83
K. Lattice Fluid Theory Applied to the Modulus of Polymer Blends	88
L. Relaxations and Motions Below T_g	92
References	100

Table of Contents (continued)

	<u>Page</u>
III. Experimental	110
A. Preparation of Blends	110
B. Injection Molding of Tensile Specimens	115
C. Tensile Testing - Technique, Corrections, and Data and Error Analysis	119
D. Differential Scanning Calorimetry . .	130
E. Gel Permeation Chromatography	131
F. ¹³ C NMR of PPO and i-PS	132
G. Wide Angle X-ray Measurements	133
H. Polymer Degradation	134
I. Scanning Electron Microscopy	134
J. Determination of Orientation	134
References	136
IV. Results and Their Discussion	137
A. Information Regarding SI Units	137
B. Moduli of the Glassy Homopolymers and Compatible Polymer Blends . .	137
C. Tensile Strengths of the Glassy Homopolymers and Compatible Polymer Blends	189
D. Elongation at Break and Yield of the Glassy Homopolymers and Com- patible Polymer Blends	198
References	206
V. Summary and Conclusions	208
VI. Suggestions for Further Study	211
APPENDIX - TABULATION OF DATA	213

LIST OF TABLES

<u>Table</u>		<u>Page</u>
2.1	Time Required for the Density of Polystyrene to Come to Within 1/e of its Equilibrium Contraction upon Quenching to Various Temperatures	48
2.2	Longitudinal and Transverse Moduli for Oriented Polystyrene	81
3.1	Summary of Molecular Weights	111
3.2	Summary of Injection Molding Temperatures	118
4.1	Summary of Molecular Parameters for PS-PPO Blends Utilizing a Corresponding States Principle According to Bondi . . .	152
4.2	Summary of Molecular Parameters for PS-PPO Blends Utilizing a Lattice Fluid Theory According to Sanchez	154
4.3	Summary of Simplex Equations Representing the Moduli of PS-PPO Blends	179
A.1	Nomenclature for Subsequent Tables . . .	214
A.2	Summary of Tensile Properties for aPS 4000/PPO Blends	215
A.3	Summary of Tensile Properties for aPS 10000/PPO Blends	216
A.4	Summary of Tensile Properties for aPS 37000/PPO Blends	217
A.5	Summary of Tensile Properties for aPS 110000/PPO Blends	218
A.6	Summary of Tensile Properties for aPS 233000/PPO Blends	219

List of Tables (continued)

<u>Table</u>		<u>Page</u>
A.7	Summary of Tensile Properties for HH101 aPS/PPO Blends	220
A.8	Summary of Tensile Properties for aPS 670000/PPO Blends	221
A.9	Summary of Tensile Properties for aPS 2000000/PPO Blends	222
A.10	Summary of Tensile Properties for α -PS/PPO Blends	223
A.11	Summary of Tensile Properties for α -PS/HH101 aPS Blends	224
A.12	Summary of Tensile Properties for Amorphous iPS/PPO Blends	225
A.13	Glass Transition Temperatures	226

LIST OF FIGURES

<u>Figure</u>		<u>Page</u>
2.1	Brittle-Ductile Transition	29
3.1	Preparation of Polymer Blends	113
3.2	Schematic of Stress-Strain Curve	120
3.3	Force-Extension Curve for 5 Kg Load Cell	122
3.4	Force-Extension Curve for 20 Kg Load Cell	123
3.5	Force-Extension Curve for 20 Kg Load Cell (4 Kg Full Scale)	124
4.1	Modulus of Blends of aPS 4000-PPO	139
4.2	Modulus of Blends of aPS 10000-PPO	140
4.3	Modulus of Blends of aPS 37000-PPO	141
4.4	Modulus of Blends of aPS 110000-PPO	142
4.5	Modulus of Blends of aPS 233000-PPO	143
4.6	Modulus of Blends of HH101-PPO	144
4.7	Modulus of Blends of aPS 670000-PPO	145
4.8	Modulus of Blends of aPS 2000000-PPO	146
4.9	Variation of the Modulus of Polystyrene with \bar{M}_n	149
4.10	Modulus and Density of Blends of PS-PPO	156
4.11	Densification and Excess Modulus for Blends of PS-PPO	156
4.12	Modulus and Packing Density of PS-PPO Blends	159

List of Figures (continued)

<u>Figure</u>		<u>Page</u>
4.13	Packing Densification and Excess Modulus for Blends of PS-PPO	159
4.14	Variation of Reduced Modulus with Blend Packing Density	162
4.15	Variation of Reduced Modulus with Reduced Density	166
4.16	Modulus and Density as a Function of PS-PPO Blend Composition	168
4.17	Variation of Reduced Modulus with Reduced Temperature and Blend Composition	170
4.18	Modulus of Blends of PS-PPO (Modeling of the Modulus)	174
4.19	Modulus of Blends of PS-PPO (Modeling of the Modulus)	176
4.20	β_{12}^E for PS-PPO Blends	180
4.21	Modulus of Blends of α -PS/PPO	182
4.22	Modulus of Blends of α -PS/PS	184
4.23	Modulus of Blends of iPS-PPO	187
4.24	Tensile Strengths of Blends of aPS 4000-PPO	191
4.25	Tensile Strengths of Blends of aPS 37000-PPO	192
4.26	Tensile Strengths of Blends of aPS 110000-PPO	193
4.27	Tensile Strengths of Blends of aPS 233000-PPO	194
4.28	Tensile Strengths of Blends of HH101-PPO	195
4.29	Percent Elongation of Blends of aPS 4000-PPO	199

List of Figures (continued)

<u>Figure</u>		<u>Page</u>
4.30	Percent Elongation of Blends of aPS 10000-PPO	200
4.31	Percent Elongation of Blends of aPS 37000-PPO	201
4.32	Percent Elongation of Blends of aPS 110000-PPO	202
4.33	Percent Elongation of Blends of aPS 233000-PPO	203
4.34	Percent Elongation of Blends of iPS-PPO	205

C H A P T E R I

INTRODUCTION

Most materials, including plastic ones, are utilized because they have desirable mechanical properties at economical cost. For this reason, the mechanical properties (particularly tensile stress-strain measurements) are considered the most important of all physical properties for most applications. High polymers have the widest variety and greatest range of mechanical properties of all materials. However, considering the present economical and environmental climate, it is often more advantageous to blend existing materials rather than to synthesize new ones to develop materials with unique or desirable properties.

The implications in the previous paragraph with regard to blending operations are impressive. Blending is a widely used technique to improve rheological, mechanical, and degradative properties in polymers. Moreover, it affords the fabricator the opportunity to custom formulate a material to predetermined desirable properties [1,2]. Finally, the blend may often be more economical than the homopolymer. With all the above considerations, there is considerable impetus to ascertain the engineering properties of a blend.

There are two important categories of polymer blends. The first category includes blends where the components are

incompatible and the second category includes blends where the components are compatible. The second category will receive primary consideration here. An example of the second category is the compatible thermoplastic blend whose components are poly(2,6-dimethyl p-phenylene oxide) (PPO) and polystyrene (PS). Blends of PPO and PS are of particular interest because compatibility exists in the entire range of possible compositions [3,4,5] and because deformation through the composition range spans the entire spectrum from brittle to ductile behavior [2].

The broad range of thermoplastic polymers which can be produced by modification of PPO resins is reviewed by Kramer [6]. This technology provides the capability of tailoring materials with predetermined combinations of properties such as melt viscosity, heat deflection temperature, impact strength, modulus, and dielectric characteristics. The results of this unique technology provide the basis for the family of engineering thermoplastics called Noryl.

In spite of the extraordinary latitude obtainable upon blending by capitalizing on the attractive properties of the parent PPO resins, PPO by itself was not a commercial success due to undesirable aging characteristics (embrittlement) and poor processibility due to high melt viscosity, autoxidation, and crosslinking of the melt [1,7,8]. It was not until the discovery of the solubilizing power of PPO by

PS that improved rheological, mechanical, and environmental resistance were obtained in the blend [1].

Still not all mechanical properties were optimized by blending PPO with PS. Better impact strength was desired, so PPO was blended with high impact PS (HIPS) finally allowing this PPO based blend to become a commercial success. Elimination of HIPS by the substitution of PS would be more economical if perhaps the correct molecular weight combination could be found for each of the components of the blend allowing the retention of the desirable impact characteristics of the PPO-HIPS blend. To this end alone, a study of the tensile properties of PPO-PS blends as a function of both composition and PS molecular weight would be invaluable.

Aside from the important practical aspects regarding knowledge of tensile properties, it would be highly desirable if they could afford an assessment of compatibility. Assessment of compatibility becomes particularly important in the case where the unblended homopolymers have glass transition temperatures so close to each other that the discernment of two glass transitions for an incompatible blend would be impossible. PPO based blends afford a unique opportunity to test the validity of tensile measurement (i.e., modulus, yield stress or ultimate stress) compatibility criteria since the level of compatibility can be varied rather readily.

Consequently, a study of the tensile properties of PPO based blends as a function of composition and molecular weight was carried out with the following goals in mind:

1. To assess the influence of composition, molecular weight and molecular weight distribution upon blend tensile properties.
2. To develop correlations between the experimentally determined properties and theory.
3. To ascertain whether compatibility criteria can be developed based upon tensile measurements.
4. To model the moduli of the blends via a Simplex lattice design.

REFERENCES

1. E. P. Cizek, U. S. Patent No. 3,383,435.
2. A. F. Yee, Polymer Preprints, ACS, Div. Polym. Chem., 17, 145 (1976).
3. J. Stoelting, F. E. Karasz, W. J. MacKnight, Polym. Eng. Sci., 10, 133 (1970).
4. H. E. Bair, Polym. Eng. Sci., 10, 247 (1970).
5. A. R. Shultz and B. M. Gendron, J. Appl. Polym. Sci., 16, 461 (1972).
6. M. Kramer, Appl. Polym. Symp., 15, 227 (1970).
7. A. S. Hay, private communication.
8. A. F. Yee, private communication.

C H A P T E R I I

THEORETICAL AND EXPERIMENTAL BACKGROUND

It is the purpose of this chapter to develop a variety of topics in sufficient depth to provide a basis for explaining the experimental results contained in Chapter IV. Essentially, these topics represent a survey of the literature.

II.A. TENSILE TESTING

Most plastic materials are used because they have desirable mechanical properties at economical cost. For this reason, the mechanical properties may be considered the most important of all physical and chemical properties of polymers for most applications.

There is a bewildering number of mechanical tests and testing instruments. Most tests are highly specialized and many have not been standardized (although it should be recognized that a standardized test is no better than one that is not). The most widely used of all mechanical tests is the stress-strain test in tensile mode. In such a test, the buildup of force is measured as the specimen is being deformed at nominally a constant rate. In spite of their popularity, these tests are more difficult than most others to interpret on a molecular level. Traditionally, stress-

strain curves have served as a guide to experienced engineers as to how a polymer will behave under a variety of usage conditions [1].

The slope of the initial straight line portion of the stress-strain curve is the elastic modulus of the material,

$$E = \frac{d\tau}{d\varepsilon} \quad . \quad (1)$$

The maximum in the curve denotes either the stress at break for a brittle material or the stress at yield for a ductile material and correspondingly either the elongation at break or the elongation at yield. The end of the curve represents the tensile strength at break (or ultimate strength) and the elongation to break.

In tensile tests, the stress, τ , is defined by

$$\tau = \frac{\text{force}}{\text{cross-sectional area}} = \frac{F}{A} \quad . \quad (2)$$

The strain, ε , can be defined in several ways, but for most purposes, the engineering strain is used:

$$\varepsilon = \frac{\ell - \ell_0}{\ell_0} = \frac{\Delta\ell}{\ell_0} \quad , \quad (3)$$

where ℓ_0 is the original length of the specimen, while its stretched length is ℓ . Another commonly used definition of strain is the true strain:

$$\varepsilon = \int_{\ell_0}^{\ell} \frac{d\ell}{\ell} = \ln \frac{\ell}{\ell_0} = \ln(1+\varepsilon) \quad . \quad (4)$$

For many practical applications, the engineering strain or nominal change in elongation is nearly equal to the true strain for strains up to 0.1, since $\ln(1+\epsilon) \approx \epsilon$ for $\epsilon \leq 0.1$. When $\epsilon = 0.1$ (percent elongation is 10%), the two strains differ by 4.9%.

It is commonly stated that the machine used in the stress-strain measurement extends the sample at a constant strain rate. This is not strictly accurate except for small strains because most machines have in fact a constant cross-head movement which implies a diminishing rate for strain because the sample length is being increased as the test proceeds. Devices can be constructed to accelerate the rate of cross-head movement to compensate for this, but the correction is only needed for rubbers which may extend several times their original length [2]. Additionally, the strain in the specimen will not match that calculated from the cross-head speed due to machine elasticity, so corrections need to be made [3].

Stress-strain tests not only give an indication of the stiffness and strength of a material, but also its toughness. The concept of toughness can be defined in several ways, one of which is in terms of the area under the stress-strain curve. Toughness, then, is an indication of the energy a material can absorb before breaking. Thus, toughness and impact strength can at least be related qualita-

tively. Toughness is also associated with ductile polymers, while materials that exhibit little toughness are brittle [1].

There is no unique value for the moduli, tensile strengths, or elongations. These parameters are dependent upon the rate of testing. In glassy polymers, a three orders of magnitude increase in testing rate influences stiffness only modestly, i.e., the Young's modulus may increase up to about 10%. The effects on the strength, which goes up, and the elongation, which goes down, are much greater. For very brittle polymers (where the tensile properties are largely determined by flaws and sub-microscopic cracks), the effects are generally smaller than for rigid ductile polymers, where the effects can be quite significant if the rate of testing is varied over several decades [1,4].

Stress-strain measurements for homopolymers are also molecular weight dependent. Polymers of very low molecular weight which have glass transition temperatures above ambient conditions tend to be very brittle. It may be impossible to prepare tensile test specimens of such materials because the thermal and shrinkage forces involved are great enough to shatter the polymer into small pieces of low strength [5]. Brittle polymers must have some molecular chain entanglements before the polymer becomes strong enough to carry any load [6]. Additionally, chain ends act as

imperfections which adversely affect the strength properties, but chain ends and molecular weight have little effect on elastic moduli [1].

The tensile strength's dependence upon molecular weight is reported by many sources to have the following form:

$$\tau_B \text{ or } \tau_Y = \tau_0 - \frac{K}{\bar{M}_n} \quad , \quad (5)$$

where τ_B is the strength at break, τ_Y the strength at yield, τ_0 the limiting strength at high molecular weight, K an empirical constant and \bar{M}_n the number average molecular weight. Actually, the molecular weight relationship is quite a bit more complex. The weight average molecular weight also has some effect as does the molecular weight distribution [7]. However, for polymers whose molecular weight distribution is rather narrow, equation (4) is quite acceptable. Additionally, a similar equation holds for elongation at break or yield for brittle and ductile polymers respectively [1].

Other authors, for example Boyer [8] or Goppel [9], find viscosity rather than molecular weight per se to be the important parameter. That would indicate that \bar{M}_w is more important than \bar{M}_n .

II.B. MODES OF DEFORMATION

Under this heading only that deformation pertaining to glassy polymers below their respective glass transitions will be discussed. This implies that crazing, shear banding, and the brittle-ductile transition will receive the majority of attention. The mechanism of deformation is still not well understood which explains the profusion of literature on identical aspects of deformation interpreted by widely differing mechanisms. Only the more common viewpoints will be presented here.

Deformation may be separated into homogeneous and heterogeneous processes. Homogeneous deformation is characteristic of a material in which each microscopic element deforms in the same way more or less simultaneously to produce the overall macroscopic shape change. The deformation of rubbers at low and high strains and of glassy polymers at very low strains can be classified as homogeneous. Two types of heterogeneous deformation, in which small volumes deform to large strains, leaving adjacent volumes undeformed, have been identified in glassy polymers: shear banding (shear yielding) and crazing (normal stress yielding). The two modes available depend on conditions of stress and ambient temperature as well as the polymer microstructure [10-12]. Crazing and shear banding have been reviewed by Kambour [13] and Bowden [14] respectively (among others).

Crazes represent a form of energy absorption or dissipation in the brittle phase [15]. They usually initiate at inherent surface flaws, then grow perpendicularly to the direction of maximum stress [16]. The main characteristics of crazes in transparent, glassy, isotropic polymers are fairly well defined and generally accepted. These characteristics are:

1. A craze is a highly localized region of plastic deformation in which the strains are of the order of 100 percent.
2. Crazes formed in a uniaxial tensile stress field have a similar shape to a crack, and the plane of the craze is at right angles to the stress axis. The planar dimensions are many orders of magnitude greater than the thickness, which is typically less than 1 mm. In a more complex stress field, the craze is normal to the maximum principal stress field [17,18,19].
3. Crazes form only in a tensile field and the criteria for visible crazing in a biaxial stress field is:

$$\tau_b = A + B/I_1 \quad , \quad (6)$$

where τ_b is the difference between the principal stresses ($\tau_1 - \tau_2$), I_1 is the first stress invariant ($\tau_1 + \tau_2$) and A and B are parameters

which depend upon testing and material variables such as temperature and molecular weight.

4. The craze volume has a lower density than the surrounding material and the microstructure consists of a high density of interpenetrating micropores surrounded by drawn material in a fibrillar form [20]. These features are responsible for such craze properties as the lower refractive index, load-bearing capacity, porosity, and the eventual breakdown of the craze by cavitation processes (e.g. void coalescence or crack propagation) [21].

In addition to these well defined characteristics, there is a range of other properties which have to be taken into account in any generalized model for the crazing process. Notably, these are the features which relate to mechanism and kinetics of craze nucleation and propagation indicating that crazing is a thermally and environmentally controlled stress-activated process involving local molecular motion. The craze characteristics relating to morphology and microstructure are qualitatively similar for all brittle glassy polymers, and they can be altered in detail only by changes in the conditions under which crazes form (e.g. temperature, environment, and strain rate) and

in molecular structure and conformation of the polymer (e.g. molecular weight, orientation, and degree of crosslinking) [17].

In addition to the main characteristics of crazes, a number of features pertaining to the microstructure can be summarized as follows:

1. The boundary between the craze and undeformed material is sharp and well defined.
2. The main feature of the structure in the early stages of craze growth is the development of an array of fibrils approximately 250 \AA thick, which are joined together by fibrils less than 50 \AA thick. This produces an interconnecting three dimensional array of fibrils similar to an open-celled foam [22]. The size of the microvoids is comparable to that of the fibril thickness.
3. The fibrils form at right angles to the craze-matrix interface.
4. Fracture occurs by progressive failure at the craze-matrix interface; the fracture path tending to oscillate between one craze-matrix interface and the other [21].
5. Crazing is the precursor of fracture in brittle polymers. The presence of some crack, flaw, or

other inhomogeneity gives a region of high strain concentration and hydrostatic tension, resulting in the formation of a craze [17].

So, to summarize, crazes appear as hairlike lines on the surface of the specimen. The thickness of the craze and the spacing between crazes both increase with increasing temperature of deformation [10]. Although they look like cracks, they are actually sheet-like structures with millions of tiny holes. From refractive index studies, it was found that craze material is 50% void.

It is now felt that fracture of thermoplastics involves generation of voids as extension takes place. In some cases, the voids are dispersed throughout the polymer; in others they concentrate into a craze which eventually leads into a crack. It is the formation of the craze and its subsequent deformation (it is a material of much lower modulus than the matrix) which is responsible for the energy absorption in an advancing crack. Deformation of up to 100 percent is possible in the craze, hence the material left behind is oriented and yields parallel surface layers [15].

Crazes are formed in brittle glassy polymers, because the substantial stress concentration at the sharp tip of a crack or flaw is sufficient for plastic deformation of the material in the immediate vicinity, thereby creating a fine craze. The crack propagates by gradual failure of the thin craze preceding the crack tip [3].

Generally, crazes initiate from a surface crack or some other stress raising flaw, but the craze can also be initiated internally at stresses well below the yield-point in pure isotropic glasses [3,23]. The importance of the stress raising flaw is not only that it localizes craze initiation, but also that it modifies the stress field in its locality. Stress magnifications of 10-50 would not be unreasonable for surface flaws, according to Gent [24]. Additionally, he proposes a mechanism for crazing. The formation of a craze is attributed to stress activated devitrification of a small amount of material, at the tip of a chance nick or flaw, to a softer rubbery state.

Clearly, craze propagation is microscopically a micro-drawing process. Yet, even though a basic craze structure is similar in all cases examined, there are several unanswered questions raised by present knowledge of morphology:

1. What are the triggering events for craze initiation?
2. What events occur ahead of the craze tip to permit additional craze growth?
3. What controls the characteristic fibril diameter at any set condition?
4. What controls the craze width at any temperature of deformation?

In conclusion, the morphology and mechanism of crazes are fairly well characterized, but not understood in molecular detail sufficient for predictive analysis.

The other mode of deformation available to a glassy polymer is shear yielding. Visually shear yielding is manifested as kink bands running at about 58° to the tensile axis in PS and in general at orientations closer to planes of maximum shear than planes of maximum normal stress. Shear bands can form under tensile, compressional, or shear loading [10].

Of the two modes of yielding, shear yielding is by far the least studied. Whitney first reported the observation of shear bands in 1963 [25]. The state of stress needed to initiate this mode of deformation has subsequently been studied by a number of investigators (e.g. see ref. 18). Formally, the critical stress state, τ_s , follows a Mohr-Coulomb criterion; τ_s is related to the yield stress in pure shear, τ_{ps} , and the mean normal stress, τ_m , ($\tau_m = 1/3[\tau_1 + \tau_2 + \tau_3]$) by

$$\tau_s = \tau_{ps} - \mu\tau_m, \quad (7)$$

where μ is a material constant. Usually, the term $\mu\tau_m$ makes the minor contribution of the two terms in the above expression.

On the other hand, the criterion for normal stress yielding (crazing) is considerably different from that for

shear yielding. The criterion is based on the average normal stress, τ_m , and a stress bias, τ_b , ($\tau_b = |\tau_1 - \tau_2|$) in biaxial stressing and is equivalent to the applied stress in uniaxial loading. The simplest hypothesis would be that the critical stress bias should be inversely proportional to τ_m :

$$\tau_b = A(T) + \frac{B(T)}{\tau_m} \quad . \quad (8)$$

It is also found that negative values of τ_m (compression) never lead to crazing. According to the model just given, crazes would be expected to always lie normal to the direction of greatest principal stress. Crazing can, in general, be produced ahead of a crack front (if the crack moves slowly enough to allow molecular reorientation before bond rupture occurs). Schematics of the envelopes for both shear and normal yielding criteria for biaxial loading are given by Sternstein and Ongchin [26].

In developing criteria for yield, the approach is usually a macroscopic one which takes no account of the mechanisms involved. If one seeks to explain yield in polymers in molecular terms, one enters a field that is not well explained, although in some cases general principles have been discovered which account for some of the observed phenomena [2].

Various criteria for yield have been proposed [2,27, 28] in the past, such as:

- a. Yield occurs when the maximum principal stress exceeds some critical value.
- b. Yield occurs when the maximum principal strain exceeds some critical value.
- c. Yield occurs when the maximum shear stress or strain exceeds some critical value.
- d. There is a critical maximum strain energy.

The yield criteria were first developed for metals, but have been extended to polymers. However, agreement is generally poor (e.g. using Tresca's or von Mises criteria for which critical stresses are tabulated [2]) and usually give little indication of molecular-level phenomena [2].

Up to now, the heterogeneous mode of deformation, crazing, has been given most of the attention. Now we turn to the other mode of heterogeneous deformation termed inhomogeneous yielding, shear yielding, bulk shearing, or shear banding. The inhomogeneity takes the form of a band of localized yield termed a "shear band". Shear yielding initiates with a delocalized strain softening [29] which occurs either at a well defined creep delay time [30] or when the elastic strain energy reaches a critical value which is a function of strain rate, temperature, and the

physical state of the material. Subsequently, the plastic deformation localizes into shear bands that propagate at approximately a 45° angle to the maximum principal stress [31]. The phenomenological explanation is usually done using Considere's construction, but it, of course, gives no explanation on a molecular level why shear yielding occurs.

Any theory of inhomogeneous yield stress must answer the following questions [32]:

1. What is the nature of the bend in the experimental stress-strain curve and what determines the critical stress, τ_c , at which cold drawing (necking) occurs?
2. Why does τ_c fall with increase in temperature and rise as the speed of drawing is increased?
3. What relations are fundamental for the cold drawing process of glassy polymers?
4. What polymer properties cause either homogeneous or inhomogeneous yielding to occur?
5. What are the conditions of a stable neck?

These questions are important since essentially all tough (ductile) polymers and those with high impact exhibit shear yielding and cold drawing. Yielding implies a yield point in the stress-strain curve. The yield point is either a distinct maximum or a region of strong curvature approaching zero slope in the stress-strain curve.

Cold drawing manifests itself as a necking of the polymer during stretching. Necking starts at a localized point in the specimen where the cross-section becomes much less than the remaining portion of the specimen, while the force remains nearly constant during stretching. Cold drawing, after the yield point, means that there must be a strain hardening process, otherwise the material would break without drawing at the reduced cross-section where necking occurred. The strain hardening generally results from molecular orientation which increases the modulus and tensile strength. Cold drawing of a given section stops at a critical elongation known as the natural draw ratio of the material. The draw ratio is a function of temperature, orientation, and stretching rate. On further stretching of the cold-drawn polymer, the stress generally increases rapidly and failure ensues [1,33].

Many theories have been proposed to explain shear banding and cold drawing, but the subject is still being actively debated.

One of the first theories invoked local rise in temperature during drawing, i.e., the work of drawing appeared as heat at the localized neck, lowering the yield stress there. The localized hot spot that developed as energy was put into the polymer, caused the temperature of a spot to rise to the T_g [33,34]. Thus, cold drawing was assumed to

be the spot-by-spot stretching of a rubbery material near T_g . Although heat is certainly generated during practical industrial rates of drawing, it cannot be the cause for necking since it can be observed at such low stretching rates as 10^{-6} m/sec [35,36,37]. Thus, this theory is now generally believed to be unacceptable.

A more common explanation is the phenomenological one that has also been successful for metals. It involves the use of a Considere plot which is a graphical construction superimposed upon the stress-strain curve indicating whether the plastic deformation has become unstable, thus causing the formation of a neck. The instability occurs for polymers where the rate of work hardening may not be sufficient to compensate for the reduction of area causing a neck to form. Work hardening, which in polymers allows the formation of stable necks, arises from molecular orientation [2].

Some theories are based upon dilation of the polymer when stress is applied. If this increase in volume is an increase in free volume, then T_g is lowered to the stretching temperature, so that the cold-drawing process becomes similar to the stretching of an elastomer [38-41]. While the above-proposed model corresponds to a stress-induced increase in free volume, some models require a reduction of the T_g by the applied stress without invoking free volume

[42]. Still another very similar model formulated by Robertson [43] is based on the idea that applied stress causes molecules to seek new, more rubber-like conformations, and when the conformation becomes similar to that at T_g , yield occurs.

Still other theories of cold drawing use a concept similar to Eyring's theory of viscosity [44]. This theory is based on the assumption that the applied stress makes the potential wells for segmental motion asymmetrical, making it easier for motion to occur in the direction of the force. The net effect of the applied stress is to reduce the height of the barrier for a jump in the forward direction and increase it in the reverse [45,46].

Possibly all the above theories have some merit. Actually, shear yielding and cold drawing may take place by several possible mechanisms, and the relative importance of different mechanisms may vary from polymer to polymer. The possible mechanisms just cited are not all-inclusive, i.e., still others can be found in the literature, but these, for the most part, are minor.

A different approach may be taken to explain necking (inhomogeneous deformation), which is based on stability. For this type of deformation to occur, homogeneous deformation must have become unstable and, of course, the strain rate locally must become higher than that of the surround-

ing material. There are two possible reasons for this instability: one, geometrical and one structural (both may occur simultaneously) [3].

The geometrical argument goes as follows. The geometrical instability here refers to the formation of a neck in a specimen tested in uniaxial tension. If part of the specimen should happen to be slightly thinner, then the stress at this location will be slightly higher. This will concentrate further deformation at that point and increase the local stress further unless the rate at which the material strain hardens is sufficient to suppress the instability.

A second reason for instability is strain softening of the material (stress is lowered as the strain increases) after the yield point. If locally, the strain should happen to be slightly higher than elsewhere (possibly due to some fortuitous stress concentration) then the material will be softer locally and it will therefore deform to a higher strain than elsewhere and become softer still. This process can only be stopped by the eventual orientation hardening of the material [3].

Thus, it is the drop in modulus that causes the curvature in the true stress versus strain diagram which eventually leads to necking and, hence, the assumption that the specimen is heated to the softening temperature is

unnecessary. Actually, the softening temperature is drastically reduced by straining, while there is only a small rise in actual specimen temperature [35,36]. So, the following conclusions can be drawn:

1. Initially, when the stress-strain curve is rising steeply, specimen non-uniformity does not lead to necking because the extra stress can be supported without too great an excess of strain (i.e., the system is stable).
2. The modulus of many polymers is much reduced by strain. The consequent downward bending of the stress-strain curve leads to mechanical instability, and so causes a neck to form.
3. Cold drawing is caused by this mechanical instability, followed by a strain-hardening process, due to molecular orientation.
4. Cold drawing is prevented by insufficient strain hardening. This may be caused by very high stretching rates or by low molecular weight [35,36].

If a test piece were perfectly uniform in cross-section and composition, it would in principle be possible for uniform extension to always take place. However, in practice this is never so; there is always a point in the test piece where the stress passes the maximum first, and

when this happens, the stress required to extend at this point falls (shear bands will form if a material exhibits strain softening). Extension, therefore, continues there while the stress in the other points of the test piece falls below that required to pass over the yield point. A constriction or neck then develops [3,34].

The degree of brittleness of a polymer glass depends upon the amount of flow that occurs during the failure process, either microscopically via crazing or shear banding or macroscopically via necking. What this means is that practically all glassy polymers under suitable conditions can undergo either crazing or shear banding or show some tendency to show both simultaneously. The flow during deformation absorbs energy during the failure process, thereby decreasing the brittleness of the polymer glass.

Flow initiation on a microscopic level depends upon the local stress concentrations in the form of flaws. The distribution of the magnitudes of the stress intensity factors associated with all flaws smaller than the primary flaw has a significant effect on the amount of flow that occurs during the deformation and failure of a polymer glass. Generally, more of these flaws lie on the surface of the glass because of its exposure during fabrication [47].

The previous paragraph leads to the question of the role of imperfections in the establishment of failure

criteria in glassy polymers. It is well known that the load and temperature history imposed upon a material affects whether a material fails in a brittle or ductile fashion. However, it is now felt that the formation and growth of defects during loading is perhaps the most important criterion in establishing the mode of failure [48]. In fact, it has been found that at a specific sample history, the average defect size was the parameter that established the mode of failure. Defect size is a complex function of strain rate and temperature; however, as long as defect size was kept below a certain critical size (or length), l_c , the failure was by shear yielding, while if the defect size was greater than l_c , the failure was brittle. The critical defect size is a function of temperature, defect density, and defect size distribution. So, if the defects grow to their critical size before the stress-strain reaches a maximum, brittle failure occurs. The importance of inherent flaws has been recognized by other principle investigators as well [49,50].

Discussions of brittle and ductile failure eventually lead to descriptions of the brittle-ductile transition. Qualitatively, a locus of points can be defined which separate the two types of behavior. However, since brittle failure is a stochastic process, one cannot predict with absolute certainty the time to failure. This implies that

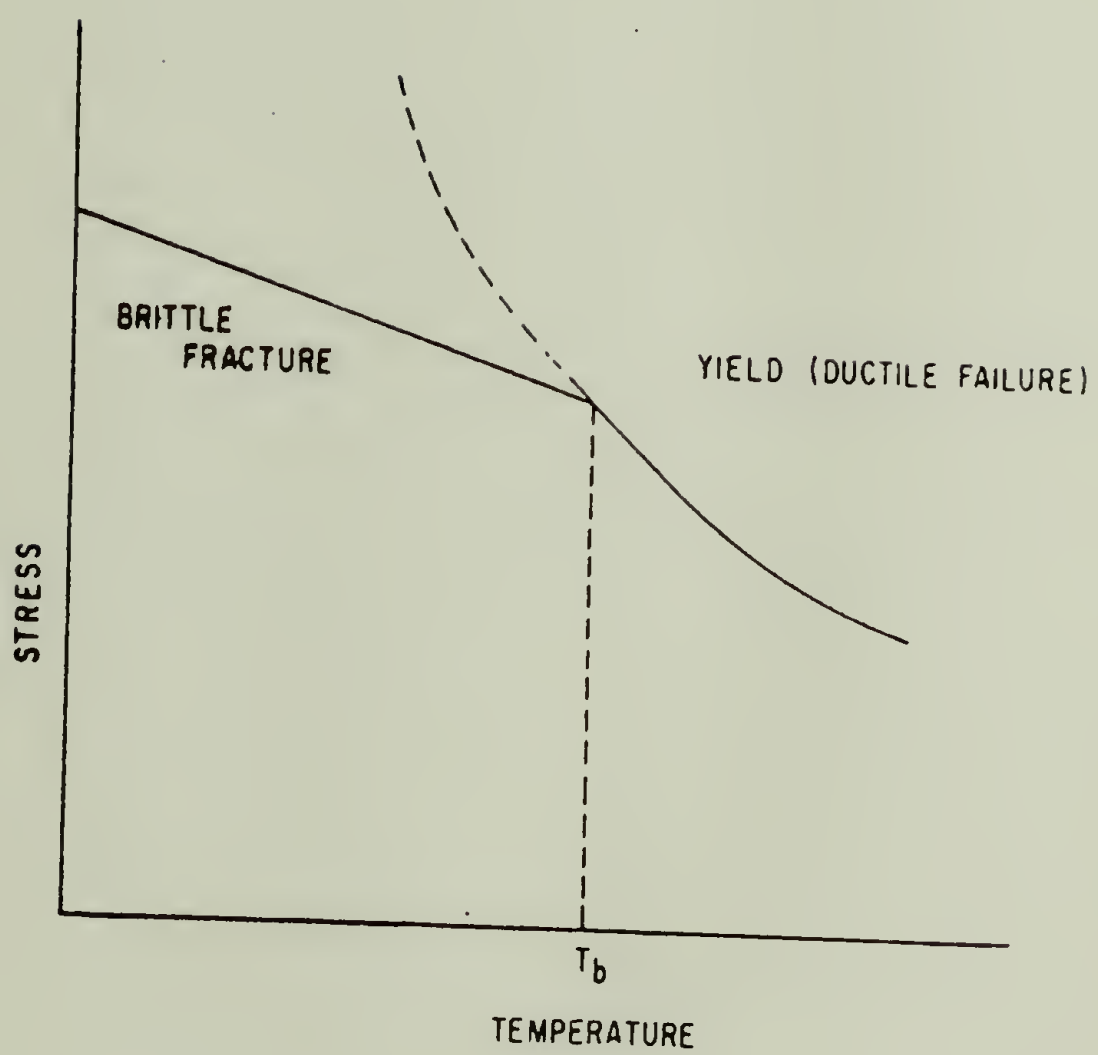
the brittle-ductile transition cannot be represented by a single locus of points, but rather there is a transition zone within which both modes of failure are probable [48].

The brittle-ductile transition is typically characterized by a transition temperature, T_b . Polymer specimens undergoing a simple tensile test fail in a brittle fashion below T_b and in a ductile fashion above T_b (at a particular strain rate and specimen history). It is to be noted that T_b is not at the T_g , but often considerably below it (e.g. $T_b = -200^\circ\text{C}$ for Polycarbonate, while $T_g = 150^\circ\text{C}$) [2].

When considering the form of the temperature variation of tensile strength of polymers, one typically finds curves of the type shown schematically in figure 2.1. The form of the temperature variation is different for the two parts of the curve. Similar behavior is found in metals and explained by assuming two failure processes: a) a brittle strength and b) a yield strength with different temperature coefficients. T_b is then defined as the temperature at which the coefficients are equal [2].

It has been established that for many polymers, T_b and T_g lie close together if there is no secondary relaxation, while T_b lies close to a secondary relaxation when one exists. There are, however, exceptions and it has been suggested that the latter statement is true only if the

FIGURE 2.1



secondary relaxation is due to the main chain and not to a side chain or side group [2].

The brittle-ductile transition temperature, T_b , increases during polymer aging. Of particular concern in the processing and application of polymers is the loss of general ductile behavior of many polymers upon annealing at temperatures below their respective T_g 's. A dramatic example of embrittlement is the transition from ductile behavior to brittle fracture for amorphous unoriented PET on aging. Even under experimental conditions involving a low strain rate, $10\% \text{ min}^{-1}$, the ductile behavior observed for freshly prepared PET film is lost after an extremely short annealing period (about 90 min. at 51°C). Although the time to embrittlement increases with decreasing temperature, it is only of the order of a few days at room temperature for amorphous PET [51]. With a brief heating to temperatures greater than T_g , and subsequent quenching, the annealed PET regains its ductile behavior and the process of embrittlement occurs again.

Another often used equation used in the discussion of brittle-ductile transitions is the Griffith equation [52]:

$$\tau_g = \sqrt{\frac{E\gamma}{c}} \quad , \quad (9)$$

where τ_g is the brittle fracture stress, E the Young's modulus, γ the surface energy, and c the size of the flaw.

The criterion for the brittle-ductile transition can be based on the magnitude of the stress necessary for the growth of the flaw versus the stress necessary to cause yielding. Using the Griffith equation, then when $\tau_g > \tau_y$, ductile failure will take place while when $\tau_y > \tau_g$, brittle failure will take place. τ_y is the yield stress.

Cracks and other stress concentrations play a vital role in the strength of materials [53]. At a tip of a crack or notch in a sheet, the stress is concentrated according to the equation:

$$\tau_m = \tau_o [1 + 2 (a/r)^{1/2}] \quad (10)$$

The applied stress is τ_o , τ_m is the maximum stress at the crack tip of radius r , and a is the length of the crack or the depth of the notch [54]. Brittle polymers usually contain flaws or inherent cracks with a length of the order of 10^{-3} to 10^{-4} cm. and with widths approaching molecular diameters, so very high concentrations of stress can occur at the tips of cracks.

In addition to cracks, inclusions and holes are also stress concentrators. For example, a circular hole in a sheet produces a stress concentration given by [55]:

$$\tau_t = \tau_o (1 - 2 \cos 2\theta) \quad (11)$$

the tangential stress at the edge of the hole is τ_t , while θ is the angle from the direction of the applied stress, τ_o .

At the poles of the hole ($\theta = 0$), the tangential stress is compressive (i.e., negative); while in the direction perpendicular to the stress (at the equator of the hole), the stress is tensile and equal to $3\tau_0$ at the edge of the hole.

Spherical inclusions also behave as stress concentrators [56]. The greatest stress concentration occurs at the equator of the sphere (90° to the applied stress); the tensile stress being concentrated by a factor of two. If the modulus of the inclusion is much greater than that of the continuous matrix, the tensile stress is reduced and may actually become compressive if there is good adhesion between the sphere and matrix. In such a case (very rigid inclusion), the stress is concentrated at the poles ($\theta = 0$) so that the sphere tends to separate from the matrix by a process termed dewetting.

II.C. ANTIPLASTICIZERS

The addition of liquids and plasticizers to polymers causes a complex series of secondary relaxational phenomena [57-67]. The secondary glass transitions may be shifted up or down in temperature, they may disappear, or new damping peaks may develop. One type of phenomenon, which has been incorrectly called antiplasticization, is quite common [68-73]. This effect, during which certain types of additives in a polymer increase its modulus and tensile strength while decreasing the elongation, is

termed antiplasticization because opposite results are obtained on plasticization: decreased modulus and tensile strength and increased elongation. Both antiplasticizers and plasticizers, however, decrease T_g .

Jackson and Caldwell [69] discuss in detail the effects and properties of antiplasticizer molecules for polycarbonates. The antiplasticizers for polycarbonates all contain polar atoms or groups. Invariably, the more polar the molecule, the more effective its antiplasticizing action is. In addition to being polar, antiplasticizer molecules have a relatively high degree of stiffness and rigidity. Cyclic structures introduce rigidity in a molecule, and most antiplasticizers for polycarbonates contain cyclic structures. The more rigid the molecule, the more effectively it serves as an antiplasticizer. Aromatic compounds are generally more effective antiplasticizers than saturated structures, perhaps because aromatic rings are thinner. Molecules containing two or more rings are usually more effective than one molecule containing one ring. In studies of additives containing more than one ring, the maximum stiffening action occurred at a concentration of about thirty percent.

The thickness of the molecule is very important in determining whether a rigid polar molecule will be a plasticizer or an antiplasticizer. Models have indicated that

the antiplasticizers included only compounds which had one dimension less than about 5.5 \AA in at least sixty-five percent of the length of the molecule. Finally, the antiplasticizer must be compatible with the polymer.

In summary, antiplasticizers are thin, polar, stiff molecules which are compatible with the polymer. They usually contain at least two nonbridged rings, have a T_g greater than -50°C and have one dimension less than 5.5 \AA in at least sixty-five percent of the molecule [68,69].

Up to now only the antiplasticizing effects on bisphenol A polycarbonates have been discussed. Actually the results are considerably more general and can be extended to other polymers which contain rigid polar groups and stiff chains such as some polyesters, cellulose triacetate, and poly (sulfone ether). In fact, these polymers could be antiplasticized by the same additives that antiplasticized polycarbonates.

Polymers with flexible chains are not antiplasticized. In fact, some compounds that are antiplasticizers for stiff polymers are plasticizers for flexible polymers. Rigidity and some polarity appear to be required in both polymer and additive in order for antiplasticization to occur.

The mechanism is not well understood. The DTA curves of antiplasticized films exhibited broad endotherms which indicated the presence of forces broken by thermal energy.

These forces are speculated to be due to interaction between the polar groups of the polymer and antiplasticizer.

Density measurements indicated that the densities were significantly higher than would be calculated by simple volume additivity. The loss in free volume should restrict the movement of polymer chains and increase the stiffness. Additionally, wideline NMR indicated that the antiplasticizer in the polymer was not mobile. The polar antiplasticizer additive must be a relatively thin molecule, perhaps because thick molecules push the polymer chains too far apart and interfere with the attractive forces between chains.

So the mechanism of antiplasticization is perhaps a combination of several factors including a reduction in free volume hindering chain mobility, interaction between polar groups of the polymer and antiplasticizer, and a physical stiffening action due to the presence of rigid antiplasticizer molecules adjacent to the polar groups of the polymer. Since the most flexible portions of a rigid polymer are its polar groups (here e.g. carboxylate, carbonate, or sulfone groups) interaction of these groups with thin, stiff, polar antiplasticizer molecules should reduce the flexibility. Additionally, it would be expected that an antiplasticizer molecule containing only one ring would be less effective than a longer molecule

containing two or more rings which would stiffen a larger portion of the polymer chain [69].

Robeson and Faucher [70,71] have continued the work of Caldwell and Jackson [68,69] in their study of secondary loss transitions in antiplasticized polymers. Since these transitions have been widely assumed to be connected with impact strength and elongation, it is reasonable to expect substantial changes to occur in secondary relaxations as a consequence of antiplasticization. Both polysulfone and polycarbonate were investigated. Upon antiplasticization with Aroclor 5460, the usual effect was obtained: increased modulus and tensile strength and reduced elongation and impact. Both polymers (additive free) have well-defined secondary relaxations at about -100°C . However, upon the addition of thirty percent antiplasticizer (Aroclor 5460) these transitions were virtually eliminated. Concomitant with the antiplasticization effect is a densification over and above simple volume additivity.

The reduction in magnitude and the eventual disappearance of the secondary loss transition upon the addition of antiplasticizer is significant. The presence of antiplasticizer and elimination of the secondary transition results in a higher modulus value above the transition temperature and is thus the cause of the increased modulus in the room temperature range. It also results in higher

tensile strength for the antiplasticized polymer. The close connection between secondary transitions and ultimate elongation and impact strength is also verified. As the secondary transition disappears; elongation and impact values drop sharply.

The density data suggest that at low antiplasticizer concentrations, the antiplasticizer molecule must initially be filling in polymer free volume. In turn, the decrease in free volume is sufficient to hinder motions associated with the secondary transition.

A further consequence of this particular theory is that the ability of polymers to be antiplasticized will be related to the magnitude of the secondary transition. Therefore, PS, which has only a very small secondary transition should not be effected as highly as PC [71]. More brittle polymers with no secondary relaxation would not be expected to be antiplasticized to any great extent. This has been verified experimentally [68,72].

The addition of certain "plasticizers" at low concentration to PVC has been shown to lead to increases in modulus and tensile strength [73-76]. Again, the elimination of the secondary transition at -40°C is very well documented and explains the increase in modulus and tensile strength [73]. In this system, of course, one must work at low enough concentrations so that the glass transition

remains above room temperature. Otherwise, the modulus and tensile strength will decrease, as in a normal plasticized system [70,71]. This is the reason why PVC can only be antiplasticized at low antiplasticizer concentration and polycarbonates and polysulfones can be antiplasticized up to concentrations of thirty percent.

The elimination of low temperature transitions which restrict the molecular flexibility of the polymer chain as well as a reduction in free volume would be expected to restrict the diffusion of penetrants at low concentrations such that the penetrant did not appreciably alter the mechanical characteristics of the polymer. This hypothesis is borne out experimentally. The CO_2 permeability of antiplasticized polysulfone is decreased noticeably when compared to pure polymer. Water takeup is also noticeably reduced. In fact, these decreases are greater than one would expect from an additivity relationship assuming no water absorption due to the antiplasticizer. Apparently, the polysulfone solubility sites for H_2O or CO_2 have been partially eliminated due to interaction with the antiplasticizer. The experimental results for permeability coincide with the observed elimination of secondary loss transitions and reduction of free volume as diffusion is restricted, since the energy required to displace polymer chains increases as the antiplasticizer eliminates the

flexibility of the polymer chain resulting from the low temperature mechanical loss transition. The free volume available for unrestricted diffusion is decreased with addition of antiplasticizer, thus resulting in a decrease in the diffusion coefficient [71].

More recently, Robertson and Joynson [77] reported densification of PC(bisphenol A polycarbonate) by combining annealing and antiplasticization to ascertain whether the two were related or would interfere with each other. The latter might be expected if annealing and antiplasticization affected the same free volume. It was found that the antiplasticizer, Aroclor 1254 (a biphenyl with an average of five chlorines per molecule), increased the modulus forty-two percent (from that of pure polymer). The tensile strength which remains roughly proportional to the modulus increased correspondingly. Concomitantly, there was a densification of two percent more than would be predicted assuming volume additivity. Tensile strength increases of fifteen percent could be obtained by annealing below T_g and resulted in a densification of 0.22 percent [78].

When antiplasticization and annealing are combined in the same specimen, the increases in modulus and yield or tensile strength are essentially the sum of the individual effects, suggesting no interference between the two. In fact, the effects of antiplasticization and annealing

remain additive even as the individual effects approach saturation [77]. This indicates that the two effects do not affect the same free volume. Antiplasticizing suppressed the -120°C loss peak in PC while annealing suppressed the shoulder just below T_g , but no work has been done to see whether annealing also suppressed the -120°C loss peak.

Litt and Tobolsky [72] antiplasticized PS with benzophenone and use somewhat different reasoning to explain their results. Specifically, by the addition of six percent benzophenone to PS, the modulus increased five percent. The percent densification (over that calculated by assuming volume additivity) was 0.6 percent. Incidentally, these data are strikingly similar to what is obtained by adding twenty-five percent PPO to PS, i.e., the modulus is five percent higher and the density 0.6 percent higher than that calculated from the simple "rule of mixtures" [37]. As usual with antiplasticizers, the elongation dropped approximately thirty-three percent for the PS-benzophenone system. The advantage of this system is the fact that benzophenone is crystalline. The implication is that it is already packed as densely as it can be and consequently contains no excess free volume. Thus, the density increase on mixing with PS must be due to efficient packing of the antiplasticizer in the polymer and loss of polymer

free volume (and not antiplasticizer free volume as would be possible if the antiplasticizer were liquid and contained excess free volume). Instead of free volume ($[\alpha_l - \alpha_g]T_g$), a better definition might be unoccupied volume, \bar{f} , where

$$\bar{f} = 1 - \rho_a/\rho_c \quad (12)$$

where ρ_a represents the amorphous density and ρ_c the theoretical crystalline density. If this definition is used the loss of ductility or the increased degree of brittleness could be correlated with \bar{f} . (As a general rule a ductile polymer has $\bar{f} > 0.07$ while for brittle polymers $\bar{f} < 0.07$) [72].

Bondi [79] reports the "antiplasticizer" phenomenon for various polymers including PVC, PS and PC. He argues that while maxima in the Young's modulus versus plasticizer concentration are observed, the T_g decreases uniformly for all plasticizer or antiplasticizer-polymer systems studied so far. The packing density of the polymer is the only equilibrium quantity which also passes through such a maximum (the packing density, ρ^* , is the ratio of the van der Waals volume over the measured volume). Unfortunately, this property has not been examined for many cases, yet Bondi feels that it is the key to the entire phenomenon of "antiplasticization". Addition of small amounts of plasticizer (antiplasticizers and plasticizers are termed

plasticizers or diluents by Bondi) loosens the glassy matrix just enough to permit a closer approach to equilibrium density at a given $T < T_g$, provided the system is cooled slowly. Plots of the resulting densification versus diluent concentration in the polymer show a maximum, the height and corresponding concentration being larger the greater θ_L , where

$$\theta_L = \frac{E^\circ}{5cR} \quad (13)$$

E° is the standard energy of vaporization, and all E° 's are calculated at $\rho^* = 0.588$. R is the gas constant and c a measure of the external degrees of freedom. Since θ_L can be related to the cohesive energy density, it is logical that the "antiplasticizing" effect can be maximized by a choice of diluents composed of large and stiff molecules. Experimentally this is verified, as typical maximum densifications range from 0.5 to 1.5 percent for the usual aliphatic to aromatic plasticizers in vinyl polymers to 2.5 percent for tetrachloroterphenyl in PC. Finally, Bondi [79] suggests that packing density alone is sufficient to explain the phenomenon of antiplasticization, including the observed decreases in secondary mechanical loss peaks. There should be no need to resort to specific molecular interactions between polymer and diluent.

The primary parameter affecting the physical properties of a glassy polymer is the free volume. Does a decrease in free volume during the incorporation of a diluent mean an increase in "order" of the glassy matrix? Some of the "holes" between the polymer chains become partially filled by the additive, restricting movement of the polymer chains. Does this mean that antiplasticizers besides causing losses in free volume also cause an increase in chain alignment in the amorphous state, thus increasing the "order" in the amorphous state? That line of reasoning appears logical if the considerable evidence for order in the amorphous state is valid.

Ever since the beginnings of polymer science, it has been generally assumed and accepted that amorphous polymers, both in the glassy state and above T_g , consist of randomly coiled, entangled chains with no local order being present [80]. Although this model should have been rejected on the basis of density considerations alone, as pointed out by Robertson [81] (a collection of randomly coiled molecules would have a considerably lower density than is observed for any amorphous polymer, which typically is about eighty-five percent of the perfect crystal density), it has remained the basis for nearly all discussions of physical properties of glassy and molten polymers.

It has been recently proposed [82,83] that amorphous polymers consist of small (about 30-100 Å) domains in

which there is local ordering or alignment of neighboring segments. An amorphous polymer, it was suggested, can most simply be looked at as being composed of numerous, small nematic-liquid-crystal-like domains, with the majority, but not all, of the molecules running from one domain to another. In the glassy state, this structure will be frozen, whereas above T_g , there will be a continual redistribution of segments among the domain, individual domains forming and disappearing.

Wecker, Davidson, and Cohen [84] also recently concluded from their detailed x-ray studies that the chain segments in atactic PS have a tendency to pack parallel to each other. The same conclusion was reached several years earlier by Corradini for amorphous polymers in general [85]. Geil [82] has proposed that the physical properties in the amorphous state are a function not only of the free volume, but also how that free volume is distributed, i.e., on the degree, type, and distribution of order in the sample.

If the addition of an antiplasticizer does indeed increase the "order" (induce or increase chain alignment) in the amorphous state, then perhaps such antiplasticization phenomena as densification, increase in modulus and tensile strength, and suppression of secondary relaxations can be explained on this basis.

II.D. DENSITY

Specific volume or its reciprocal, density, may be regarded as one of the most important polymer properties. This is obvious not only from a practical, but also from a theoretical point of view. For the calculation of many properties, especially in thermodynamics, it is necessary to know the density. In spite of its importance, it is surprising how little accurate and reliable data exist in this field [86].

Theoretical predictions of density (molar volume) of organic liquids and polymers can be made on the basis of group contributions using such elementary formulae as

$$V = \sum_i V_i + \Omega \quad (14)$$

where V is the molar volume and Ω is an additional value termed a "residual volume" (for high molecular weights, Ω is neglected). The group contributions have received some refinement more recently by recognizing that group contributions are not constant, but are dependent upon the surrounding atoms. Still, these estimations have standard deviations of \pm one percent [86]. So theory, at best, can do no better than yield two place accuracy in density. Even empirical measurements found in the literature are not reported with sufficient accuracy. As shall be shown later under this heading, four place accuracy with perhaps some inaccuracy in the last place is needed.

Density has a marked influence on the other physical properties of the glassy material [79]. Thus, those properties of glassy materials that are sensitive to volume changes will be a function of the details of the preparation of the glass and of its subsequent thermal history. Precise measurements of the volume and enthalpy and their time dependencies are extremely tedious. In molding and extruding operations, the level of orientation, its profile throughout the sample, and pressure effects must be considered as well. Rigorous characterization of fabricated glassy polymers is difficult, if not impossible to achieve, nevertheless progress is being made [87].

The most common cause of easy vitrification is a high melt viscosity somewhat above the glass transition temperature. In the glass transition temperature range, the viscosity of the melt increases very steeply (several orders of magnitude) and eventually becomes so high that during cooling the volume change with temperature experiences a significant delay [79,88]. This is the reason why a glass cannot be considered as fully described unless the cooling rate that prevailed during its preparation is specified. A rapidly cooled liquid becomes glassy at higher temperatures and is likely to exhibit a lower density than one that has been cooled slowly from the melt state [89].

As an example of the effect of cooling rate on the physical properties, one can note the far greater creep rate of rapidly chilled PMMA as compared with slowly cooled PMMA. This greater weakness of quenched glass is in keeping with its lower density. One should be able to characterize the comparative thermal history of given glasses by their density; however, the small maximum density difference caused by varying cooling rates (usually less than one percent) and the difficulty of measuring the density of solids militate against the fulfillment of this need. Measurement of the refractive index and its conversion to density may be a solution to this problem [79,90]. Again, it is clear that in all elastic modulus and relaxation measurements (as well as other physical measurements) of the glass, the rate and amplitude of deformation as well as the thermal history of the sample must be specified.

That glasses do not obtain their equilibrium specific volume or density instantaneously because of their high viscosity can best be seen by referring to Table 2.1. On the other hand we also see that equilibrium is unattainable for practical purposes at temperatures far below T_g . So, we can treat a glass as an ordinary solid at $(T_g - T) > 20^\circ\text{C}$, i.e., a glass at $(T_g - T) > 20$, whether at its equilibrium volume or not, is a dimensionally stable solid with

TABLE 2.1

Time Required for the Density of Polystyrene
to Come to Within 1/e of its Equilibrium
Contraction upon Quenching to Various Temperatures

$T - T_g$ ($^{\circ}\text{C}$)	t (1/e) (sec)	t (1/e) (years)
11	0.01	--
6	1	--
2	40	--
1	120	--
0	300	--
-1	1.1×10^3	--
-2.5	3.6×10^3	--
-4	1.8×10^4	--
-7	1.8×10^5	--
-10	5.2×10^6	0.16
-12	3.2×10^7	1
-50	3.2×10^8	10

See ref. [91]. The refractive index n was used as a measure of the density. Time was calculated from the ratio

$$[n(t) - n(\infty)]/[n(0) - n(\infty)] = e^{-1}.$$

reproducible properties as long as it is not heated to within $(T_g - T) < 20^\circ\text{C}$ [79,91].

The sensitivity of glass density, and therefore of its elastic properties, to thermal history, makes it unsafe to compare results obtained by different authors on different samples of a given (usually insufficiently characterized) material. The evaluation of literature data must therefore be of a more qualitative than quantitative nature [79]. Quenched amorphous polymers typically have densities from 10^{-4} to 10^{-2} $\text{g}\cdot\text{cm}^{-3}$ less than annealed polymers. Annealing at temperatures near the glass transition temperature after quench cooling of polyvinylacetate raises the Young's modulus. This result is expected since the density increases with annealing time, indicating a decrease in free volume. Molecular mobility due to greater than equilibrium free volume manifests itself by a lowering of the modulus [92].

The principal ordering process taking place in glassy polymers on annealing are those ordering processes associated with the changes in the normal liquidlike packing to be anticipated as the glassy polymers approach their corresponding equilibrium glassy stage. Aligning of chains is not a principal factor in the annealing process and does not significantly contribute to the enthalpy relaxation process associated with the non-equilibrium nature of the glass states. This was discerned by investigating the

glassy state of smectic phases in which the molecules are essentially aligned and comparing their relaxation behavior with isotropic glasses [83,93].

In inorganic glasses it is possible to produce changes in density of one percent or more by changing the rate at which the glass is cooled through the glass transition temperature. Similar effects, as already mentioned, occur in organic polymeric glasses, although the density differences are not so large. Those density differences have been observed to cause significant differences in the mechanical properties of the glass. Struik [94] has recorded density gradients in quenched samples of PS involving changes of up to 0.2 percent and has shown the creep rate to be very sensitive to the annealing treatment after quenching. The yield stress is also sensitive to annealing treatment. Raha and Bowden [95] prepared samples of PS by quenching into an ice-water mixture from 110°C and found that the yield stress measured at 20°C was twelve percent lower than the yield stress of samples annealed at 110°C and slowly cooled to room temperature over twenty-four hours. The density difference was 0.2 percent, only just detectable by the method used. Golden and coworkers [78] have reported increases in tensile yield of PC of up to fifteen percent on annealing quenched samples, associated with a density increase of about 0.2 percent.

Other than by annealing below the glass transition (usually 10 to 20°C below T_g), it is also possible to produce a compaction of a percent or more by cooling through the glass transition under a hydrostatic pressure of a few kilobars and subsequently releasing the pressure [96].

Upon densifying by either technique, the modulus and tensile strength are raised while the elongation is reduced. The explanation in the case of PS [96,97] is that the β relaxation disappears upon densification. In addition, the degree of brittleness is increased (or some loss in ductility for ductile polymers occurs) due to loss of independent segmental mobility. Finally, there is more extensive interchain cohesion for the densified material than for the undensified material. These arguments actually can be generalized for all glassy polymers studied so far. In some aspects, these studies have been quite extensive, since numerous articles on density, densification, specific volume, volume relaxation, and PVT thermodynamics can be found in the literature besides those already referenced [98-125]. In many of these literature references, the specific volume is given as a function of temperature and pressure and sometimes it is mentioned that modulus and tensile strength increase with increasing density. However, the tabulation of

modulus and tensile strength as a function of percent densification was not found (particularly for PS and PPO) although Jacques and Hopfenberg [126] present data representing the densification occurring in PS-PPO blends indicating a maximum negative excess volume of mixing, while Yee [127] additionally presents some concomitant tensile strength data for the compatible PS-PPO mixtures. Unfortunately, the paucity of data in this field does not allow as yet an answer to the question: can the amount of densification alone explain the increase in mechanical properties above that predicted by additivity in compatible polymer blends?

Some progress in this direction may be to use an approach similar to that of Bondi [79]. Since in homopolymers, it appears that the density, without regard to the means by which it has been varied, correlates satisfactorily with mechanical behavior, it might be advantageous to attempt to correlate a reduced modulus with a reduced density. The packing density $\rho^* = V_w/V$ is commonly used. V_w is the van der Waals volume in $\text{cm}^3\text{-mole}^{-1}$ calculated from bond distances and van der Waals radii. V is the measured molal volume. The procedure brings the density of all polymer glasses into a common range (typically between 0.6 and 0.8). The modulus is reduced via $E^* = E V_w/H_s$, where E is the measured modulus and H_s is the heat of sublimation.

Because of the extreme sensitivity of E^* to the packing density ρ^* , there is only tolerable agreement in the prediction of the tensile modulus [79,128]. Probably better agreement could be reached with more accurate data.

In the case of polymer blends, such as PS-PPO, what needs to be plotted is E^* vs. ρ^* for the compositional possibilities at constant reduced temperature, T^* (or $\bar{T} = T/T_g$). The reduced temperature, T^* , is equal to $5 CRT/E^\circ$. E° ($E^\circ = \Delta H_v - RT$) is the standard heat of vaporization at $V/V_w = 1.7$ or $\rho^* = 0.588$. Although \bar{T} is not a corresponding state parameter, it is often also used. Then a comparison should be made between E^* versus ρ^* of the homopolymer and E^* versus ρ^* of the blend. Such plots would confirm or negate the premise that densification can account for observed mechanical properties in the blend. Of course, all glassy polymers and mixtures should have a well characterized thermal history. The major problem at this time with such experiments lies with the accessibility and reliability of the empirical and theoretical data. Accessibility is enhanced with the use of lattice fluid theory formulated recently by Sanchez and Lacombe [129-131]. This theory, however, will be presented later in this chapter.

Finally, some additional comments should be made about the packing density, ρ^* , for mixtures. The packing density

of hard spheres is increased, in general, when spheres of different radii are mixed. The increase is not large when only binary mixtures are considered. However, the random densely packed mixture of spheres with log normal size distribution can reach packing densities of the order of 0.80. Higher densities can be achieved when hard spherical and non-spherical particles are mixed. This consideration of forceless mixtures suggests that the mixing of unequally sized molecules at equal reduced temperatures should proceed generally with volume contraction (excess volume, $v^E < 0$). Because forceless systems or mixtures of components at equal reduced temperatures are rarely met in practice, one usually takes the more realistic case of mixtures with unequal force fields (and thus at unequal T^*). The prediction of the excess volume of mixing

$$v^E = V_{\text{mix}} - (x_1 v_1 + x_2 v_2) \quad (15)$$

is the severest test for any theory of mixtures and none as yet has met this test [79], although qualitative predictive methods are available [132,133]. Quantitative prediction is difficult because in most cases v^E/V_{mix} is of the order of 0.01 or less (in rare cases up to 0.02) so that either

$$V_{\text{mix}} \approx \sum x_i V_i \quad (16)$$

$$\bar{V}_{\text{mix}} \approx \sum w_i \bar{V}_i \quad (17)$$

holds for many practical cases to within ± 1 percent. Equation (16) is on a molar basis while equation (17) is on a weight basis.

II.E. THERMAL HISTORY

Significant variations are observed in many of the physical properties of glassy polymers as a result of the differences in the methods of preparation and/or thermal histories to which the polymers have been subjected. Some of the variability of the measured physical properties of glasses is a consequence of the rate of cooling and the instrumental rate of measurement. In general, with slower cooling rates and/or increased annealing periods, the density, tensile and flexural yield stresses, and elastic moduli increase, while impact strength, fracture energy, ultimate elongation and creep rate decrease [87,88].

Because of the kinetic aspects of the process of transformation of a melt to a glass, the glassy states of materials prepared under normal cooling conditions have excess volume and enthalpy relative to those of the corresponding equilibrium states; the levels of excess volume and enthalpy being functions of the cooling rate. Thus, those physical properties that are sensitive to such changes as excess volume and enthalpy will be influenced by the details of the preparation of the glass and by the subsequent thermal history of the glass [87].

The Young's moduli for glassy polymers well below their respective T_g 's are not very sensitive to the decreases in the excess thermodynamic properties that occur during annealing regimes [51,134,135], whereas the yield stresses are [51,52,134,135]. It would appear that the expected increase in modulus as a result of densification is masked because of the experimental error involved in moduli measurements [79]. On the other hand yield strengths are very sensitive to the thermal history and, therefore, excess thermodynamic properties [135]. During isothermal annealing, the tensile yield stress changes in a manner that parallels the changes in excess enthalpy, i.e., with increasing annealing time, the tensile yield stress increases regularly and approaches a limiting value asymptotically.

Another concern is in the area of processing and application of polymers. It is the loss of general ductile behavior on annealing at temperatures below T_g . The transition from ductile behavior to brittle fracture for tough glassy polymers such as PC, PET, and PPO on aging has been observed [51,136,137]. So again, thermal history can influence this important transition. Since ductile behavior can be restored to these polymers when they are reheated to temperatures above their respective T_g 's, direct correlations between the time to embrittlement and changes in excess volume or enthalpy can be established. Observations

in the literature support the conclusion that the ductile behavior of tough glassy polymers is a function of the thermodynamic state of the polymer. Further, they indicate that ductility is associated, at least in part, with modes of motion that are enhanced by greater levels of excess thermodynamic properties trapped in the glass during glass formation [87]. These results are consistent with the correlation between impact strength and free volume noted independently by several authors [72,138,139].

II.F. MODULUS

The rigidity of a solid is measured by its short time modulus. However, with polymeric glasses, the different moduli are not completely independent of the time scale of the experiment, although there is a tendency for the magnitude of the change in modulus as a function of time to diminish at low temperatures, small strains, and high frequencies. Below their respective T_g 's, however, the change in modulus for a polymeric glass is generally less than five percent for a decade in time [3]. Under conditions when the modulus is essentially independent of time, a polymer glass will obey the conventional equation for an elastic solid:

$$E = 2G(1 + \nu) = 3B(1 - 2\nu) \quad (18)$$

where E is the Young's modulus, ν the Poisson's ration, B the bulk modulus, and G the shear modulus. The Poisson's

ratio is a measure of the volume change during deformation and is defined as the ratio of the lateral contracting strain over the elongation strain when a rod is stretched by a force applied at its ends. It is commonly written in terms of volume change via

$$\nu = \frac{1 - \frac{\partial v}{\partial \epsilon}}{2} \quad (19)$$

Further, since ν is found to be about 0.33 for most polymer glasses ($\nu = 0.33$ for PS [3,79] and 0.35 for PPO [39]), it follows that $E \approx 2.7 G$ and that $E \approx B$. However, to avoid ambiguity the term modulus, unless otherwise stated, will refer to the Young's modulus or tensile modulus, E , as defined in equation (1), section A of this chapter.

The modulus of unoriented glassy polymers is determined primarily by the strength of intermolecular forces and not by the strength of the covalent bonds along the polymer chain. These intermolecular forces are mostly of the van der Waals type and include dipole-dipole, induction, and London dispersion forces. Ionic forces and hydrogen bonding are somewhat less frequently encountered [3,86].

The intermolecular forces are related to the cohesive energy density of the polymer. The higher the cohesive energy density, the higher the modulus. An equation relating the cohesive density, δ^2 , to Young's modulus is

$$E \approx 13.38(\delta^2) \quad (20)$$

where δ^2 is in ergs/cm³. Unfortunately, this equation is empirical in nature [140]. In going from one kind of polymer to another, the cohesive energy density correlation is not very good, probably because chain packing (density) is also important [1,141]. The correlation would incorrectly predict a higher modulus for PPO than PS since δ is 9.57 (cal/cm³)^{1/2} and 8.82 (cal/cm³)^{1/2} for each polymer respectively [86].

Since most organic polymers have only the relatively weak dispersion and dipolar forces, their moduli in the glassy state are all fairly similar. Strongly polar polymers with hydrogen bonding have higher moduli, while polyelectrolytes with strong electrostatic bonding have the highest moduli [1].

A more promising approach to the level of moduli and the changes in moduli actually found in glasses might lie in the understanding of the compressibility of liquids. Two changes, which occur under the influence of pressure, would have to be considered: a reduction in unoccupied volume and a contraction in occupied volume related to the intermolecular forces between the molecules themselves. From this it would certainly appear that density is one of the most important empirical parameters related to the modulus [3]. Indeed, some investigators, such as Bondi [79]

do supply correlations of E_o^* vs. ρ_{ref}^* where E_o^* is the reduced modulus at $0^\circ K$ and ρ_{ref}^* is the packing density at room temperature or at $0.9 T_g$ if $T_g < 298^\circ K$.

Actually, there is a rather good correlation between the experimentally determined reduced modulus E_o^* and the packing density at room temperature for semi-crystalline polymers with a degree of crystallinity greater than fifty percent. Unfortunately, the corresponding correlation for glasses is rather poor. One cause may be the rather larger differences in thermal expansion among the glasses than among the crystals, so that the ordering of the glasses by their density at $0^\circ K$ may differ from their order at room temperature. In any event, the correlation curve for glasses that may be drawn through the scatter of points with some justification is [79]

$$E_o^* \approx 85.9 \rho_{ref}^* - 47.6 \quad (21).$$

The obvious question relevant to this work would be if a similar equation, i.e., $E = E(\rho)$, could be written for compatible polymer blends. Ideally, data should be available at the same reduced temperature.

The effect of molecular structure on the modulus is fairly well represented by the reducing parameter H_s/V_w where H_s is the heat of sublimation increment per group. Young's modulus may then be theoretically calculated by an equation such as

$$E_o = \frac{H_s}{V_w} \left[41.6 \left(\frac{\rho V_w}{M} \right)^{1/2} - 22.4 \right] \quad (22)$$

The units of H_s/V_w are typically in dynes/cm² and $\frac{\rho V_w}{M}$ is dimensionless. The good correlation with H_s/V_w again is an indication that elastic moduli of isotropic glasses reflect primarily (to within a factor of 2/3) the van der Waals interaction between molecules.

The anisotropic force distribution around an individual repeating unit on a polymer chain, i.e., the strong coupling to its chemically bonded neighbors and the weak van der Waals coupling to its nonbonded neighbors, is observed only indirectly when dealing with an isotropic polymer glass, namely, a factor of 3/2 has to be used for normalization in comparison with crystals or glasses from nonpolymeric substances. Orientation of the molecules by drawing leads to anisotropy in elastic properties. For example, the bulk modulus parallel to the draw direction, B_{11} , is raised above that of the isotropic glass, B_o , and the modulus normal to the draw direction, B_1 , is correspondingly reduced below B_o . In general,

$$\frac{1}{B_o} = \frac{2}{3B_1} + \frac{1}{3B_{11}} \quad (23)$$

A search through the literature leads one to the conclusion that packing density (ρ^*), cohesive energy density (e.g. as represented by H_s/V_w), and the glass transition temperature are, in the order given, the major factors that

determine the magnitude of the elastic moduli. All three factors are interrelated. If the supposition holds that the thermal history of the sample is reflected in its packing density, only two other factors need be considered. One is the effect of secondary relaxation transitions, at each of which the elastic moduli make a step change. The relaxational effect causes complications in correlations between density and modulus (for example, deviation of PMMA and PVC from simple behavior can be attributed to relaxation processes near room temperature [79]). The other effect (already mentioned previously) is the effect of the time scale of the imposed deformations. These phenomena will always exercise a blurring effect on any correlation attempt, so the best one can expect from a generalized scheme is a rough guidance regarding the manner in which given structural elements may determine the elastic properties of the molecular glass. More explicitly, the percent error expected in a correlation of ρ^* versus B^* or E^* for PS is approximately five percent and goes as high as one hundred percent for poly (vinyl acetate) [79]. Unfortunately, tensile moduli can usually be measured experimentally to no better than five percent, again exercising a blurring effect on any correlation attempts.

Up to now, only correlations of modulus for homopolymers have been mentioned. What about polymer mixtures?

There are four categories one might consider when dealing with homogeneous or compatible mixtures. The first pertains to the elastic moduli of low molecular weight glass-forming mixtures. These have apparently not been investigated. Most polymers are not miscible with each other. Hence correlations of moduli for compatible high molecular weight polymer blends cannot be found. The elastic moduli of copolymers which have been investigated fall in the expected range between that of homopolymers [142,143] and are, therefore, of little interest. Only the elastic properties of several glass-forming homogeneous blends of plasticizers and antiplasticizers have been studied in some depth so that comparisons can be made with compatible polymer-polymer systems. However, those points worthy of attention have already been enumerated in section C of this chapter. The general lack of correlations for homogeneous systems naturally leads one to the large number of correlations found for elastic moduli of heterogeneous mixtures. Specifically, it might be fruitful to investigate whether any relations that apply to two phase systems can be extended to apply to homogeneous systems. Heterogeneous systems include filled polymer systems (either fiber or particulate), incompatible polymer blends, semi-crystalline polymers, and interpenetrating networks. A common word used to describe these heterogeneous systems is composite. The properties of the composite materials are determined by

the properties of the components, by the shape of the filler phase, by the morphology of the system, and by the nature of the interface between phases. Actually, a polymeric matrix is strengthened or stiffened by a particulate second phase in a very complex manner. The particles appear to restrict the mobility and deformability of the matrix by introducing a mechanical restraint, the degree of restraint depending upon the particulate spacing and on the properties of the particle and matrix [144]. To calculate the behavior of a composite exactly, it would be necessary to ensure that the equilibrium and compatibility conditions around the individual inclusions were satisfied. For most cases, this would be a long and difficult task, so most models adopt assumptions of uniform stress or strain throughout the composite [145].

In the simplest case, an upper and lower bound can be predicted for the composite elastic modulus. The maximum possible modulus for a filled system which is the result to be expected when the two materials making up the composite are connected in parallel is given by the "rule of mixtures":

$$M = \phi_1 M_1 + \phi_2 M_2 \quad (24)$$

where the M's represent the composite and component moduli respectively, while ϕ is the volume fraction. An example

would be an aligned fibrous composite with the force applied parallel to the fibers.

On the other hand, the lowest possible modulus is obtained when the two materials comprising the composite are connected in series. The equation then becomes:

$$\frac{1}{M} = \frac{\phi_1}{M_1} + \frac{\phi_2}{M_2} \quad (25)$$

The parallel model (Voigt model) assumes uniform strain in an assembly to predict the overall modulus, while the series model (Reuss model) assumes a uniform stress in the composite assembly. Hill [146] has shown that the Voigt estimate is always greater than the Reuss and that typically the actual moduli will lie between the two estimates. Strictly speaking, the Voigt estimate is identical to the rule of mixtures only when the Poisson's ratios of the two components are equal.

More complicated expressions utilized for estimating the modulus will be found to lie between the Voigt and Reuss estimates. In practice more complicated expressions may be useful. For polymers containing nearly spherical particles of any modulus, the Kerner equation [147],

$$\frac{G}{G_m} = \frac{G_f \phi_f / [(7-5\nu) G_m + (8-10\nu) G_f] + \phi_m / [15(1-\nu)]}{G_m \phi_f / [(7-5\nu) G_m + (8-10\nu) G_f] + \phi_m / [15(1-\nu)]} \quad (26)$$

or the equivalent equation of Hashin and Shtrikman [148]

can be used to calculate the modulus of the composite if there is some adhesion between the phases. In this particular case, G represents the shear modulus of the composite, ϕ is the volume fraction, ν is the Poisson's ratio of the matrix, while the subscripts m and f represent the matrix and filler respectively. In general, particle size does not appear in the Kerner equation. It is especially useful in predicting the moduli of composites of a spherical filler randomly dispersed in a glassy matrix [147].

For fillers which are more rigid than the polymer matrix, the Kerner equation up to moderate filler concentrations becomes:

$$\frac{G}{G_m} = 1 + \frac{15 (1-\nu)}{(8-10\nu)} \frac{\phi_f}{\phi_m} \quad (27)$$

For foams and rubber-filled rigid polymers (such as HIPS) the Kerner equation reduces to:

$$\frac{1}{G} = \frac{1}{G_m} \left[1 + \frac{15 (1-\nu)}{(7-5\nu)} \frac{\phi_f}{\phi_m} \right] \quad (28)$$

The theories indicate that the elastic moduli of a composite material should be independent of the size of the filler particles; however, experiments sometimes show an increase in modulus as the particle size decreases [149]. One possible explanation has to do with the surface area of

the particles. As their size decreases, the surface area increases. Now, if the polymer is changed in some manner at the interface, then the properties should change with particle size because of the change in surface area.

The Kerner and similar equations all assume that there is good adhesion between the filler and matrix phases. Actually, good adhesion is not important as long as the frictional forces between the phases are not exceeded by the applied external forces. In most filled systems there is a mismatch in the thermal coefficients of expansion so that cooling down from the fabrication temperature imposes a squeezing force on the filler by the matrix. Thus, in most cases, even if the adhesion is poor, the theoretical equations are valid because there may not be any relative motion across the filler-polymer interface [1].

Halpin [150] has shown that the Kerner equation and many other equations for moduli can be put in a more general form:

$$\frac{M}{M_m} = \frac{1 + AB\phi_f}{1 - B\phi_f} \quad (29)$$

where M is any modulus-shear, Young's, or bulk.

Additionally,

$$A = \frac{7 - 5\nu}{8 - 10\nu} \quad (30)$$

and

$$B = \frac{M_f/M_m - 1}{M_f/M_m + A} \quad (31)$$

These so-called Halpin-Tsai equations are actually generalized Kerner equations and are used for both rubbery-filled systems and glassy-filled systems. When A approaches infinity, equation (29) becomes the rule of mixtures (i.e., $M = M_m\phi_m + M_f\phi_f$ and when A approaches zero, the equation becomes $\frac{1}{M} = \frac{\phi_m}{M_m} + \frac{\phi_f}{M_f}$).

Nielson [151] has shown that the Kerner or Halpin-Tsai equation can be generalized even further to:

$$\frac{M}{M_m} = \frac{1 + AB\phi_f}{1 - B\psi\phi_f} \quad (32)$$

The factor ψ depends upon the maximum packing fraction ϕ_p of the filler. The two empirical equations fulfilling the necessary boundary conditions are

$$\psi = 1 + \left(\frac{1 - \phi_p}{2\phi_p} \right) \phi_f \quad (33)$$

and

$$\psi\phi_f = 1 - \exp\left(\frac{-\phi_f}{1 - \phi_f/\phi_p}\right) \quad (34)$$

Phase inversion may occur in some systems so that the more rigid phase becomes the continuous matrix phase.

Such systems are called inverted composites. For the inverted case, equation (29) becomes [152]:

$$\frac{M_m}{M} = \frac{1 + AB\phi_f}{1 - B\phi_f} \quad (35)$$

where

$$A = \frac{8 - 10\nu}{7 - 5\nu} \quad (36)$$

and

$$B = \frac{M_m/M_f - 1}{M_m/M_f + A} \quad (37)$$

In some systems, such as polyblends and block copolymers, an inversion of the phases occurs at a volume fraction of about one half. The exact composition at which phase inversion occurs can be changed considerably by the intensity of mixing [153]. In addition, there is generally a range of compositions where both phases are partly continuous and where the modulus changes rapidly with composition.

There is often a discrepancy between theoretical predictions and experimental results for the moduli of particulate filled polymers due to the present limitations of understanding of these materials. It is for this reason that the simple parallel and series models which represent the upper and lower bounds to the composite moduli, respectively, are so useful [154]. However, the Kerner or Halpin-Tsai equations seem to agree with experiment as well as any other equations that have been proposed [1].

Other than the most widely used Kerner equation [155], there are, of course, many other equations describing the modulus of a composite. These will be discussed briefly now.

One of the first fundamental studies illustrating the effects of fillers on the modulus was described by Nielson et al [156], who showed that the shear modulus of PS was increased by the incorporation of mica, calcium carbonate, or asbestos. The proposed equation was of the form:

$$G = G_m \phi_m + A G_f \phi_f \quad (38)$$

where A is an empirical term to give a measure of the filler-matrix adhesion. It allows for the fact that upper bound modulus values are not found consistently in practice with such systems.

Equation (38) is very similar to that used for fiber-filled polymers. If fibers are long and oriented in the direction of applied stress, the rule of mixtures is found to hold:

$$E_{11} = E_f \phi_f + E_m \phi_m \quad (39)$$

which again represents an upper bound (or maximum obtainable modulus). In general, long oriented fibers in a matrix tend to yield upper bound values of modulus, while

particulate filled systems tend to yield lower bound values (as predicted by relationships such as Kerner's). Another similar equation commonly used for fiber-resin composites is the Kelly-Tyson equation [157] which predicts the composite longitudinal modulus:

$$M_L = K M_f \phi_f + M_m \phi_m \quad (40)$$

The value for K is unity for parallel continuous filaments and is less for randomly arranged filaments. Degree of adhesion has little effect on modulus, but a great effect on strength and ultimate elongation.

It should be remembered that most fiber-filled composites are highly anisotropic, so that the equation relating the elastic moduli to composition depends upon the orientation of the test. The rule of mixtures only holds in the case of very long fibers oriented parallel to the stretching deformation. For truly randomly oriented three dimensional composites, Nielson [158] has proposed a logarithmic rule of mixtures:

$$\log E = \phi_m \log E_m + \phi_f \log E_f \quad (41)$$

This equation has no theoretical basis.

The logarithmic rule of mixtures has also been applied to semicrystalline polymers [159]. The equation then has the following form:

$$\log_{10} G = W_a \log G_a + W_c \log G_c \quad (42)$$

In this equation W_a is the fraction of amorphous phase and W_c the fraction of crystalline phase. The logarithmic rule of mixtures has also been found empirically to be useful for predicting the moduli of block copolymers and polyblends when both polymeric phases are continuous.

Davies [160,161] has theoretically derived equations which are applicable when both phases are continuous in contrast to the usual theories in which one phase is assumed to be dispersed. His equations are specific examples of the very general mixing equation:

$$G^n = \phi_1 G_1^n + \phi_2 G_2^n; \quad -1 \leq n \leq 1 \quad (43)$$

where ϕ_1 and ϕ_2 are volume fractions of phases 1 and 2, respectively. As a special case, Davies' equation for the shear modulus of systems containing two continuous phases is:

$$G^{1/5} = W_a G_a^{1/5} + W_c G_c^{1/5} \quad (44)$$

Equation (44) fits many experimental data on crystalline polymers over a wide range of crystallinities [159]. It works well also for interpenetrating networks (IPN's) [155]. IPN's, one can say, exhibit dual phase continuity.

The Hashin-Shtrikman theory of the elastic properties of a hard matrix with randomly dispersed soft inclusions

appears to work quite well also for semi-crystalline polymers [79,148]. The equation has the following form:

$$\frac{B - B_c}{B_c} = \frac{1 - \phi_c}{(B_a/B_c - 1)^{-1} + \phi_c f(\nu)} \quad (45)$$

where ϕ_c is the volume fraction crystallinity, a and c represent the amorphous and crystalline regions respectively, and $f(\nu)$ is a slowly varying function of the Poisson's ratio of the crystalline phase. For example, when $\nu = 0.33$, $f(\nu) = 0.50$ so that equation (45) becomes:

$$\frac{B - B_c}{B_c} = \frac{1 - \phi_c}{(B_a/B_c - 1)^{-1} + 0.5\phi_c} \quad (46)$$

In the crystallinity range, $\phi_c > 0.5$, experimental evidence strongly suggests that the crystalline regions form the load-bearing phase. The elastic moduli of such a structure can be estimated by the method of Hashin and Shtrikman [148], who assume the discontinuous phase to be present as randomly distributed spheres and obtain as the representative equation:

$$\frac{G - G_c}{G_c} = \frac{1 - \phi_c}{\frac{G_c}{\frac{G_a - G_c}{a} + \phi_c f(\nu)}} \quad (47)$$

where $f(\nu)$ is a slowly varying function of Poisson's ratio ($f(\nu) = 0.467$ when $\nu = 0.33$).

Because the elastic properties depend very strongly on packing density and to some extent on the proximity of the melting point, these properties should be known before any correlation of elastic moduli can be attempted. When both these properties are known, the correlation of the bulk modulus has succeeded quite well, while those of the Young's and shear modulus are only suggestive, but far from quantitative [79].

II.G. TENSILE STRENGTH

The theoretical strength for a brittle material is of the order:

$$\tau_{th} \approx \frac{1}{10} E \quad (48)$$

where E is Young's modulus. However, the observed brittle strength is generally quite variable and usually 10 to 100 times less than the theoretical value. The reason is the presence of flaws or cracks in the material (especially at the surface) which act as stress concentrators [86].

For a ductile material, Tabor [162] has shown that the yield strength is proportional to the indentation hardness. Since the indentation hardness is a power function of the modulus, the yield stress will be:

$$\tau_Y = \tau_{max} \propto E^n \quad (49)$$

where $n \approx 0.75$ or

$$\tau_{\max} = (9.0) E^{3/4} \quad (50)$$

τ is the tensile strength at break for a brittle polymer and the tensile strength at yield for a ductile polymer. Equation (50) is empirical.

The presence of a filler has been shown to have marked and complex effects on the strength of polymers. Unfortunately, rigorous treatment of these phenomena (magnitude of tensile or yield strength) is not yet available for even unfilled systems [155]. Generally the tensile strength of particulate filled systems is reduced, when compared to the unfilled polymer matrix, although there are numerous exceptions [1,155]. Often the following is assumed:

$$\tau_{\text{break}} = E \epsilon_{\text{break}} \quad (51)$$

Then, since for a particulate filled matrix

$$\epsilon_{\text{break}} = \epsilon_{\text{matrix}} (1 - K \phi_f^{1/3}) \quad (52)$$

where K is an empirical constant (usually very nearly equal to one), equation (51) becomes:

$$\tau = E[\epsilon_m (1 - K \phi_f^{1/3})] \quad (53)$$

Equation (53) predicts a decrease in tensile strength and this generally occurs at low ϕ_f (filler volume fraction).

At higher concentrations of ϕ_f , the tensile strength is predicted to increase somewhat if Kerner's equation is used to predict the modulus of the composite [155].

As already mentioned, rigid fillers may increase or decrease the tensile strength of a glassy polymer. For polymers with good interfacial bonding, there is generally an increase. It is important when considering rigid fillers added to a glassy matrix to also compensate for the mismatch in coefficients of thermal expansion and to properly transmit most of the stress to the filler, otherwise the addition of filler, while increasing the modulus, will decrease the tensile strength. Chances for success in achieving higher tensile strength are therefore best with ductile polymers where there is good adhesion to the filler. In brittle polymers, these chances are markedly reduced with dewetting a serious problem. Also the squeezing of filler particles due to mismatch of thermal expansion coefficients may produce such high tensile stresses in the polymer that it may crack and reduce the strength of the composite [155].

Although particle size has little effect on the modulus of a composite, it has a large effect on the tensile strength [163]. Tensile strength increases as particle size decreases; however, the reason for this is not clear, but the increase in interfacial area per unit volume filler as particle size decreases should be an important factor.

Additionally, the probability of finding a larger flaw around a larger particle should be greater because the volume of polymer that experiences the stress concentration increases with filler size.

In spite of its great practical importance, the strength and stress-strain behavior of fiber filled composites is not as clearly understood as the moduli of such materials. The fracture phenomena of fiber filled composites is extremely complex not only because of anisotropy and heterogeneity, but also because of the possibility of several modes of fracture and the great importance of interfacial bonding, dewetting, perfection of fiber alignment, stress concentration at the ends of fibers, and relative brittle or ductile nature of the components. Only in the case of infinitely long fibers aligned in one direction and tested in tension parallel to the fibers is the strength given by a simple relationship. In this special case, the rule of mixtures holds:

$$\tau_{BL} = \tau_{BM} \phi_M + \tau_{BF} \phi_F \quad (54)$$

where the τ_B 's represent tensile strength and the subscripts L, M, and F refer to longitudinal, matrix, and filler (fiber) respectively.

For uniaxially oriented fiber composites, there are at least three important modes of failure and three important

strengths. These strengths are the longitudinal, the transverse, and the shear strength. The relative importance of these strengths depends, among other factors, upon the angle between the fibers and the applied load. Between 0° and 5° , where a tensile load is approximately parallel to the fibers, the longitudinal tensile strength is the important factor in determining the mode of failure. For fiber orientation angles between 5° and 45° , the important factor determining strength and mode of failure is the shear strength. At still higher angles, the transverse strength tends to determine the mode of failure [1].

II.H. ELONGATION AT YIELD AND BREAK

Generally, fillers in a composite system cause a dramatic decrease in elongation at yield and break. The decrease in elongation to break, ϵ_B , (rigid fillers) arises from the fact that the actual elongation experienced by the polymer matrix is much greater than the measured elongation by the specimen. Although the specimen is part filler and part matrix, practically all of the elongation comes from the polymer, if the filler is rigid. The theory is still incomplete and at best gives semi-quantitative understanding of experimental results. For good adhesion, the following equation is expected [164]:

$$\epsilon_b = \epsilon_m (1 - \phi_f^{1/3}) \quad (55)$$

This equation is nearly identical to equation (52) which contains an adjustable parameter to account for variation in adhesion.

Only in rare cases, where fillers induce additional crazing and act as stoppers to crack growth at the same time, will polymers filled with rigid fillers have elongations to break which are equal or greater than that of the unfilled polymer [165].

II.I. ORIENTATION

Nearly all polymeric objects have some orientation. During the forming or shaping of a specimen, the molecules are oriented by viscous flow and part of this orientation is frozen if the object is cooled relatively rapidly. But this kind of orientation is negligible compared with the directed orientation applied in drawing or stretching processes [166].

Orientation is generally accomplished by deforming a polymer at or above its T_g . Fixation of the orientation takes place if the stretched polymer is cooled below its T_g before the molecules have a chance to return to their random orientation. By heating above T_g , the oriented polymer will tend to retract; in amorphous polymers, the retractive force obtained is a measure of the degree of orientation obtained [86,166].

Orientation has a pronounced effect on the physical and mechanical properties of polymers. Uniaxially oriented amorphous glassy polymers will exhibit a higher modulus, tensile strength, and elongation to break in the direction of orientation in a tensile stress-strain measurement. At low degrees of orientation, the effect is not great for modulus, tensile strength, and elongation at break, although the effect is greater for tensile strength than for modulus, and greatest for elongation at break [167].

The properties of plastics are dependent upon processing history. During injection molding some orientation occurs particularly for samples that are quenched below the T_g . However, during moderate cooling rates from above T_g to T_g these orientational effects should be minimized due to relaxation effects. The relaxation time for PS, for example, is of the order of one second or so 11 C° above T_g [79].

The influence of the draw ratio upon the longitudinal and transverse moduli of PS is reported by Kennig [168]. Some of the values he obtained are reproduced in Table 2.2.

Since the draw ratio is a measure of the orientation in a polymer, one can conclude that the modulus is not severely affected by orientation until it becomes quite large. In fact, E_0 increases by only 2.4 percent in going from unoriented PS to PS with a draw ratio of two. The implication is that the effect is practically negligible since

TABLE 2.2

Longitudinal (E_0) and Transverse (E_{90})
Moduli for Oriented Polystyrene in Units
of Gigapascals (GPa)

<u>Draw Ratio</u>	<u>E_0</u>	<u>E_{90}</u>
1.0	3.30	3.30
2.0	3.38	3.29
3.0	3.46	3.28

it is difficult to even obtain moduli to an accuracy of 2.4 percent. Orientation in this case was achieved by drawing above the T_g , quenching to below T_g , and testing at room temperature.

The changes in moduli of polymer glasses made elastically anisotropic by drawing can be correlated quite well with independent measures of orientation, such as birefringence [168] but not so well with draw ratio because of the great sensitivity of the final moduli to the applied drawing rate [79].

Quantitative determinations of the degree of orientation are difficult to obtain. The easiest qualitative technique is generally the birefringence. Another relatively simple qualitative technique is based upon environmental stress crazing. Uniaxial orientation increases the resistance to crazing by external loads acting parallel to the direction of orientation and decreases the resistance to loads acting in the perpendicular direction. This phenomenon can be quickly used to make visible the orientation and flow pattern in injection molded objects. If an object molded from PS is soaked for some time in warm methanol and then exposed to hexane, the flow pattern of the molten polymer becomes visible. For an unoriented polymer, the hexane induced crazes show random orientation [170].

While orientation does not greatly influence the modulus at low levels of orientation, the influence at high

levels of orientation can become quite large. For very highly drawn fibers, E_L , the longitudinal modulus can be at least ten times as great as E_o , the modulus of the un-oriented polymer. The explanation for this experimental observation is that in unoriented or mildly oriented polymers, the modulus is largely determined by the relatively weak intermolecular (van der Waals) forces while in oriented polymers a tensile force in the direction of orientation acts along the polymer chains to either deform the much stronger covalent bond angles or possibly even stretch covalent bonds. A convenient measure of orientation in such cases is [1,166,171]:

$$(\text{Degree of Orientation}) = 1 - \frac{E_o}{E_L} \quad (56)$$

The degree of orientation predicted by the above equation agrees quite well with those obtained by birefringence measurements [172].

II.J. MODELING THE PROPERTIES OF MIXTURES - SIMPLEX LATTICE DESIGN

To a first approximation linear additivity is usually employed for the prediction of thermodynamic properties of multicomponent systems. Higher precision calculation is often unattainable because the excess property, P^E , cannot be predicted. As a generalization during mixing, the deviation of a property from linearity is unattainable or difficult to predict.

Nevertheless, the empirical data resulting from a mixing or blending experiment can usually be modeled. Often, semi-empirical significance can be attached to the coefficients of the model equation. One convenient modeling technique arises from a statistical method for investigating properties of multi-component systems as a function of composition [173-175]. The method was originally devised by Scheffé [173] for designing experiments of multi-component systems. The fraction of components making up any mixture must add to unity and hence factor space may be represented by a regular simplex (an element or figure contained within a Euclidean space of a specified number of dimensions having one more boundary point than number of dimensions).

The method is particularly useful when several properties are of interest. For example, the method has been applied to octane blending [174] and polymer blends in solution [175]. The regression equations used for the modeling of mixtures are polynomials. In principle any mixture response can be represented by a polynomial, if enough terms are included. In practice, polynomial models are limited to low order because of the large number of coefficients in higher order models. For the sake of simplicity, the cubic model for a three component system will initially be presented, although equations could easily be generated for any order model for any number of components.

So, the representation for a three component system (using a polynomial model of third order to express the response of a property, P , as a function of composition χ) is:

$$P = \beta_1\chi_1 + \beta_2\chi_2 + \beta_3\chi_3 + \beta_{12}\chi_1\chi_2 + \beta_{13}\chi_1\chi_3 + \beta_{23}\chi_2\chi_3 + \gamma_{12}\chi_1\chi_2(\chi_1 - \chi_2) + \gamma_{13}\chi_1\chi_3(\chi_1 - \chi_3) + \gamma_{23}\chi_2\chi_3(\chi_2 - \chi_3) + \beta_{123}\chi_1\chi_2\chi_3 \quad (57)$$

or more compactly

$$P = \sum_{1 \leq i \leq q} \beta_i \chi_i + \sum_{1 \leq i < j \leq q} \beta_{ij} \chi_i \chi_j + \sum_{1 \leq i < j \leq q} \gamma_{ij} \chi_i \chi_j (\chi_i - \chi_j) + \sum_{1 \leq i < j < k \leq q} \beta_{ijk} \chi_i \chi_j \chi_k \quad (58)$$

The β 's and γ 's are the coefficients of the composition and q is equal to the number of components. In this work we will be interested primarily in a quadratic two component model. Hence, we can reduce equation (57) to

$$P = \beta_1\chi_1 + \beta_2\chi_2 + \beta_{12}\chi_1\chi_2 \quad (59)$$

The first two terms of equation (59) correspond to the linear rule of mixtures for which all higher order coefficients are zero. The magnitude of β_{12} expresses the extent of deviation from non linearity. A positive β_{12} represents a nonlinear synergism while a negative β_{12} expresses an antagonism effect.

The quadratic model for binary systems describes a response curve with no more than one maximum or one minimum, but not both, and with no point of inflection.

Deviation from linearity is symmetrical and is a maximum at the 50:50 mixture. Of course, all equations are subject to the constraint $\sum \chi_i = 1$.

One can readily solve for the coefficients of equation (59) which for the sake of convenience will be represented in the following form:

$$P = \sum_{1 \leq i \leq 2} \beta_i \chi_i + \sum_{1 \leq i < j \leq 2} \beta_{ij} \chi_i \chi_j \quad (60)$$

The solution is

$$\beta_i = P_i \quad (61)$$

and

$$\beta_{ij} = 4P_{ij} - 2P_i - 2P_j \quad (62)$$

P_i and P_j now represent the response of the pure components and P_{ij} represents the response of the 50:50 mixture. More explicitly, the solution can be written:

$$\beta_1 = P_1 \quad (63)$$

$$\beta_2 = P_2 \quad (64)$$

and

$$\beta_{12} = 4P_{12} - 2P_1 - 2P_2 \quad (65)$$

The at least semi-empirical nature of equation (59) can now be better illustrated by allowing P_1 to represent a property of PS and P_2 a property of PPO. Then we would obtain:

$$\bar{V}_{\text{mix}} = \chi_1 \bar{V}_1 + \chi_2 \bar{V}_2 + \beta_{12} \chi_1 \chi_2 \quad (66)$$

Here the excess volume of mixing, \bar{V}^E , would be equal to $\beta_{12} \chi_1 \chi_2$ and one can think of β_{12} as a type of interaction term. Of course similar expressions could be written for other properties. In this work, primary interest will be in excess modulus, tensile strength and density, represented by the following equations, respectively:

$$E = E_1 \chi_1 + E_2 \chi_2 + \beta_{12}^E \chi_1 \chi_2 \quad (67)$$

$$\tau = \tau_1 \chi_1 + \tau_2 \chi_2 + \beta_{12}^\tau \chi_1 \chi_2 \quad (68)$$

$$\rho = \rho_1 \chi_1 + \rho_2 \chi_2 + \beta_{12}^\rho \chi_1 \chi_2 \quad (69)$$

A superscript has been placed on each interaction term, β_{12} , to emphasize that β_{12} will have a different value for different properties. A logical goal in this work would necessarily be to ascertain whether or not at least some semi-quantitative significance can be attached to the β_{12} term. More explicitly, does the magnitude and sign of β_{12} correlate with the level of compatibility or incompatibility in a blend and how does β_{12} vary with molecular weight?

II.K. LATTICE FLUID THEORY APPLIED TO THE MODULUS OF POLYMER BLENDS

Earlier in this chapter (see section II.D.), allusion was made to the lattice fluid theory recently formulated by Sanchez and Lacombe [129-131]. One of its advantages lies with the accessibility of empirical and theoretical data in the application of the theory (in comparison e.g. to the theory reported in Bondi's book [79]). In particular, the lattice fluid theory departs markedly from a corresponding states theory in that it does not require the separation of internal and external degrees of freedom [176]. Since the lattice fluid or Ising fluid is not based on a cell model, the introduction of a "c" parameter (characterizing the decrease in external degrees of freedom) is not required [130].

The equation of state for a lattice fluid is:

$$\tilde{\rho}^2 + \tilde{P} + \tilde{T} \left[\ln(1 - \tilde{\rho}) + \left(1 - \frac{1}{r}\right)\tilde{\rho} \right] = 0 \quad (70)$$

where $\tilde{\rho}$ is the reduced density ($\tilde{\rho} = \rho/\rho^*$; ρ^* is the maximum packing density at 0°K and is very close to the crystalline density), \tilde{P} is the reduced pressure ($\tilde{p} = P/P^*$; P^* is the cohesive energy density in the close packed state at 0°K), \tilde{T} is the reduced temperature ($\tilde{T} = T/T^*$; T^* is the interaction energy per mer in the close packed state at 0°K), and r is the number of lattice sites occupied by the r -mer [130,177]. The fluid is completely characterized by

the three equation of state parameters T^* , P^* , and ρ^* or equivalently by the three molecular parameters ϵ^* , v^* , and r^1 . The molecular parameters can be obtained from the equation of state parameters:

$$\epsilon^* = k T^* \tag{71}$$

$$v^* = k T^*/P^* \tag{72}$$

$$r = M/\rho^*v^* \tag{73}$$

ϵ^* is the total interaction energy per mer (it is also the energy required to create a lattice vacancy), while v^* is the closed packed volume [131,176].

Since r remains explicit in the reduced equation of state, a simple corresponding-states principle is not, in general, satisfied. However, for most polymers, $r \rightarrow \infty$, and the equation of state reduces to a corresponding states equation:

$$\tilde{\rho}^2 + \tilde{P} + \tilde{T} [\ln (1-\tilde{\rho}) + \tilde{\rho}] = 0 \tag{74}$$

T^* , P^* , and ρ^* can be calculated if experimental values of α , β and ρ or of α , β and γ are known. α , β , γ ,

¹Note that these parameters do not have the same significance as those dimensionless parameters, T^* and ρ^* , introduced in Section C and D of this chapter. T^* and ρ^* in those sections were analogous but not equivalent to \tilde{T} and $\tilde{\rho}$ in this section. Parameters with a star for a superscript have dimensions while parameters with a tilde are dimensionless in this section.

and ρ represent the thermal expansion coefficient, the isothermal compressibility, the thermal pressure coefficient, and the density respectively. For example, if α , β , and ρ are known, the pertinent equations are equation (74) and

$$T\alpha = 1/[\tilde{T}/(1-\tilde{\rho}) - 2] \quad (75)$$

and

$$P^* = T\alpha/\tilde{\rho}^2\beta \quad (76)$$

Since the modulus, E , is related to the cohesive energy density and recalling that P^* is the cohesive energy density in the close packed state, it would seem natural to define a reduced modulus:

$$\tilde{E} = E/P^* \quad (77)$$

The goal is to extend the lattice fluid theory to the modulus of compatible polymer blends. The following correlations would be useful if they could be obtained:

1. $\tilde{E}_{\text{blend}} = \tilde{E}(\tilde{\rho}_{\text{blend}})$. This is important since $\tilde{\rho}$ is a measure of the occupied lattice volume. It is expected that when $\tilde{\rho}$ increases, \tilde{E} increases.
2. $\tilde{E}_{\text{blend}} = \tilde{E}(\tilde{T}_{\text{blend}})$. \tilde{T} is inversely proportional to the interaction energy; hence the larger \tilde{T} , the smaller \tilde{E} .
3. $\tilde{\rho}_{\text{blend}} = \tilde{\rho}(\tilde{T}_{\text{blend}})$. Since $\tilde{\rho}$ is a measure of the occupied volume, $\tilde{\rho}$ should decrease with increasing \tilde{T} . Sanchez and Lacombe [130] show that the lattice

fluid equation of state correlates polymer density (as a function of \tilde{T}) as well as more complicated equations derived from modified cell models and illustrate that a corresponding-states principle is indeed satisfied.

In order to apply the lattice fluid theory to blends, additional equations or rules of mixing are required [176]. As a starting point, the following equation is useful:

$$P_{\text{mix}}^* = \epsilon_{\text{mix}}^* / v_{\text{mix}}^* \quad (78)$$

However,

$$\epsilon_{\text{mix}}^* = \phi_1^2 \epsilon_{11}^* + 2\phi_1\phi_2 (\epsilon_{11}^* \epsilon_{22}^*)^{1/2} + \phi_2^2 \epsilon_{22}^* \quad (79)$$

where

$$\phi_1 = 1 - \phi_2 = \frac{m_1/\rho_1^*}{m_1/\rho_1^* + m_2/\rho_2^*} \quad (80)$$

The subscripts refer to the components of the two component blend. ϵ_{11}^* is the interaction energy, ϕ is the volume fraction and m is the mass fraction. Equation (79) can be simplified by dividing by the Boltzmann constant and completing the square:

$$\epsilon_{\text{mix}}^*/k = 1/k [\phi_1 (\epsilon_{11}^*)^{1/2} + \phi_2 (\epsilon_{22}^*)^{1/2}]^2 \quad (81)$$

and finally reduced to a more useful form:

$$\epsilon_{\text{mix}}^*/k = [\phi_1 (T_1^*)^{1/2} + \phi_2 (T_2^*)^{1/2}]^2 \quad (82)$$

Finally, blending laws are needed for ρ^* and v^* . For ρ^* ,

$$\frac{1}{\rho^*} = \frac{m_1}{\rho_1^*} + \frac{m_2}{\rho_2^*} \quad (83)$$

and for v^* ,

$$v^* = \phi_1^o v_1^* + \phi_2^o v_2^* \quad (84)$$

where

$$\phi_1^o = 1 - \phi_2^o = \frac{\frac{m_1}{\rho_1^* v_1^*}}{\frac{m_1}{\rho_1^* v_1^*} + \frac{m_2}{\rho_2^* v_2^*}} \quad (85)$$

In Chapter IV, these equations will be utilized to calculate $\tilde{E} = E/P^*$, $\tilde{\rho} = \rho/\rho^*$, and $\tilde{T} = T/T^*$ as a function of blend composition.

II.L. RELAXATIONS AND MOTIONS BELOW T_g

Most polymers exhibit transitions (e.g. in elastic modulus or dielectric properties) in addition to the main glass-rubber transition. The glass transition represents the maximum amount of chain flexibility, short of solution in a suitable solvent, that a polymer network can possess. When this flexibility is frozen at the glass transition temperature, there may remain some limited freedom either of short segments or of side groups. Damping peaks occurring below T_g in polymers are called secondary glass transitions, secondary relaxations or dispersions, or beta, gamma, etc.

relaxations. The energy involved in secondary relaxations will be less than for full movement and so will occur at lower temperatures. These secondary relaxations have been studied in a number of polymers and in some cases assignments have been made of definite groups of molecules or of side groups as being the cause of the relaxations [1,2,74].

So, it can be asserted that the entire area under the energy absorption versus frequency, time, or temperature is a measure of the population of mobile molecules or segments (under the test conditions). This population of mobile molecules or segments, in turn, determines the frequency limit below, or the temperature limit above, which there will be enough relaxing mechanisms available to permit small scale deformation at a particular rate and temperature. Knowledge of the location and the area of the loss curve versus frequency or temperature coordinates permits, therefore a reasonable prediction of the possibility of high speed deformation, or more crudely, of adequate impact strength under various operating conditions [79].

A consequence of the availability of secondary molecular deformation mechanisms is then that a glass is not always brittle. So the practical importance of these transitions is that nearly all tough ductile glassy polymers have prominent secondary relaxations [74]. Closely associated with ductility and high impact strength is a decreased notch sensitivity. In very brittle polymers a scratch or a

notch acts as a stress concentrator causing a drastic decrease in strength; however, in ductile polymers some types of secondary transitions appear to decrease notch sensitivity [1]. So as a generalization, brittle polymers, such as PS, have insignificant relaxations at $T < T_g$, while some polymers exhibit high ductility at $T < T_g$, such as PC, in conformity with the large areas under their loss curves at $T < T$ (test). However, it should be noted that only certain types of secondary relaxations increase ductility and impact, even if this transition lies well below the test temperature. In particular, those transitions due to side chain motion are considerably less important than backbone motions in increasing ductility and impact strength [178].

The energy-loss spectrum can be modified appreciably by molecular orientation, annealing, and mixing with plasticizers and antiplasticizers. The modification by orientation is of little concern here; while that accomplished by annealing and mixing is of considerable significance.

As mentioned previously in this chapter (see section D), annealing treatments can densify the glass with subsequent decrease in excess thermodynamic properties. Concomitantly, the secondary relaxation that is related to the degree of ductility of the polymer diminishes or disappears. For example, the β relaxation exhibited by atactic PS (a-PS) like that of amorphous PC, is sensitive to the thermodynamic state of the glass. In PS, the β loss peak at approximately 75°C

can be eliminated by annealing at 92°C. Thus, the modes of motion involved in the β relaxation can be completely suppressed by appropriate annealing treatment [87].

As just mentioned, a-PS has a β relaxation which appears just below T_g [179]. This transition is not observed in i-PS [180]. The β relaxation in a-PS is apparent in both dynamic-mechanical loss spectra and in dielectric loss measurements [3]. At frequencies higher than 40 hertz, the β relaxation peak merges with the primary relaxation. There is also considerably more plastic deformation at extremely slow rates of deformation in tensile testing than at "normal" speeds, suggesting that this relaxation may in part contribute to what toughness PS does possess [37].

There is still some controversy as to the precise origin of the β -relaxation. The available evidence suggests that this transition results from a local mode transition, such as local mode twisting of the main chains [3]. The time dependence of the β -relaxation of PS could also be of significance in general with respect to the physical aging of glassy materials. It has often been proposed [181,182] that brittleness, embrittlement, etc., of amorphous polymers are closely related to the β -relaxation range. Above the β -process stresses can be relaxed by molecular rearrangements. Below the β -process, changes in molecular position are hindered. In this way, mechanical work done on a specimen cannot be dissipated; the material is hard and brittle. More

dynamic mechanical measurements supplemented by thermodynamic data (especially volume measurements) are needed to clarify this point.

PS also has γ and δ relaxation peaks. They are less pronounced in i-PS than in a-PS and it has been suggested that the γ and δ peaks are due to restricted phenyl group motion and phenyl oscillation respectively [3].

PPO has a β -relaxation that occurs at approximately -50°C [183]. This loss peak is attributed to hindered torsional oscillatory motions of the phenylene units in the backbone around the $0-\phi-0$ axis. The activation energy is around 16 kcal/mole, indicating that the barrier is predominantly intermolecular. This and other secondary relaxation peaks appear to be very sensitive to thermal history [127,137,183].

As mentioned, one of the effects of densification is often a suppression of secondary relaxations (e.g., the β -relaxation in both PPO and PS), which may, at least in some part, account for polymer embrittlement. However, that does not imply that all β , γ , etc. relaxations depend upon free volume for their mobility. For example, the β and γ relaxations of PMMA have been found to be independent of hydrostatic pressure (and therefore specific volume) indicating some molecular motions are not associated with volume changes [184]. Of course, molecular processes involving segmental motion should be associated with volume changes; while pro-

cesses involving only small side group rotations (e.g. methyl group rotation) would be unlikely to cause detectable changes in volume.

Other than by annealing and orientation, secondary relaxations can also be modified by mixing with plasticizers, antiplasticizers, or other polymers. All plasticizers drive the relaxation peaks to lower temperatures, although small amounts of some plasticizers will increase the elastic moduli and also suppress the strength of secondary relaxations [74] (see also section C of this chapter for more details), and thus embrittle the glass. The stiffer the plasticizing molecule, the more effective the suppression. The motions of the plasticizer molecules in the glassy matrix can be observed by their dielectric loss (if they are polar) and/or by NMR measurements. In spite of their importance in elucidating mechanisms of plasticizer action, the data is surprisingly fragmentary [79]. It, however, appears from their comparatively small activation energy for dipole rotation that plasticizer molecules dissolved in glasses, just as polymer molecules, carry out only segmental motions. The NMR measurements of Kosfeld [185] suggest that a certain temperature dependent fraction of plasticizer is distributed in microcavities in the polymeric glass rather than in molecular dispersion. That fraction becomes smaller with decreasing temperature and the molecules in it have the mobility of free plasticizer.

The mixing of two compatible polymers also involves the suppression or inhibition of secondary relaxations. The broad β peak of PPO is suppressed even by small amounts of PS, implying a strong interaction between the molecules of the two polymers. The interaction may be the cause for the negative excess volume of mixing, thus hindering local mode motions. Also important is that concomitant with the suppression of the β relaxation is an increase in the elastic modulus. This observation is phenomenologically similar to antiplasticization. Similar, but somewhat less significant suppression effects are observed on the addition of small amounts of PPO to PS, in that both the β and γ relaxations are suppressed. The suppression of the γ relaxation of PS (ascribed to restricted phenyl group motions) again indicates a segmental level of mixing where the aromatic rings are apparently coupled. In addition, small amounts of PPO inhibit the growth of crazes in PS during deformation [12,127,186-188].

Baer and Wellinghoff [12,187,188] distinguish between iPS-PPO and aPS-PPO blends. Both UV and FTIR measurements indicate an increasing distortion of PPO from its minimum intramolecular energy configuration upon addition of PS. The increase of PPO energy in the blends is apparent in the enhancement of the PPO intermediate relaxation and its movement to lower temperatures. At the same blend composition, the PPO component has a higher configurational energy in an aPS blend than in a blend with iPS. This observation is

consistent with the greater low temperature anelasticity of aPS blends relative to iPS blends. Finally, they attribute the strong dispersion interaction between the phenylene ring of PPO and the phenyl ring of PS for being responsible for the compatibility and negative excess volume of mixing of these polymers and also for the suppression of the β relaxation in PPO.

Obviously, the mechanical properties undergo enormous changes at the glass transition; in the glassy state, however, it has been usual to assume that there are no further abrupt changes in the mechanical behavior of polymers. Closer investigation has shown that this is not so, i.e., mechanical properties are affected by secondary relaxation regions. The presence of secondary loss peaks can make some improvement in toughness and impact strength, while their suppression can lead to embrittlement and an increased elastic modulus. Moreover, creep, stress relaxation, modulus, tensile strength and elongation can be altered somewhat by the alterations of those secondary relaxations that also affect the free volume [3].

REFERENCES

1. L. E. Nielson, "Mechanical Properties of Polymers and Composites," Marcel Dekker, Inc., New York, 1974.
2. R. G. C. Arridge, "Mechanics of Polymers," Oxford University Press, London, 1975.
3. R. N. Haward, ed., "The Physics of Glassy Polymers," Halsted Press, New York, 1975.
4. I. M. Ward, ed., "Structure and Properties of Oriented Polymers," John Wiley, New York, 1975.
5. E. H. Merz, L. E. Nielson, and R. Buchdahl, Ind. Eng. Chem., 43, 1396 (1951).
6. A. N. Gent, J. Polym. Sci., A-2, 10, 571 (1972).
7. H. W. McCormick, F. M. Brower, and L. Kin, J. Polym. Sci., 39, 87 (1959).
8. R. F. Boyer, J. Polym. Sci., 9, 289 (1952).
9. J. M. Goppel in "Plastics Progress," P. Morgan, ed., Hiffe London, 1960.
10. S. Rabinowitz and P. Beardsmore, CRC Critical Rev. Macromol. Sci., 1, 1 (1972).
11. D. Hull in "Polymeric Materials," E. Baer and S. V. Radcliffe, eds., Amer. Soc. of Metals, Metals Park, Ohio, 1975.
12. S. Wellinghoff and E. Baer, Coatings and Plastics Preprints, 36(1), 140 (1976).
13. R. P. Kambour, J. Polym. Sci., D, "Reviews," 1973.
14. P. B. Bowden, in "Physics of Glassy Polymers," R. N. Haward, ed., Halsted Press, New York, 1973.
15. R. P. Kambour, J. Polym. Sci., A-2, 4, 349 (1966).
16. H. El-Hakeem, G. P. Marshall, E. L. Zichy, and L. E. Culver, J. Appl. Polym. Sci., 19, 3093 (1975).
17. H. H. Kausch, J. A. Hassell, R. J. Jaffee, eds., "Deformation and Fracture of High Polymers," Battelle Institute Material Science Colloquia, Plenum Press, New York, 1973.

18. S. S. Sternstein, L. Ongchin, A. Silverman, Appl. Polym. Symp., 7, 175 (1968).
19. M. Bevis and D. Hull, J. Mat. Sci., 5, 983 (1970).
20. R. P. Kambour and R. R. Russell, Polymer, 12, 237 (1971).
21. J. Murray and D. Hull, Polymer, 10, 451 (1969).
22. R. P. Kambour, Appl. Polym. Symp., 7, 215 (1968).
23. R. N. Haward, B. M. Murphy, and E. F. T. White, J. Polym. Sci., A-2, 9, 801 (1971).
24. A. N. Gent, J. Mat. Sci., 5, 925 (1970).
25. W. Whitney, J. Appl. Phys., 34, 3633 (1963).
26. S. S. Sternstein and L. Ongchin, Polymer Preprints, 10(2), 1117 (1969).
27. R. Hill, Proc. Phys. Soc., A, 65, 349 (1952).
28. R. Hill, "Mathematical Theory of Plasticity," Clarendon Press, Oxford, 1950.
29. S. Wellinghoff and E. Baer, J. Macromol. Sci.-Phys., B-11(3), 367 (1975).
30. R. D. Andrews, Polymer Preprints, 10(2), 1110 (1969).
31. A. S. Argon, R. D. Andrews, J. A. Godrick, J. Appl. Phys., 39, 1899 (1968).
32. J. S. Lazurkin, J. Polym. Sci., 30, 595 (1958).
33. I. M. Ward, "Mechanical Properties of Solid Polymers," Interscience, New York, 1971.
34. I. Marshall and A. B. Thompson, Proc. R. Soc., A, 221, 541 (1954).
35. P. I. Vincent, Polymer, 1, 7 (1960).
36. P. I. Vincent, Polymer, 13, 558 (1972).
37. Unpublished data of L. Kleiner.
38. A. T. DiBenedetto and K. L. Trachte, J. Appl. Polym. Sci., 14, 2249 (1970).
39. L. Nicholais and A. T. DiBenedetto, J. Appl. Polym. Sci., 15, 1585 (1971).

40. S. Newman and S. Strella, J. Appl. Polym. Sci., 9, 2297 (1965).
41. F. R. Eirich, Appl. Polym. Symp., 1, 271 (1965).
42. G. M. Bryant, Textile Res. J., 31, 399 (1961).
43. R. E. Robertson, Appl. Polym. Symp., 7, 201 (1968).
44. H. Eyring, J. Chem. Phys., 4, 283 (1936).
45. R. E. Robertson, J. Chem. Phys., 44, 3950 (1966).
46. C. Bauwens-Crowet, J. C. Bauwens, and G. Homes, J. Mater. Sci., 7, 76 (1972).
47. R. D. Deanin and A. M. Crugnola, eds., "Toughness and Brittleness of Polymers," ACS Adv. Chem. Ser., 154, 13 (1976).
48. L. Nicolais and A. T. DiBenedetto, J. Appl. Polym. Sci., 15, 1585 (1971).
49. S. S. Sternstein, Polymer Preprints, 17(1), 136 (1976).
50. M. L. Williams and A. R. Rosenfield in "Deformation and Fracture of High Polymers," Battelle Institute Material Science Colloquia, Plenum Press, New York, 1973.
51. R. M. Mininni, R. S. Moore, J. R. Flick and S. E. B. Petrie, J. Macromol. Sci., B8, 343 (1973).
52. D. G. LeGrand, J. Appl. Polym. Sci., 13, 2129 (1969).
53. S. F. Pugh, Brit. J. Appl. Phys., 18, 129 (1967).
54. R. A. Horsley, Appl. Polym. Symp., 17, 117 (1971).
55. S. Timoshenko and J. N. Goodier, "Theory of Elasticity," McGraw Hill, New York (1951).
56. J. Rehner, J. Appl. Phys., 14, 638 (1943).
57. J. Janacek and J. Kolarik, J. Polym. Sci., C16, 279, 441 (1967).
58. J. Janacek, J. Polym. Sci., C23, 373 (1968).
59. M. Baccareda, E. Butta, V. Frosini, and S. dePetris, J. Polym. Sci., A-2, 5, 1296 (1967).
60. K. H. Illers and E. Jenckel, Rheol. Acta, 1, 322 (1958).

61. M. C. Shen and J. D. Strong, J. Appl. Phys., 38, 4197 (1967).
62. M. C. Shen, J. D. Strong, and H. Schlein, J. Macromol. Sci., A3, 1315 (1969).
63. M. C. Shen, and E. H. Cirlin, J. Macromol. Sci., B4, 293 (1970).
64. R. J. Morgan and L. E. Nielson, J. Polym. Sci., A2, 10, 1575 (1972).
65. J. Janacek and J. D. Ferry, J. Macromol. Sci., B5, 219 (1971).
66. J. Kolarik and J. Janacek, J. Polym. Sci., A2, 10, 11 (1972).
67. T. Kawaguchi, J. Polym. Sci., 32, 417 (1958).
68. W. J. Jackson, Jr. and J. R. Caldwell in "Plasticization and Plasticizer Processes," Adv. Chem. Series, 48, 185 (1965).
69. W. J. Jackson, Jr. and J. R. Caldwell, J. Appl. Polym. Sci., 11, 211, 227 (1967).
70. L. M. Robeson and J. A. Faucher, J. Polym. Sci., B7, 35 (1969).
71. L. M. Robeson, Polym. Eng. Sci., 9, 277 (1969).
72. M. H. Litt and A. V. Tobolsky, J. Macromol. Sci., B1(3), 433 (1967).
73. G. Pezzin, J. Appl. Polym. Sci., 11, 2553 (1967).
74. L. Bohn, Kunststoffe, 53, 826 (1963).
75. P. Ghera, Modern Plastics, 36, 135 (1958).
76. R. A. Horsley in "Plastics Progress 1957," P. Morgan, ed., Hiffe, London, 1958.
77. R. E. Robertson and C. W. Joynson, J. Appl. Polym. Sci., 16, 733 (1972).
78. J. H. Golden, B. L. Hammant, and E. A. Hazell, J. Appl. Polym. Sci., 11, 1571 (1967).
79. A. Bondi, "Physical Properties of Molecular Crystals, Liquids, and Glasses," John Wiley, New York, 1968.

80. P. J. Flory, "Principles of Polymer Chemistry," Cornell University Press, 1953.
81. R. E. Robertson, J. Phys. Chem., 69, 1575 (1965).
82. P. H. Geil in "Polymer Materials," E. Baer and S. V. Radcliffe, eds., Amer. Soc. of Metals, Metals Park, Ohio (1975).
83. G. S. Y. Yeh, CRC Crit. Rev. Macromol. Sci., 1, 173 (1972).
84. S. M. Wecker, T. Davidson, and J. B. Cohen, J. Mat. Sci., 7, 1249 (1972).
85. P. Corradini, in Proceedings, R. A. Welch Foundation Conference on Chemical Research, X, Polymers, Houston, 1967.
86. D. W. Van Krevelen and P. J. Hoftyzer, "Properties of Polymers," Elsevier, New York, 1972.
87. S. E. B. Petrie in "Polymeric Materials," E. Baer and S. V. Radcliffe, eds., Amer. Soc. of Metals, Metals Park, Ohio, 1975.
88. A. J. Kovacs, Fortschr. Hochpolymer Forschg., 3, 394 (1963).
89. R. S. Marvin and J. E. McKinney in "Physical Acoustics," W. P. Mason, ed., Academic Press, New York, 1965.
90. J. R. McLoughlin and A. V. Tobolsky, J. Polym. Sci., 7, 658 (1951).
91. E. Jenckel and R. Heusch, Kolloid-Z., 130, 89 (1953).
92. A. J. Kovacs, R. A. Stratton, and J. D. Ferry, J. Phys. Chem., 67, 152 (1963).
93. G. S. Y. Yeh, J. Macromol. Sci., 136, 465 (1972).
94. L. C. E. Struik, Rheol. Acta., 5, 303 (1966).
95. P. B. Bowden and S. Raha, Phil. Mag., 22, 463 (1970).
96. R. W. Douglas and B. Ellis, eds., "Amorphous Materials," John Wiley and Sons, Inc., New York, Chap. 12 (1972).
97. W. C. Dale and C. E. Rogers, J. Appl. Polym. Sci., 16, 21 (1972).
98. T. E. Brady and G. S. Y. Yeh, J. Appl. Phys., 42, 4622 (1971).

99. D. H. Ender, J. Macromol. Sci.-Phys., B4, 635 (1970).
100. R. M. Kimmel and D. R. Uhlmann, J. Appl. Phys., 41, 2917 (1970).
101. R. M. Kimmel and D. R. Uhlmann, J. Appl. Phys., 42, 1892 (1971).
102. R. M. Kimmel and D. R. Uhlmann, J. Appl. Phys., 42, 4917 (1971).
103. R. M. Kimmel and E. Gamberg, J. Non-Cryst. Solids, 13, 399 (1974).
104. R. Straff and D. R. Uhlmann, J. Polym. Sci.-Phys., 14, 1087 (1976).
105. D. R. Uhlmann, J. F. Hays, and D. Turnbull, Phys. and Chem. Glas., 8, 1 (1967).
106. R. M. Kimmel and D. R. Uhlmann, J. Appl. Phys., 40, 4254 (1969).
107. R. M. Kimmel and D. R. Uhlmann, Phys. and Chem. Glas., 10, 12 (1969).
108. R. M. Kimmel and D. R. Uhlmann, Bull. Amer. Phys. Soc., 14, 406 (1969).
109. H. Breuer and G. Rehage, Koll. Zeit., 216, 159 (1967).
110. R. N. Haward, H. Breuer, and G. Rehage, Polym. Lett., 4, 375 (1966).
111. G. Rehage and G. Goldbach, Rheol. Acta., 6, 30 (1967).
112. G. Rehage and G. Goldbach, Ber. Bunsenges., 70, 1144 (1966).
113. G. Rehage and G. Goldbach, Rheol. Acta., 5, 302 (1966).
114. G. Rehage and G. Goldbach, Koll.-Z., Z. Polymere, 206, 116 (1965).
115. G. Rehage, Koll.-Z., Z. Polymere, 194, 16 (1964).
116. G. Rehage, Koll.-Z., Z. Polymere, 196, 97 (1964).
117. G. Rehage, Koll.-Z., Z. Polymere, 199, 1 (1964).
118. P. Heydemann and H. D. Guicking, Koll.-Z., Z. Polymere, 193, 16 (1963).

119. S. Ichihara, A. Komatsu, Y. Tsiyita, T. Nose, and T. Hata, Polym. J., 2, 530 (1971).
120. S. Ichihara, A. Komatsu and T. Hata, Polym. J., 2, 640 (1971).
121. S. Ichihara, A. Komatsu, and T. Hata, Polym. J., 2, 644 (1971).
122. S. Ichihara, A. Komatsu, and T. Hata, Polym. J., 2, 650 (1971).
123. A. Quach and R. Simha, J. Phys. Chem., 76, 416 (1972).
124. A. Quach and R. Simha, J. Appl. Phys., 42, 4606 (1971).
125. G. Allen, R. C. Ayerst, J. R. Cleveland, G. Gee and C. Price, J. Polym. Sci. C., 23, 127 (1968).
126. C. H. M. Jacques and H. B. Hopfenberg, Polym. Eng. and Sci., 14, 441 (1974).
127. A. F. Yee, Polym. Eng. and Sci., 17, 213 (1977).
128. E. Butta and P. Sinisti, Ric. Sci. II, 2, 362 (1962).
129. I. C. Sanchez and R. H. Lacombe, J. Phys. Chem., 80, 2568 (1976).
130. I. C. Sanchez and R. H. Lacombe, J. Polym. Sci., Polym. Letters Ed., 15, 71 (1977).
131. R. H. Lacombe and I. C. Sanchez, J. Phys. Chem., 80, 2352 (1976).
132. I. Prigogine, "The Molecular Theory of Solutions," Interscience, New York, 1957.
133. J. H. Hildebrand and J. Dymond, J. Chem. Phys., 46, 624 (1967).
134. K. Neki and P. H. Geil, J. Macromol. Sci., 8, 295 (1973).
135. J. R. Flick and S. E. B. Petrie, Bull. Amer. Phys. Soc., 19, 238 (1974).
136. G. Pielstöcker, Kunststoffe, 51, 509 (1961).
137. A. F. Yee, private communication.
138. R. F. Boyer, Rubber Chem. Technol., 36, 1393 (1963).

139. J. P. Mercier, J. J. Aklonis, M. Litt, and A. V. Tobolsky, J. Appl. Polym. Sci., 9, 447 (1965).
140. L. Holliday and J. M. White, Pure and Appl. Chem., 26, 545 (1971).
141. J. A. Sauer and R. G. Saba, J. Macromol. Sci., A-3, 1217 (1969).
142. W. Albert, Kunststoffe, 53, 86 (1963).
143. G. Schreyer, Rheol. Acta., 3, 218 (1964).
144. L. J. Broutman and R. H. Krock, "Modern Composite Materials," Addison-Wesley, Reading, Mass. 1967.
145. John Gittus, "Creep, Viscoelasticity, and Creep Fracture in Solids," Applied Science Publishers, London, 1975.
146. R. Hill, Proc. Phys. Soc., A, 65, 349 (1952).
147. E. H. Kerner, Proc. Phys. Soc., B69, 808 (1956).
148. Z. Hashin and S. Shtrikman, J. Mech. Phys. Solids, 11, 127 (1963).
149. T. B. Lewis and L. E. Nielson, J. Appl. Polym. Sci., 14, 1449 (1970).
150. J. C. Halpin, J. Composite Mater., 3, 732 (1969).
151. L. E. Nielson, J. Appl. Phys., 41, 4626 (1970).
152. L. E. Nielson, Appl. Polym. Symp., 12, 249 (1969).
153. T. Miyamoto, K. Kodama, and K. Shibayama, J. Polym. Sci., A2, 8, 2095 (1970).
154. Z. Hashin, Appl. Mech. Rev., 17, 1 (1964).
155. J. A. Manson and L. H. Sperling, "Polymer Blends and Composites," Plenum Press, New York, 1976.
156. L. E. Nielson, R. A. Wall, and P. G. Richmond, SPE J., 11, 22 (1955).
157. R. B. Seymour, Polym.-Plast. Technol. Eng., 7(1), 49 (1976).
158. L. E. Nielson, Rheol. Acta., 13, 86 (1974).
159. L. E. Nielson, J. Appl. Polym. Sci., 19, 1485 (1975).

160. W. E. A. Davies, J. Phys., D4, 1176, 1325 (1971).
161. G. Allen, M. J. Bowden, S. M. Todd, D. J. Blundell, G. M. Jeffs, and W. E. A. Davies, Polymer, 15, 28 (1974).
162. D. Tabor, Proc. Roy. Soc., A192, 247 (1948).
163. H. Alter, J. Appl. Polym. Sci., 9, 1525 (1965).
164. L. E. Nielson, J. Appl. Polym. Sci., 10, 97 (1966).
165. L. Nicolais and M. Narkis, Polym. Eng. Sci., 11, 194 (1971).
166. I. M. Ward, ed., "Structure and Properties of Oriented Polymers," John Wiley, New York, 1975.
167. G. B. Jackson and R. L. Ballman, Soc. Plast. Eng. J., 16, 1147 (1960).
168. J. Hennig, Kunststoffe, 57, 385 (1967).
169. K. H. Hellwege, Kolloid-Z, 188, 121 (1963).
170. L. E. Nielson, J. Appl. Polym. Sci., 1, 24 (1959).
171. W. W. Mosely, Jr., J. Appl. Polym. Sci., 3, 266 (1960).
172. H. M. Morgan, Textile Res. J., 32, 866 (1962).
173. H. Scheffé, J. Roy. Stat. Soc., London, B-20, 344 (1958).
174. J. W. Gorman and J. E. Hinman, Technometrics, 4(4), 463, (1962).
175. K. Dimov, E. Dilova, and S. Stoyanov, J. Appl. Polym. Sci., 19, 2087 (1975).
176. I. Sanchez, unpublished manuscript, University of Massachusetts.
177. I. Sanchez, private communication.
178. J. Heijboer, J. Polym. Sci., C16, 3755 (1968).
179. K. H. Illers and E. Jenckel, Rheol. Acta., 1, 322 (1958).
180. O. Yano and Y. Wada, J. Polym. Sci., A-2, 9, 669 (1971).
181. J. Heijboer, Brit. Polym. J., 1, 1 (1969).
182. R. F. Boyer, Polym. Eng. and Sci., 8, 161 (1968).

183. A. Eisenberg and B. Cayrol, J. Polym. Sci., C, 35, 129 (1971).
184. P. Heydeman and H. D. Guicking, Koll.-Z., 193, 16 (1963).
185. R. Kosfeld, Adv. Chem. Ser., 48, 49 (1965).
186. A. F. Yee, Polymer Preprints, 17(1), 145 (1976).
187. E. Baer and S. Wellinghoff, Bull. Amer. Phys. Soc., 21, 375 (1976).
188. E. Baer and S. Wellinghoff, Polymer Preprints, 18(1), 836 (1977).

CHAPTER III
EXPERIMENTAL

III.A. PREPARATION OF BLENDS

The materials utilized in the making of the polymer blends were poly(2,6-dimethyl-1,4-phenylene oxide) (PPO) received in the form of a fine crystalline powder courtesy of Dr. A. Katchman of the General Electric Company, narrow molecular weight distribution (NMWD) atactic polystyrene (aPS) received in the form of a powder from the Pressure Chemical Company, commercial atactic polystyrene (HH 101) received in the form of pellets courtesy of Mr. T. Boyd from the Monsanto Company, and isotactic polystyrene (iPS) and poly (α -methyl styrene) (α -PS) both received in pellet form from Polysciences, Inc. The molecular weights of all polymers are summarized in Table 3.1. In the case of PPO, aPS (NMWD), and HH 101 the molecular weights were furnished by each of the respective suppliers. The iPS molecular weight was determined by the D & R Testing Institute in Enfield, Connecticut after the iPS had been dissolved in toluene, reprecipitated in methanol and washed in boiling methyl ketone to remove the atactic component. The molecular weight of α -PS was obtained from an intrinsic viscosity measurement (courtesy of Mr. P. Alexandrovich) in toluene at 25.0°C and utilizing the equation [1]:

TABLE 3.1

Summary of Molecular Weights

Narrow Molecular Weight Distribution aPS	Molecular Weight	Polydispersity \bar{M}_w/\bar{M}_n
aPS - 4000	4000	<1.06
aPS - 10000	10000	<1.06
aPS - 37000	37000	<1.06
aPS - 110000	110000	<1.06
aPS - 233000	233000	<1.06
aPS - 670000	670000	<1.15
aPS - 2000000	2000000	<1.20
HH 101 Monsanto Polystyrene	$\bar{M}_n = 90,000 - 95,000$ $\bar{M}_w = 260,000 - 280,000$ $\bar{M}_z = 470,000 - 500,000$	
PPO	$\bar{M}_n = 17,000$ $\bar{M}_w = 35,000$ $\bar{M}_z = 54,000$	
iPS (MEK purified)	$\bar{M}_n = 133,000$ $\bar{M}_w = 724,000$ $\bar{M}_z = 2,490,000$	
α -PS (reppt.)	$\bar{M}_v = 18,000$ (toluene at 25°C) $\bar{M}_n \approx 10,000$ (estimated from T_g)	

$$[\eta] = 1.01 \times 10^{-4} \bar{M}^{0.72}$$

(86)

The number average molecular weight \bar{M}_n , was estimated from the experimentally determined (by DSC) T_g [1].

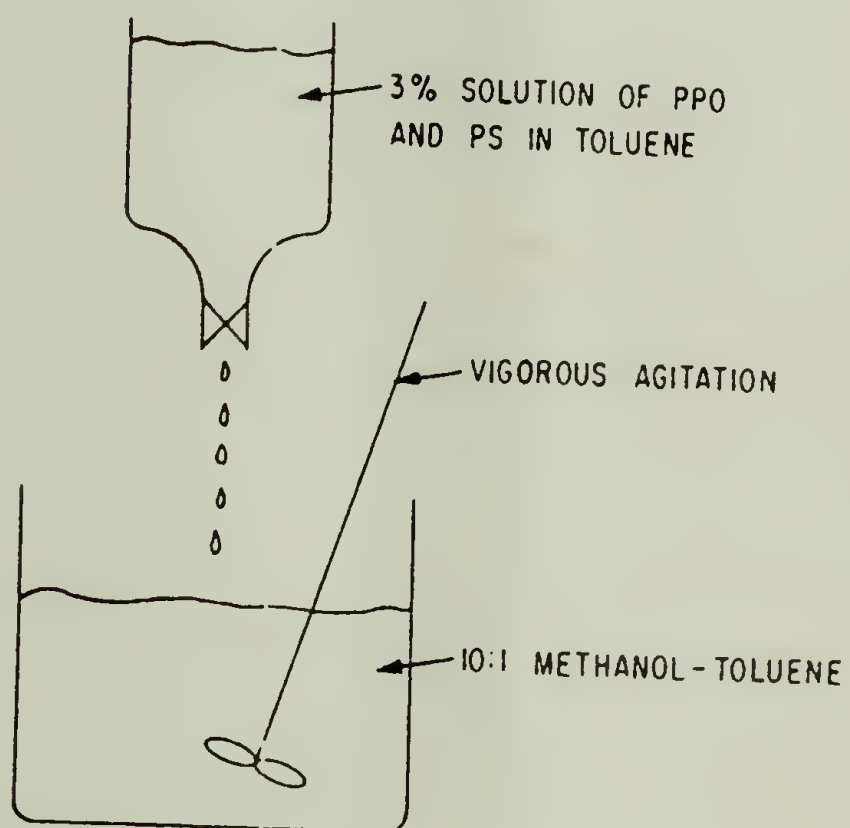
Polymer blends were generally prepared as depicted schematically in Figure 3.1. More specifically, PPO-based blends (with NMWD aPS, HH 101, α -PS) and blends of HH 101 and α -PS were prepared by dissolving the appropriate weight fractions of the polymers in boiling toluene (3g polymer/100 ml toluene) and coprecipitating into methanol (10:1). Vigorous agitation is required during the entire coprecipitation process to ensure the obtaining of a fine polymer powder. The fine powder in the 10:1 methanol-toluene mixture was filtered and dried in a vacuum oven for 48 hours at 100°C.

All iPS based blends (with PPO and HH 101) were prepared somewhat differently. First, the as-received pellets were compression molded at 300°C between steel plates and aluminum foil at 10,000 psi for about one minute and then removed and quenched into an ice-water mixture. This procedure aids in the subsequent dissolution process. Next, the compression molded films are shredded and placed into boiling toluene (2g/100 ml) and upon dissolution, reprecipitated into methanol (10:1). The precipitated iPS is then charged into boiling methyl ethyl ketone (MEK) for a period of six hours to extract the atactic component from the iPS.

FIGURE 3.1

PREPARATION OF POLYMER BLENDS

1. DISSOLVE IN COMMON SOLVENT.
2. CO-PRECIPITATE INTO A NON-SOLVENT WHICH IS MISCIBLE WITH THE SOLVENT



3. FILTER AND DRY FINE POLYMER POWDER IN VACUUM OVEN FOR 48 HOURS AT 100° C.

The remaining iPS is then placed in a vacuum oven and dried for 48 hours at 100°C. After this period, the iPS is suitable for blending with PPO or with HH 101. The procedure is similar to the dissolution in toluene and reprecipitation into methanol described in the previous paragraph except that a somewhat more dilute toluene solution (~2g/100 ml) was coprecipitated into methanol.

The composition of the material prepared for subsequent studies was varied in increments of 25 percent by weight from 0 percent to 100 percent. The following two component blends were prepared:

1. PPO - aPS where aPS includes the whole series of NMWD aPS listed in Table 3.1.
2. PPO - HH 101.
3. PPO - iPS.
4. PPO - α -PS.
5. HH 101 - α -PS.
6. HH 101 - iPS.

The final blend compositions obtained by the coprecipitation into methanol are slightly different than the starting weight percentages due to some losses during the blending and precipitation procedure. Possibly some of the low molecular weight tail of a dissolved homopolymer will not be recovered upon precipitation. Typically when dissolving 10g of PS (aPS or iPS), 9.8 grams will be recovered. Starting with 10g of PPO, 9.2g will be recovered upon precipitation. These

losses are not severe since they alter the final composition by 1.5 percent at the most. The usual shift is about one percent. In the case of α -PS, a correction has to be made in the calculation of the final composition. Starting with 10g of α -PS dissolved in toluene, only 5.7g will be recovered upon precipitation into methanol. In the case of as-received iPS, 2 grams of atactic material are extracted from 10g starting material by treatment in boiling MEK. This purified iPS, when dissolved in toluene and reprecipitated into methanol will suffer a loss of 0.2g out of 10g starting material. How these losses affect the final composition is tabulated in the next chapter.

Finally, since the densities of PPO and PS (aPS and iPS) are very close (1.07g cm^{-3} and 1.05g cm^{-3} , respectively) the weight percent composition never deviates from volume percent by more than 0.67 percent. Again, some of these differences will be tabulated in the next chapter.

III.B. INJECTION MOLDING OF TENSILE SPECIMEN

The vacuum dried blend and pure component polymer precipitates were next prepared for injection molding by compacting them into irregular films in small aluminum foil packets at approximately 100°C and 10,000 psi for a very brief period of time. These polymer containing packets were immediately removed from the press and quenched in cold water. The aluminum foil was then stripped off and the thin

films were cut into small squares suitable for charging an injection molder.

The injection molder is a Mini-Max Molder designed by Bryce Maxwell, manufactured by Custom Scientific Instruments, Inc. and modified for high temperature operation at the University of Massachusetts. Its description and operation can be found in the recent literature [21]; however, for optimum performance, the described operating procedure is somewhat modified.

The injection molding machine is schematically depicted in Figure 4 of reference [2]. It operates as follows: the mixing cup and mold (in place below the cup) are preheated to approximately 20°C above the injection temperature to accommodate the typical drop in temperature from heat losses to the rotor which occur during mixing and melting in the stator (mixing cup). The cup is heated via an electrical resistance 180 watt band heater, while the mold is heated via a retaining C-clamp containing two electrical resistance cylindrical heaters. Next, a pre-weighed charge of polymer, typically 0.3g, is placed in the cup. The charge consists of cut pieces from a compression molded film. The rotor is then lowered into the cup and rotation is started. The rotor is then raised and lowered via a lever attached to a rack and pinion gear until the polymer is fully in the melt state and ready for injection. This should take no longer than ten seconds. When the

charge is ready for injection, the rotor is slightly raised, the valve opened, and the melt injected into the mold cavity by pushing down on the lever while the rotor is turning. The mold is then removed and air cooled on an insulated block to ensure uniform cooling. Typically it takes five minutes to cool from the injection temperature to the T_g of the polymer. Excess material in the cup is extruded and the valve closed in preparation of the next cycle. During preparation for the next cycle, the mixing cup and rotor were thoroughly cleaned by extruding HH 101 through the mixing cup and then removing any residual polymer with an Exacto knife, copper wire, and curved forceps with serrated jaws.

The mold cavity is for a miniature tensile test specimen of approximately $3/4$ inch in total length, $1/16$ inch in diameter by $5/16$ inch long section. More accurate values were obtained through the use of a traveling microscope and micrometer. The molded test specimen (dumbbell) had a gauge length of 0.89 cm and a cross-section diameter of 0.157 cm^2 (giving a cross-sectional area of 0.0195 cm^2).

The processing temperatures were generally from 110 to 150°C greater than the T_g of the blended or unblended polymers and are listed in Table 3.2. Care was taken to ensure that the mold and mixing cup temperatures were nearly identical.

TABLE 3.2

Summary of Injection Molding Temperatures (T°C)

Polymer Temperature	100% HH 101 250	25% PPO 275	50% PPO 300	75% PPO 325	100% PPO 300
	100% aPS-4000 too brittle	25% PPO 225	50% PPO 290	75% PPO 325	
	100% aPS-10000 200	25% PPO 225	50% PPO 290	75% PPO 325	
	100% aPS 37000 200	25% PPO 250	50% PPO 290	75% PPO 325	
	100% aPS-110000 250	25% PPO 275	50% PPO 300	75% PPO 325	
	100% aPS-233000 260	25% PPO 275	50% PPO 300	75% PPO 325	
	100% aPS-670000 260	25% PPO 275	50% PPO 300	75% PPO 325	
	100% aPS-2000000 270	25% PPO 280	50% PPO 300	75% PPO 325	
	100% iPS 300	25% PPO 300	50% PPO 310	75% PPO 325	
	100% α -PS 270	35% PPO 275	61.7% PPO 300	75% PPO 325	
	100% α -PS 270	36.4% HH101 270	63.2% HH101 270	83.8% HH101 270	
	100% iPS 300	25% HH101 300	50% HH101 300	75% HH101 300	

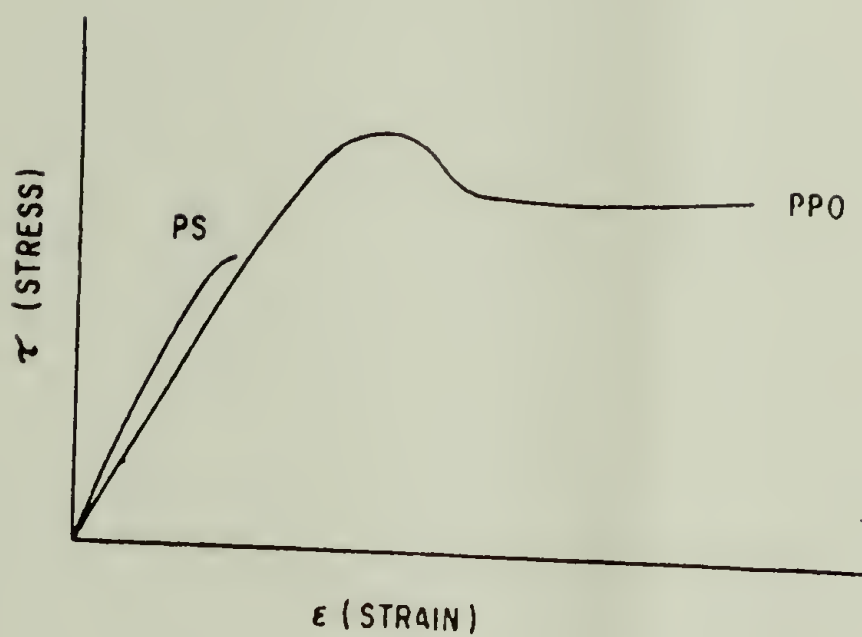
III.C. TENSILE TESTING - TECHNIQUE, CORRECTIONS, AND DATA AND ERROR ANALYSIS

The tensile specimen were tested on a Tensilon/UTM-II mechanical tester manufactured by the Toyo Baldwin Company, Ltd. at a constant crosshead speed of 0.2 mm min^{-1} at room temperature. Based on a sample gauge length of 8.9 mm, this crosshead speed yields an initial strain rate of $3.75 \times 10^{-4} \text{ sec}^{-1}$. For most cases, a 20 kg load cell was used, although in some cases a 5 kg load cell was also used. The load deformation curve was recorded on a SS-105D-B-UTM manufactured by Toyo Measuring Instruments Company, Ltd. at a chart speed of 200 mm min^{-1} . Typical load deformation curves for PS and PPO are depicted schematically in Figure 3.2.

Modulus, tensile strength at break (or yield) and elongation at break (or yield) were calculated from the recorded force deformation curves according to the equations presented in Chapter II, Section A. To ensure accuracy, since in the determination of Young's modulus it is difficult to know when the initial straight line portion of the stress-strain ends and curvature begins, Young's modulus was arbitrarily defined as the ratio of stress over strain at 100 percent pen deflection at recorder range 1. This corresponds to a 4 kg load or approximates the secant modulus at 0.6 percent elongation. Another way of explaining the above situation is that characteristic non-linearity in

FIGURE 3.2

SCHEMATIC OF STRESS-STRAIN CURVE



MODULUS

TENSILE STRENGTH AT BREAK

TENSILE STRENGTH AT YIELD

ELONGATION AT BREAK

ELONGATION AT YIELD

the force-extension curves of polymers makes it impossible to define a unique modulus from the slope, as one is able for inorganic solids [3]; hence, to insure accuracy one resorts to a more accessible manner in calculating the modulus, such as the one just described. Tensile strength at break and yield were calculated from the height of the pen deflection and knowledge of the cross-sectional area. Elongations were calculated from knowledge of chart speed, crosshead speed, and sample gauge length. Since all elongations measured were considerably under 10 percent, the engineering strain was used, since use of the true strain would contribute to a negligible increase in accuracy.

While the tensile strength at break or yield could essentially be calculated directly from the recording paper, this is not really the case for the modulus and the strain. That is the actual strain differs from the measured strain due to instrumental compliance and a clamping effect. The instrumental compliance was accounted for by running a force-extension experiment without a tensile specimen, but with the crosshead attached directly to the load cell. In theory, one should obtain a force-elongation line having infinite slope. In practice, due to the "softness" of the load cell one obtains a force-extension curve for the instrument as depicted for a 5 kg and 20 kg load cell in Figures 3.3 and 3.4 respectively. Figure 3.5 is identical to 3.4 except that the recorder was on 4 kg full scale rather than 20 kg full

FIGURE 3.3

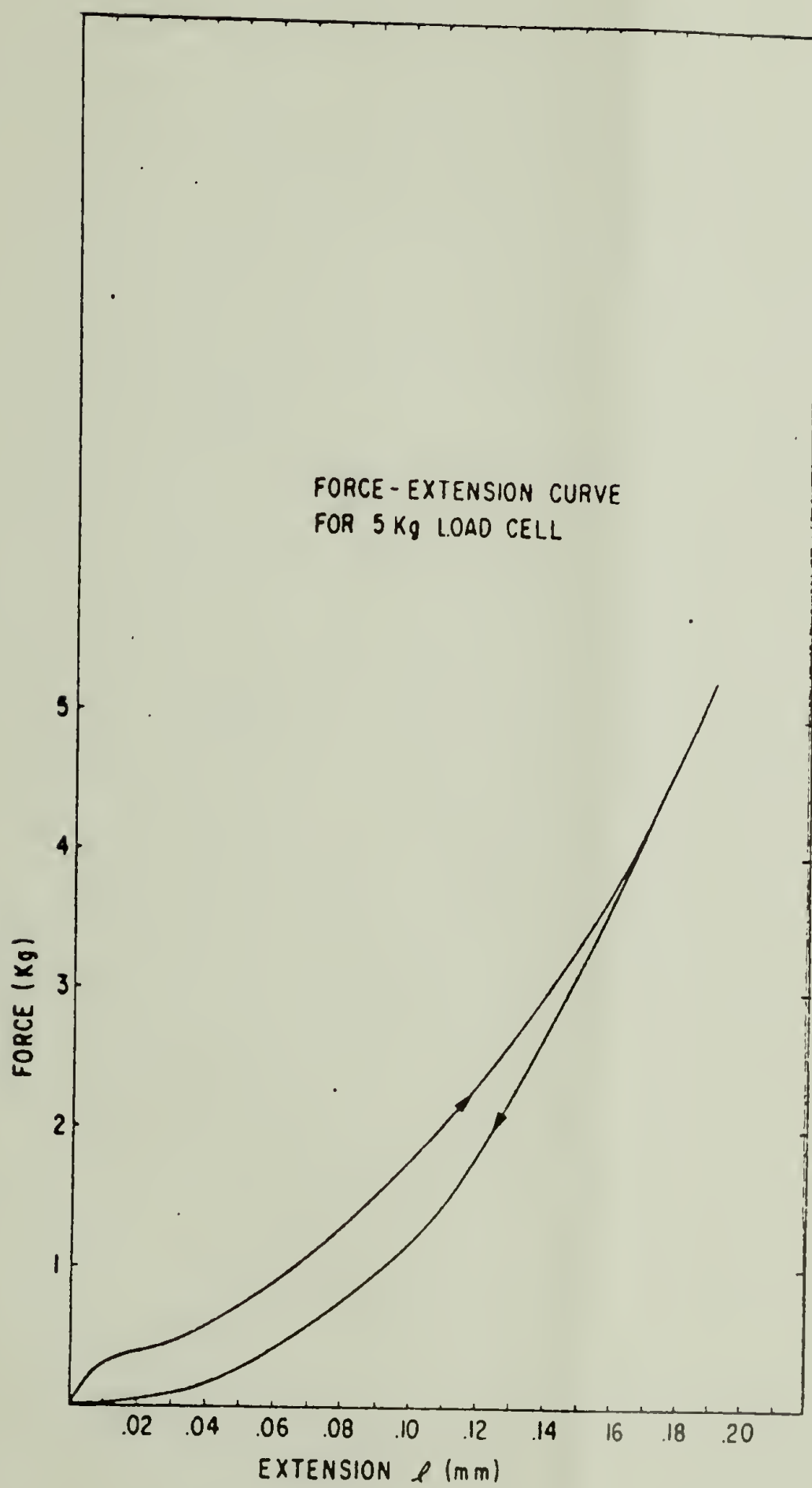


FIGURE 3.4

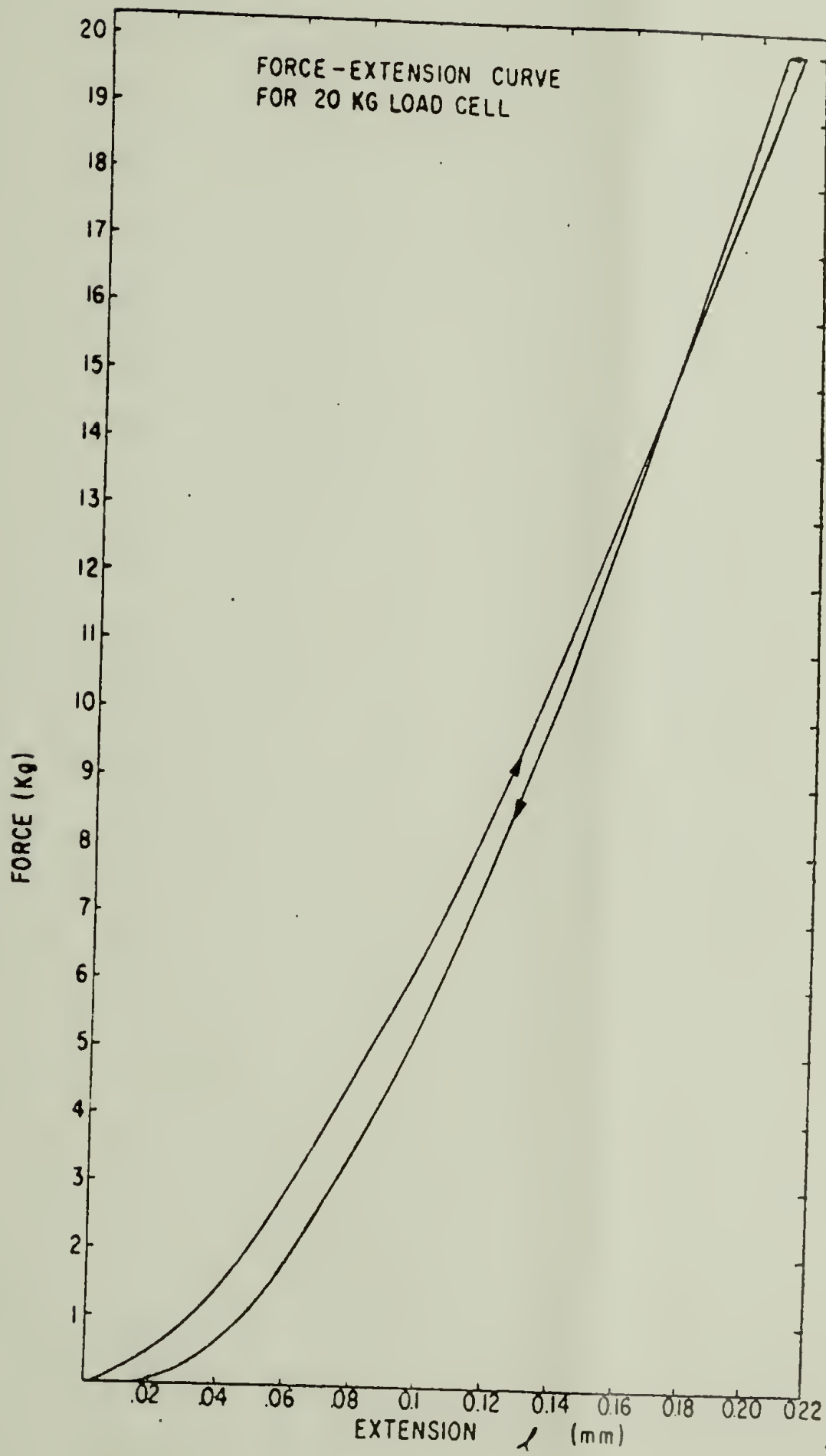
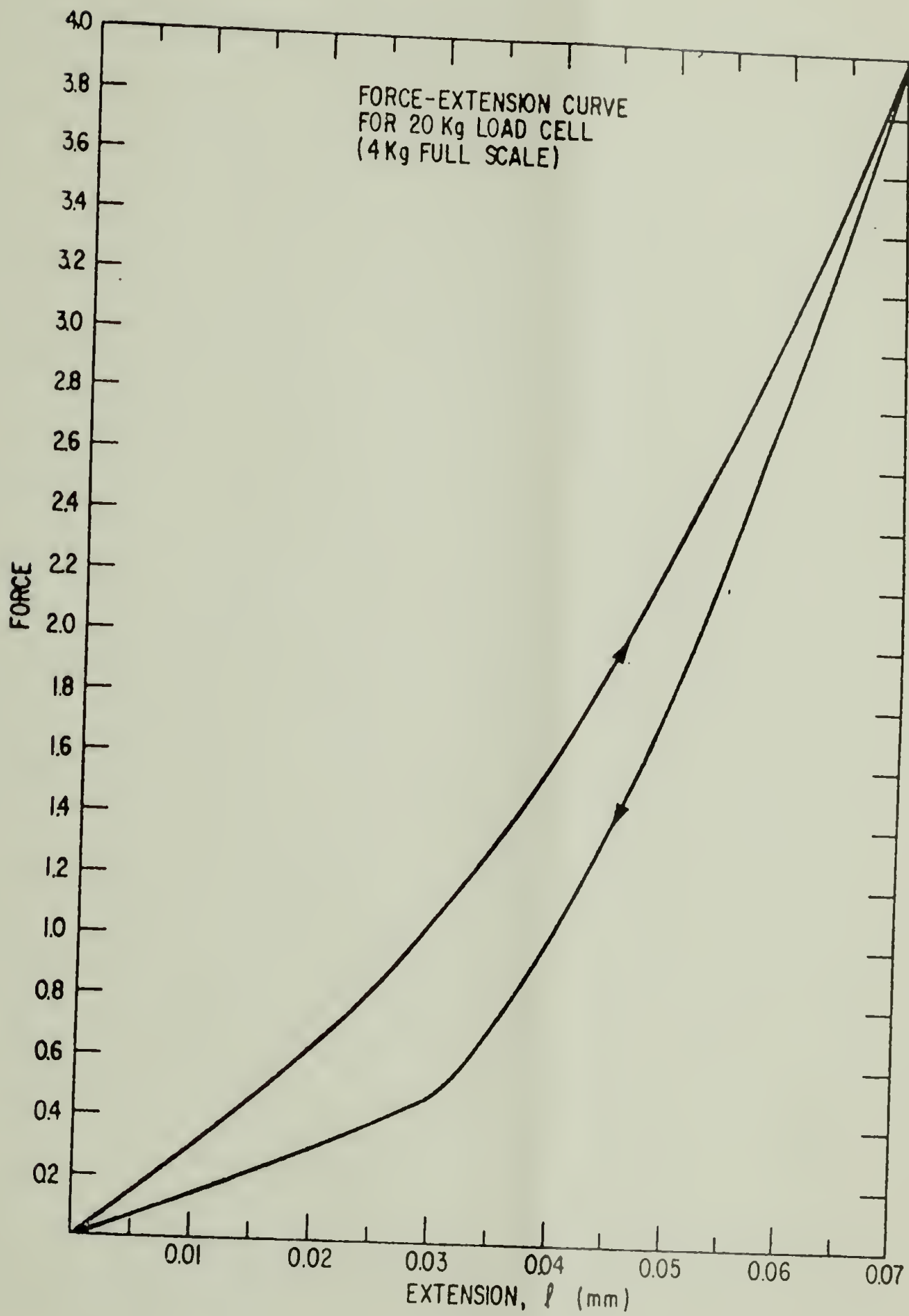


FIGURE 3.5



scale. In Figures 3.3 to 3.5 one observes a hysteresis indicated by arrowheads on the curves. The curve with the upward-oriented arrow (extension curve) represents the load-extension calibration with the crosshead moving away from the load cell. At the maximum rated load for a particular range for the load cell, the crosshead is momentarily stopped and then movement of the crosshead is reversed toward the load cell until the no-load condition is reached. This procedure is represented by the force-extension curve (recovery curve) with the downward-oriented arrow. These curves are remarkably reproducible to ± 0.005 mm or better for three independent calibrations. Additionally, no stress relaxation was encountered in these calibrations, i.e., crosshead movement could be stopped for a period of time during calibration without a noticeable decrease in force being registered by the recorder.

After the instrumental "softness" force-extension calibration curve was obtained (no-specimen run), the force-extension curve for a tensile specimen was obtained. This was a completely uncorrected force-extension curve and so will be given the designation "measured". Next, at any given force, F , the calibrated instrumental extension Δl_i , was subtracted from the measured extension, Δl_m , yielding a compliance-corrected force-extension relationship, $F(\Delta l_m - \Delta l_i)$. From knowledge of the gauge length and cross-sectional area of the tensile specimen (8.9 mm and 0.0195 cm^2 respectively), the

modulus was calculated, based upon the compliance-corrected force-extension relationship. The tensile experiment was then repeated for a specimen of identical cross-section, but longer gauge length (12.8 mm) again yielding a completely uncorrected force-extension curve. Again, at any given force, the instrumental extension was subtracted from the measured extension and a modulus calculated from the corrected relationship. Finally, the so-calculated moduli ($E_{8.9}$ and $E_{12.8}$, where the subscripts refer to the gauge length) were plotted against reciprocal gauge length. A straight line was drawn through these points and a new modulus was determined by extrapolation to infinite gauge length. This extrapolation corrects the strain for any clamping or jaw effects and is based on the assumptions that such effects are independent of sample length and that correction becomes negligible for a specimen with an infinitely long gauge length. In general, without the aid of an extensometer, instrumental and clamp corrections have to be made for short stiff specimens as there are three contributions to the strain, all of similar magnitude, during a tensile test: the sample strain, ϵ_s ; the instrumental or machine strain, ϵ_i ; and the clamping strain, ϵ_c . Without taking these into account, there will be a serious error in modulus and strain at low elongation. For example, out of a total measured extension at break of 0.50 mm for HH 101 PS with an initial gauge length of 8.9 mm, 0.14 mm is due to the instrument,

0.21 due to the clamp, and 0.15 due to the specimen. The elongation at break for PS is therefore $(0.15/8.9)(100) = 1.69$ percent and not $(0.50/8.9)(100) = 5.62$ percent, which would have been calculated without corrections.

Tensile measurements for a particular molecular weight and blend composition were repeated as often as possible in order to do statistical error analysis. The primary constraints on the number of repetitions was quantity of polymer and time. Quantity of polymer usually allowed for the fabrication of at least 20 0.2g tensile specimens, although in some cases less was available.

Reference was made to two standards texts [4,5] to aid in the error analysis. For any series of tensile measurements, the standard deviation, σ_s , was first calculated via

$$\sigma_s = \left(\frac{\sum_{i=1}^N (\chi_i - \bar{\chi})^2}{N-1} \right)^{1/2} \quad (86)$$

where χ_i represents the i^{th} measurement, $\bar{\chi}$ the mean of a series of measurements, and N the measurement population. The standard deviation applies to a population of values and assesses their variability; i.e., how widely dispersed the values are from the mean. In most cases it provides the most reliable estimate of the error involved in a single measurement taken from a population of similar measurements.

The standard error was next calculated according to

$$s_m = \frac{\sigma_s}{\sqrt{N}} . \quad (87)$$

The standard error is the standard deviation of a hypothetical population and represents the standard deviation of the mean of N equally reliable measurements taken from an infinite population.

Unfortunately, it is usually impractical to make enough measurements for the sample size to even approach the size of a population. Therefore, one must be content to take only enough measurements to calculate \bar{x} instead of μ , the so-called true mean or the mean of an infinite number of equally reliable measurements. Statistical theory may then be used to predict within what limits the sample mean, \bar{x} , is likely to agree with μ , the true mean.

The theory will not enable this prediction to be made with 100 percent probability. There is always some fraction of risk involved in a prediction. The limits predicted for a certain probability are called confidence limits. These limits depend upon the t or "Student's t " distribution curve.

The confidence limits for \bar{x} are reported as follows:

$$\bar{x} \pm \frac{t \sigma_s}{\sqrt{N}} \quad (88)$$

Thus, for example, if we have ten equally reliable measured values of tensile modulus whose \bar{x} is 3.1 GPa (gigapascals) and whose σ_s is 0.17, confidence limits can be obtained from a

standard statistics book. For ten measurements, $t = 2.262$ at the 95 percent confidence level. Then $\bar{\chi}$ should be reported as:

$$\bar{\chi} = 3.1 \pm \frac{(0.17)(2.262)}{\sqrt{10}} \quad (89)$$

or

$$\bar{\chi} = 3.1 \pm 0.1 \text{ GPa.} \quad (90)$$

If the ten measured values were truly equally reliable, then there would only be a five percent risk that the μ of the modulus is greater than 3.2 or less than 3.0. All tensile measurements in this work are reported with error bars indicating values of t calculated with 95 percent confidence.

In order to obtain truly reliable tensile measurements, it is important to standardize the tests since mechanical properties are very dependent upon molecular weight, rate of testing, temperature, method of sample preparation, size and shape of specimens, and the conditioning of samples before testing. All tests were run in identical fashion throughout this work. The only variables were molecular weight and composition; otherwise, all tests were run at the same rate of testing and temperature. Additionally, only samples of the same size, in particular, cross-sectional diameter were tested. After cooling from the mold, all specimens were conditioned for 24 hours at room temperature. Finally, the method of testing was identical for all specimens in that

sample orientation and initial tension was kept the same just prior to starting the test. Some initial tension (≈ 1.7 MPa) was given to each specimen prior to testing in order to avoid backlash.

III.D. DIFFERENTIAL SCANNING CALORIMETRY

A Perkin-Elmer DSC II was used to study the glass transitions of some of the blends and blend components. It was also used to ascertain whether or not the iPS and iPS-based blends were crystalline. However, before running experimental thermograms, temperature calibration DSC thermograms were obtained using Indium and Tin as standards. Indium was also used as a calibration standard for the heat of fusion determinations.

For all experimental glass transition and heat of fusion determinations, 10-20 mg of polymer sample (as measured by a Perkin-Elmer AD-2 Autobalance with a precision of 0.01 mg) were placed into aluminum DSC pans and sealed. A heating rate of $20^{\circ}\text{C}\text{-min}^{-1}$ and a range of $5\text{ mcal}\text{-sec}^{-1}$ was used for each sample, while chart recorder settings (Perkins-Elmer model 56 recorder) were 10 mV for the sensitivity of the recording pen and $20\text{ mm}\text{-min}^{-1}$ for the chart speed. Typically, samples were heated from 330 to 530°K under a nitrogen purge.

The glass transitions in a DSC thermogram are observed as a step change in the baseline. The transition temperature was defined as that temperature at which the change in heat capacity is one-half its maximum value. Reproducibility was

usually $\pm 1^\circ\text{C}$ and sometimes $\pm 2^\circ\text{C}$. The heat of fusion of a sample was calculated from the following equation [6]:

$$\Delta H_{\text{sam}} = (\Delta H_{\text{ind}}) \left(\frac{W_{\text{ind}}}{W_{\text{sam}}} \right) \left(\frac{A_{\text{sam}}}{A_{\text{ind}}} \right) \left(\frac{R_{\text{sam}}}{R_{\text{ind}}} \right) \left(\frac{S_{\text{ind}}}{S_{\text{sam}}} \right) \quad (91)$$

where ΔH_{ind} is the heat of fusion of indium and ΔH_{sam} is the heat of fusion of the sample. W , A , R , and S represent weights, areas under peaks, ranges and chart speeds respectively. The degree of crystallinity was then calculated via:

$$\frac{\Delta H_{\text{sam}}}{\Delta H_{\text{pc}}} \quad (92)$$

where ΔH_{pc} is the heat of fusion in the pure crystalline (100% crystalline) state. For iPS, 20 cal-g^{-1} was used for ΔH_{pc} [7].

III.E. GEL PERMEATION CHROMATOGRAPHY

A Waters Associates Model 200 Gel Permeation Chromatograph was used to determine chromatographs of two different 0.0270g samples of HH 101 PS. One sample was taken from an as-received pellet, while the other was cut from an extrusion obtained from the Mini-Max Molder (see Section III.B.). The two GPC chromatographs were entirely superposable indicating that molecular weights and molecular weight distributions were essentially identical and that no detectable polymer degradation had occurred.

III.F. ^{13}C NMR OF PPO AND i-PS

Natural abundance ^{13}C nuclear magnetic resonance was used to probe the microstructure of PPO and iPS. In both cases a Brücker HFX-90 spectrometer at 22.63 Mhz was used. Field/frequency control (lock) was effected by means of a solvent deuterium resonance (deuterated acetone).

In the case of PPO, 0.3g was dissolved in one ml. chloroform. The NMR spectral data was obtained (courtesy of Mr. F. Cummings) in ppm at 41.5°C, downfield from an internal tetramethylsilane (TMS) standard. The assignments of all carbons in the PPO molecule was quite straightforward with the aid of a recent reference [8], i.e., all major peaks in the spectrum were accounted for. However, there were some extremely minor peaks that could not be given a definitive assignment. These minor peaks could be an indication of very mild chain branching, probably at the open position on the main chain [8,9]. Overall, however, the spectrum of PPO suggests that the molecule is essentially linear.

In the case of iPS, a ^{13}C NMR spectrum was obtained at 93°C from a 33 percent solution in chlorobenzene. The iPS had been purified in MEK and the objective was to ascertain whether this treatment (described in more detail in Section III.A.) resulted in essentially 100 percent isotactic PS. Within the accuracy of the instrument, the iPS was judged to be nearly 100 percent isotactic when given the described

treatment in MEK. All judgments in this study were qualitative rather than quantitative because of the Nuclear Overhauser Effect [8].

III.G. WIDE ANGLE X-RAY MEASUREMENTS

WAXS measurements were performed with a Phillips-Norelco wide angle goniometer on as-received iPS and iPS that had been treated with MEK as described in Section III.A. In both cases, the specimens were annealed at 170°C for 26 hours in a vacuum oven. These conditions were chosen in order to obtain the highest degree of crystallinity possible for iPS [10].

The degree of crystallinity was obtained (courtesy of R. Hammel) by measuring the total area under the scattering curve and the areas under the crystalline peaks. From these areas (measured between $2\theta = 7^\circ$ and $2\theta = 30^\circ$) the degrees of crystallinity were calculated using the following relationship:

$$X_{cr} = \frac{A_{cr}}{A_{amor} + A_{cr}} = \frac{A_{cr}}{A_{total}} \quad (93)$$

The as-received iPS had a maximum degree of crystallinity of 22.8 percent, while the MEK extracted iPS had a maximum degree of crystallinity of 32.1 percent, again verifying the importance of the MEK treatment.

III.H. POLYMER DEGRADATION

Polymer degradation due to the injection molding process, described in Section III.B., was investigated. Previously tested tensile specimens were cut, weighed, and injection molded into new tensile specimens. No detectable differences in the tensile properties were observed between the previously tested tensile specimens and the regrind, indicating that degradation was not severe enough to affect mechanical properties.

III.I. SCANNING ELECTRON MICROSCOPY

Scanning electron micrographs were taken (utilizing an ETEC U-I SEM) of fracture surfaces of two tensile specimens, in particular of HH 101 aPS and iPS (annealed at 170°C for 24 hours). The two samples were fractured at room temperature by the Tensilon/UTM-II mechanical tester and then the fracture surfaces were coated with gold. Polaroid film type 57 was used for the capturing of images of the fracture surfaces at magnifications of 56X, 560X, and 5600X. The HH 101 fracture surface, although smooth in texture, revealed considerable localized plastic deformation, while the iPS fracture surface was relatively featureless, somewhat rougher in texture, and revealed little localized plastic deformation.

III.J. DETERMINATION OF ORIENTATION

The qualitative technique introduced in Chapter II, Section I was used in determining the surface orientation of an injection molded HH 101 tensile specimen. The conditions

for the injection molding are described in Section B of this Chapter, while the processing temperature can be found in Table 3.2. It is important to recall that it took approximately five minutes for the specimen to cool from the processing temperature to its glass transition of 105°C (air quench at room temperature).

After fabrication of the specimen (dumbbell) and a room temperature aging of 24 hours, the specimen was soaked in warm methanol for 24 hours. After this treatment, the specimen was immersed in n-hexane at room temperature. After a short period of time crazes were induced on the surface of the dumbbell. The sample was then removed and air dried and finally observed under a microscope at 20X. The induced surface crazes exhibited random orientation. This experiment was then repeated for an injection molded specimen that was quenched into an ice bath immediately after injection. Again crazes were induced in the prescribed fashion; however, most of these crazes were observed to be oriented parallel to the injection direction. These experiments indicate that the thin section of the air-cooled tensile specimen essentially exhibited no orientation, while the ice-water quenched specimen exhibited considerable orientation.

REFERENCES

1. H. Endo, T. Fujimoto, and M. Nagasawa, J. Polym. Sci., A-2, 7, 1669 (1969).
2. B. Maxwell, SPE J., 28(2), 24 (1972).
3. H. H. Kausch, J. A. Hassell, and R. I. Jaffee, eds., "Deformation and Fracture of High Polymers," Battelle Institute Material Science Colloquia, Plenum Press, New York, 1973.
4. A. J. Lyon, "Dealing with Data," Pergamon Press, New York, 1970.
5. D. A. Skoog and D. M. West, "Fundamentals of Analytical Chemistry," Holt, Rinehart, and Winston, Inc., New York, 1966.
6. Perkin-Elmer DSC-II Operating Manual.
7. R. A. Neira, PhD Dissertation, University of Massachusetts, 1974.
8. D. M. White, Polymer Preprints, 13(1), 373 (1972).
9. J. C. W. Chien, private communication.
10. S. L. Aggarwal and G. P. Tilly, J. Polym. Sci., 18, 17 (1955).

CHAPTER IV

RESULTS AND THEIR DISCUSSION

IV.A. INFORMATION REGARDING SI UNITS

The tensile data in this chapter is presented in accordance with "The International System of Units (SI)." Therefore, the pascal (Pa) is the dimension given for the modulus and tensile strength. A pascal is a pressure or stress quantity equivalent to 1 Newton per square meter (N/m^2). One pascal is equivalent to 10 dynes/cm^2 or to 1.45×10^{-4} psi. Typically, moduli are given in gigapascals (GPa) and tensile strengths in megapascals (MPa).

IV.B. MODULI OF THE GLASSY HOMOPOLYMERS AND COMPATIBLE POLYMER BLENDS

The tensile modulus was determined for all glassy polymers and compatible polymer blends via the techniques detailed in the previous chapter (see III.C.) and through the use of equation (1). Numerical values for all mechanical measurements are tabulated in the Appendix. The data were subjected to error analysis as explained in Chapter III.C. All tensile tests that revealed fracture at the clamps or that deviated from the mean by more than two standard deviations were discarded. Finally, the numbers found either above or below error bars (95 percent confidence "Student's t" test) indicate the number of measurements used in calculating the mean and analyzing the probable error.

The modulus as a function of composition for PPO-aPS blends is presented in Figures 4.1 through 4.8. In each of these figures the PPO had the same molecular weight and molecular weight distribution while aPS's of progressively higher molecular weights were blended with the PPO (see Table 3.1 of Chapter III). The number after each aPS refers to its molecular weight (either its \bar{M}_n or \bar{M}_w since each aPS has a NMWD) except for HH 101 which is a polydisperse commercial additive-free polystyrene. Its molecular weight is also indicated in Figure 4.6.

Several features of these curves (Figures 4.1 to 4.8) are particularly noteworthy. First, the modulus at each blend composition is higher than that which would be calculated by the simple "rule of mixtures": $E = w_1E_1 + w_2E_2$ or $E = \phi_1E_1 + \phi_2E_2$ ¹, where 1 refers to PS and 2 to PPO while w is the weight fraction and ϕ the volume fraction. The rule of mixtures represents the upper bound in the modulus of a multi-phase system; however, here we have the rare example of a polymer alloy. An enhancement in properties, in this case the modulus, is observed over and above each of the homopolymers. Other examples of glassy polymer alloys are

¹Note that when plotting mechanical properties as a function of composition, the weight fraction is traditionally used; however, when using theoretical modeling equations, particularly as they apply to composites, the volume fraction naturally falls out of the derivation. In this case, weight or volume fraction values can be used interchangeably (as will be shown later in this chapter) with negligible error since the density of each component is nearly identical.

FIGURE 4.1

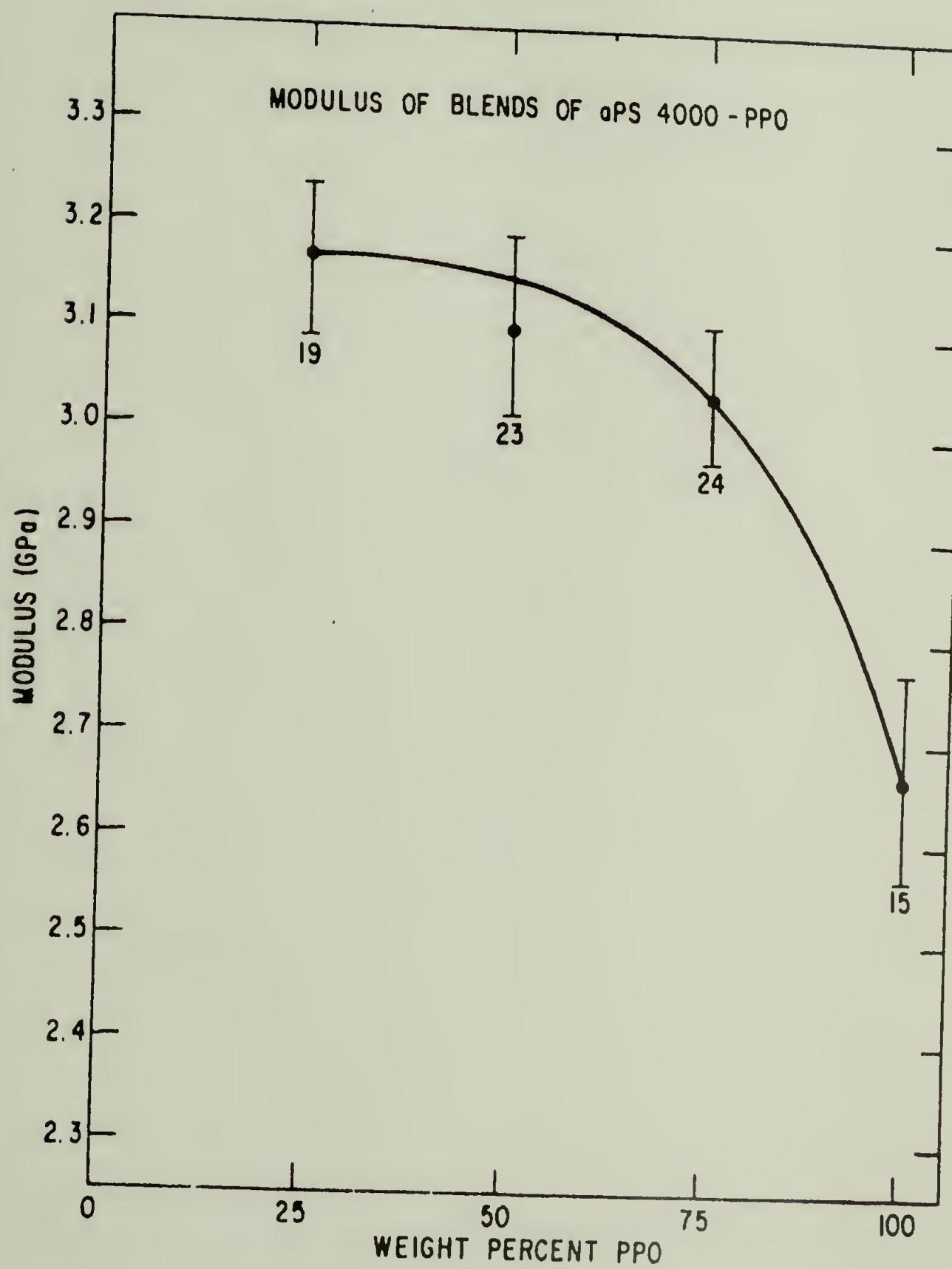


FIGURE 4.2

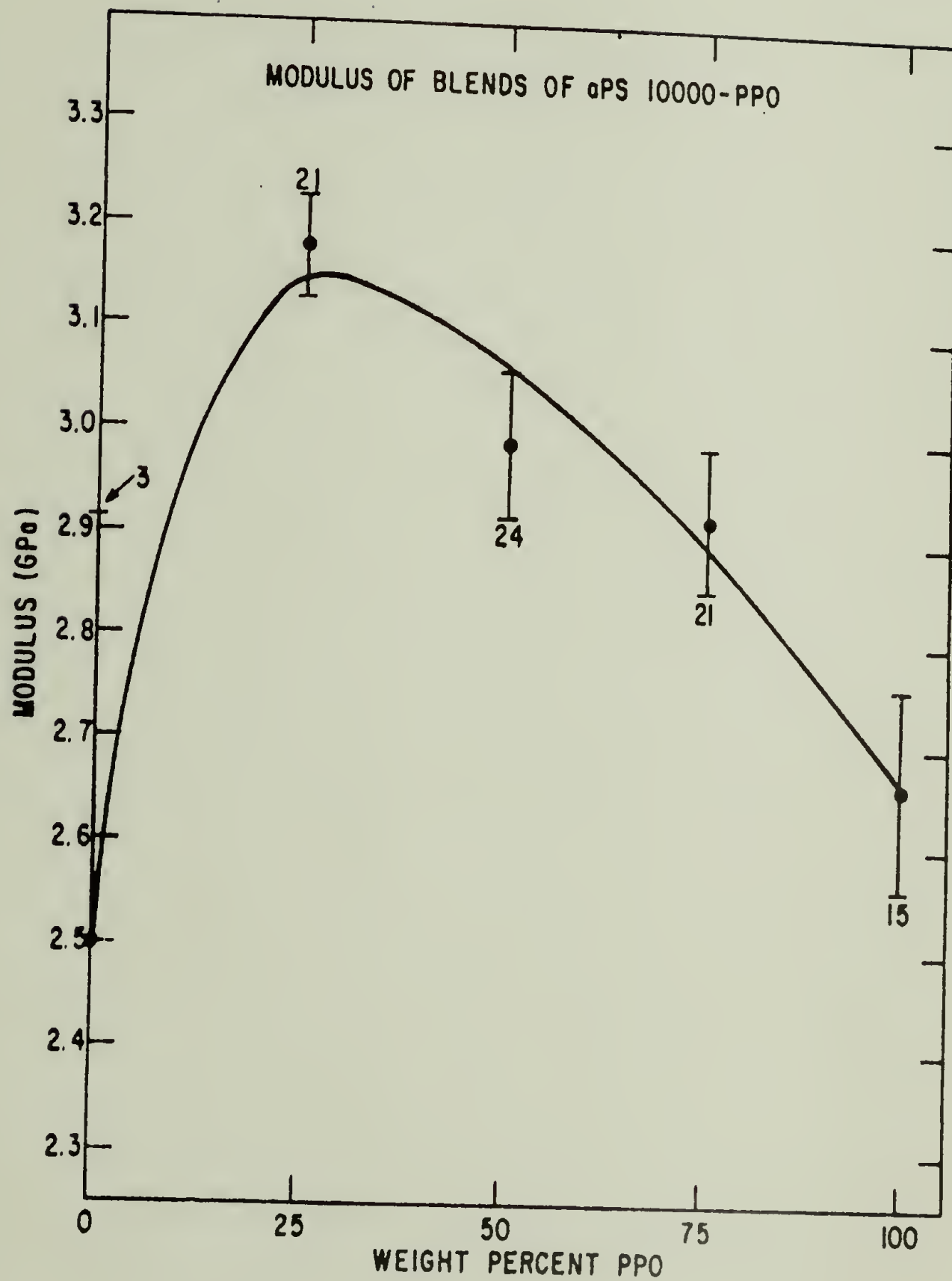


FIGURE 4.3

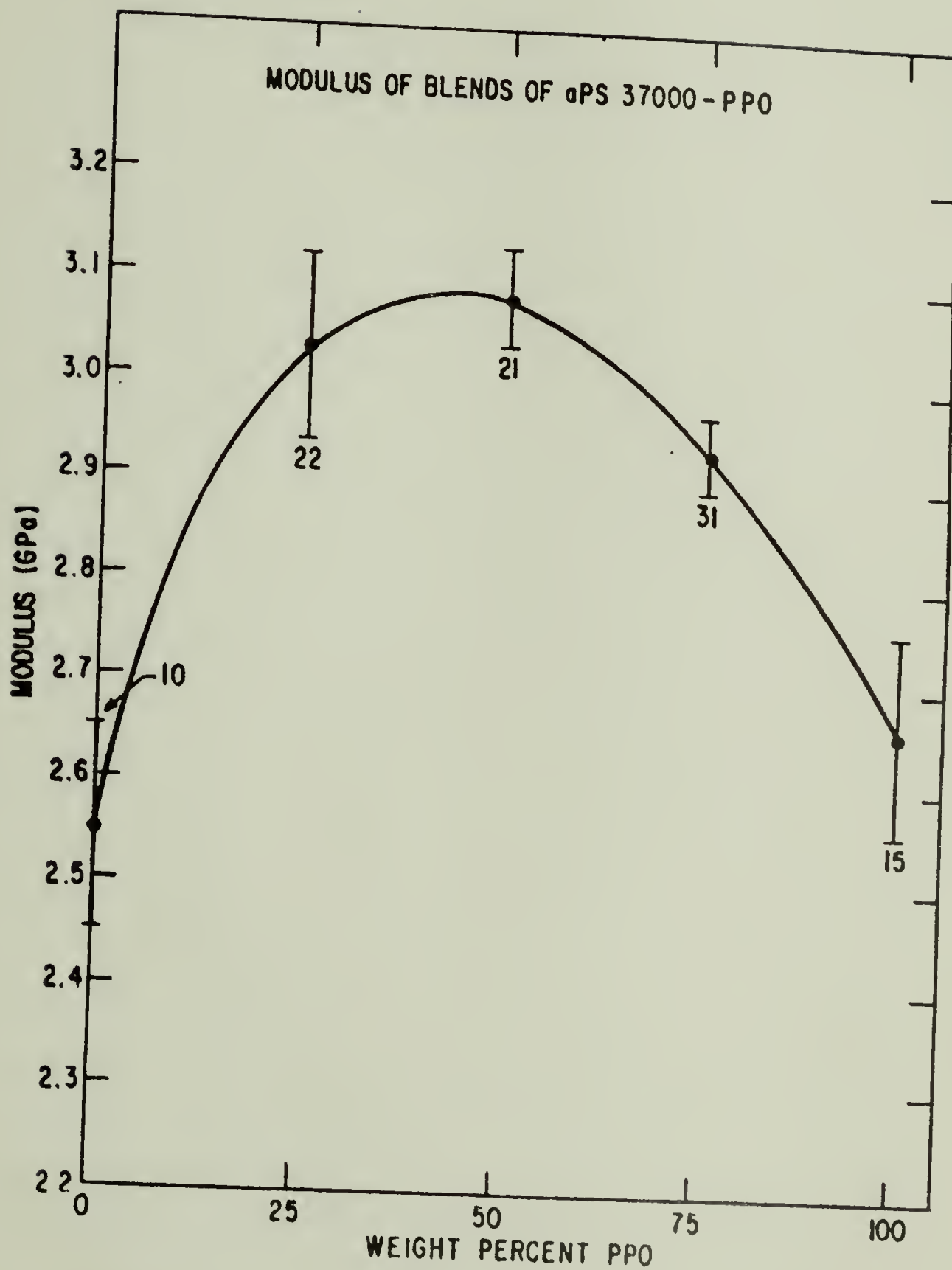


FIGURE 4.4

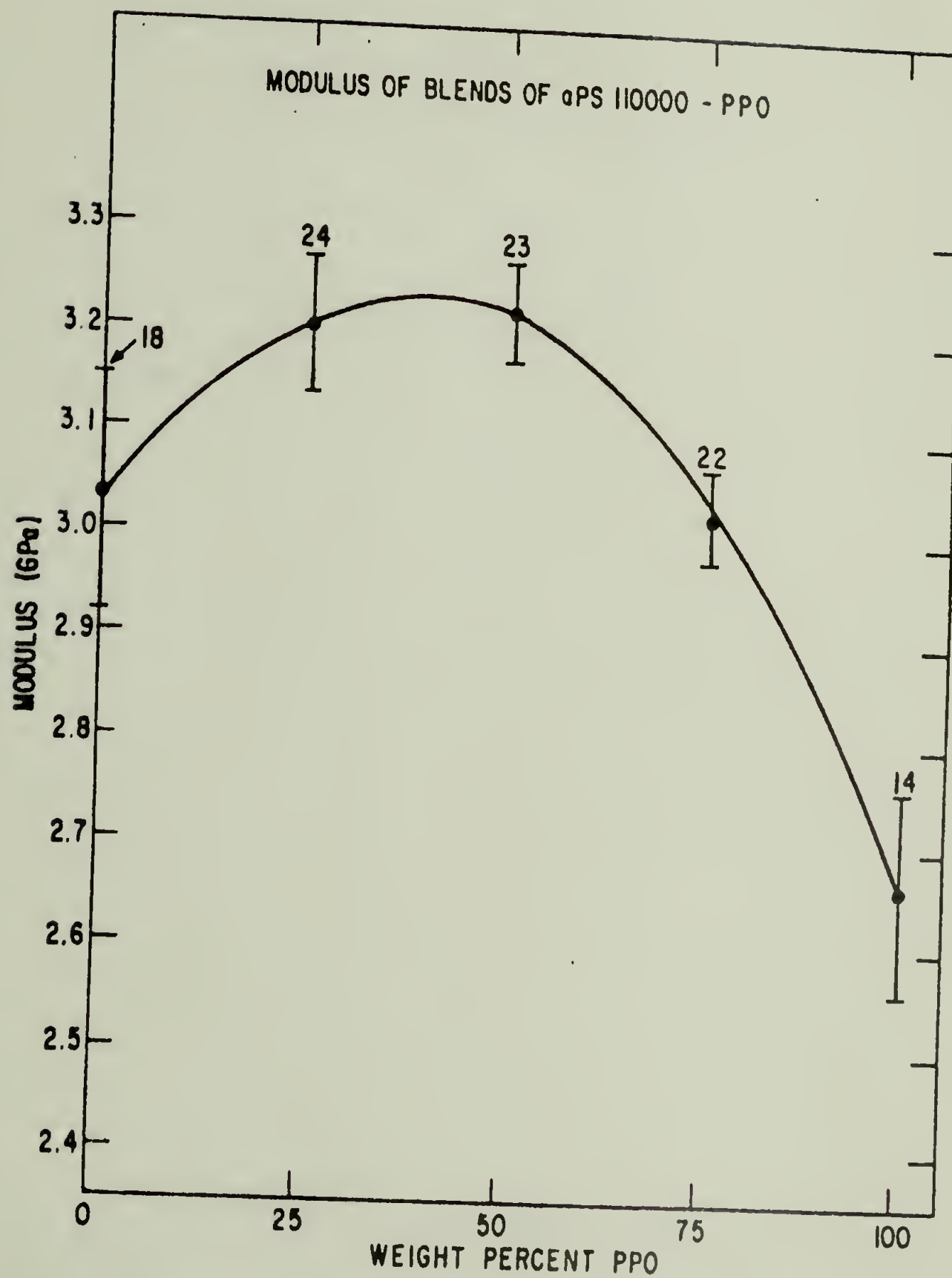


FIGURE 4.5

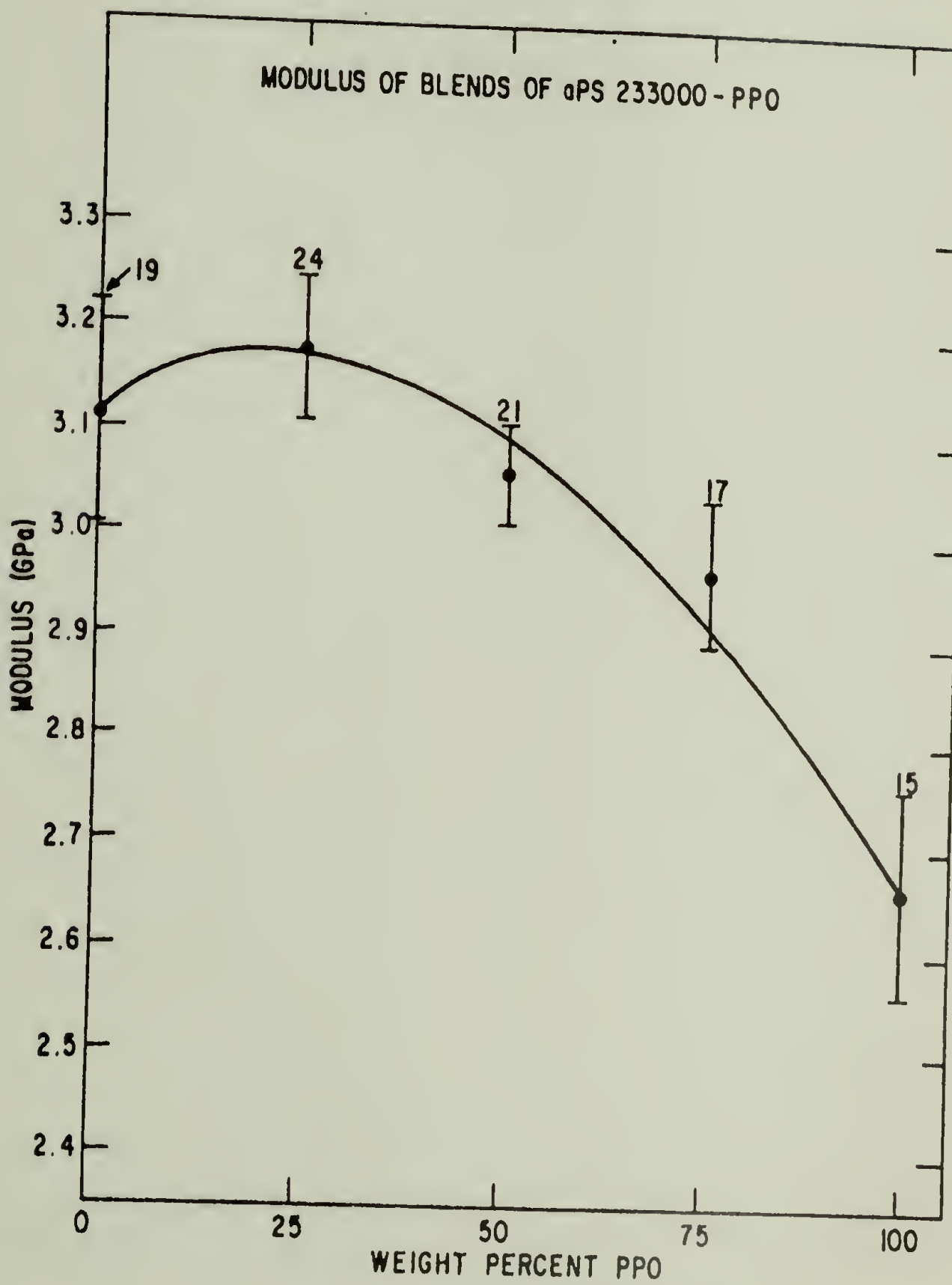


FIGURE 4.6

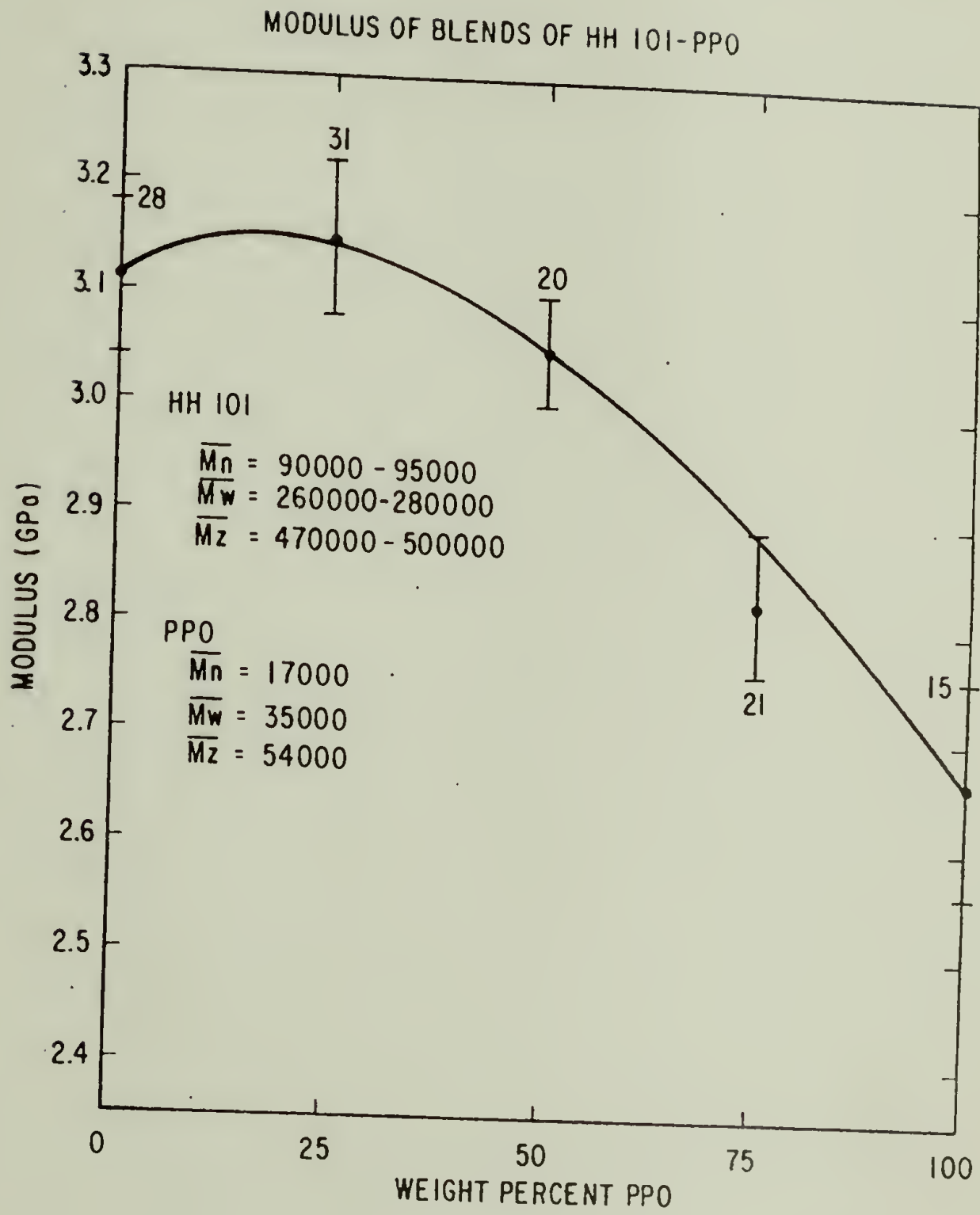


FIGURE 4.7

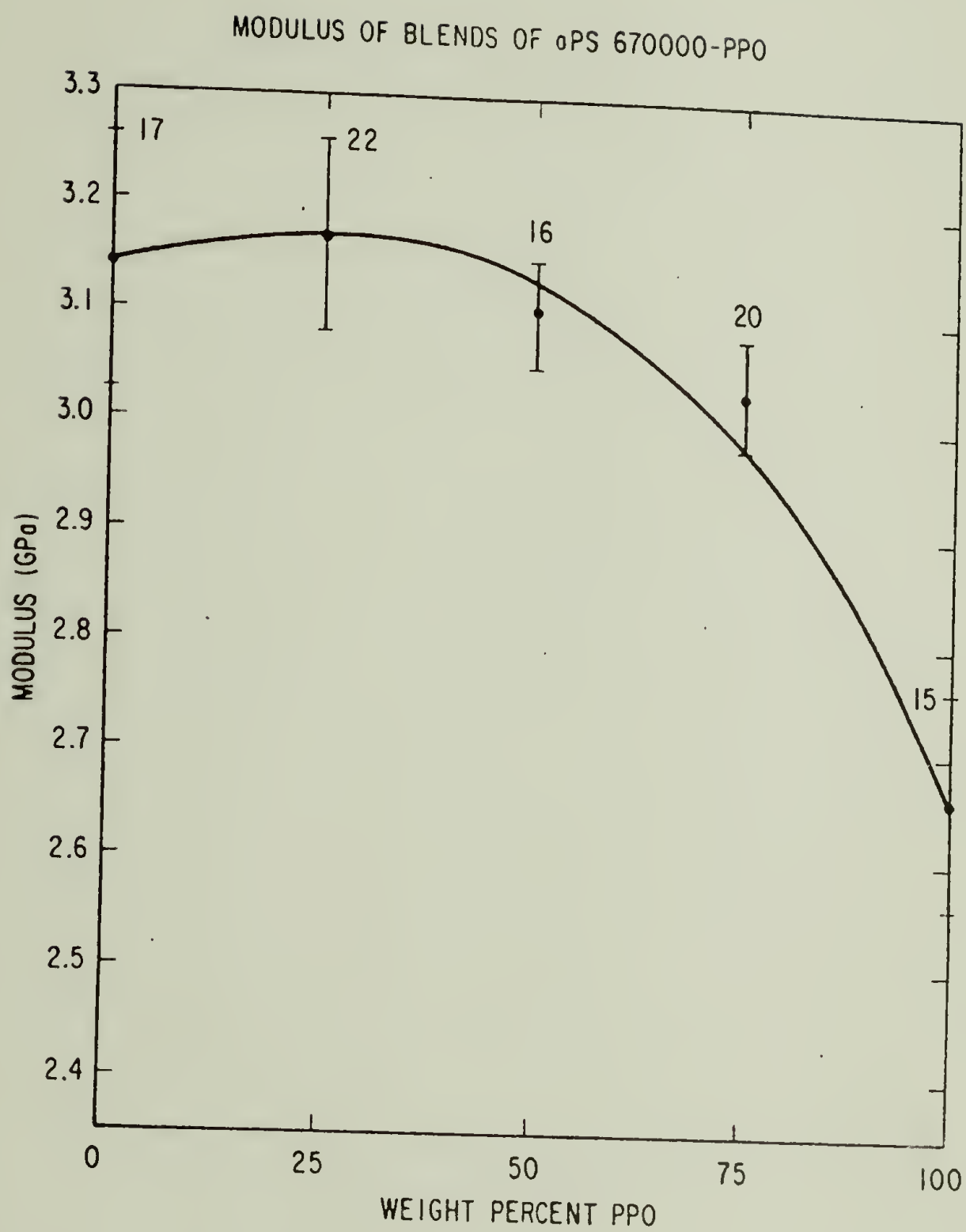
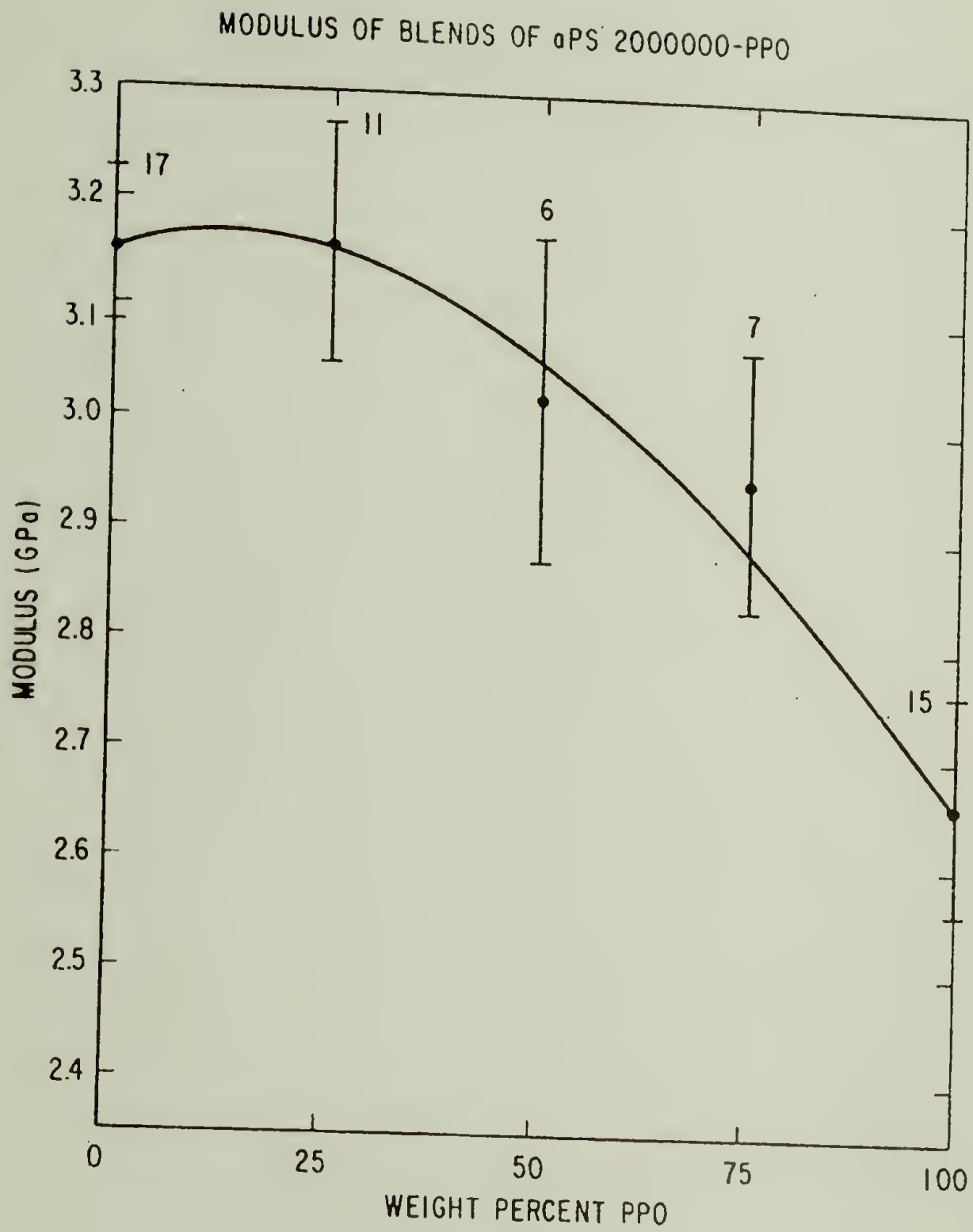


FIGURE 4.8



comparatively rare in the literature. More frequently observed enhancements (greater than that calculated from additivity) are noted upon the addition of "antiplasticizers" to certain polymers such as PC and PVC. However, these effects are usually noted only for low antiplasticizer concentrations of only a few percent and on rare occasions up to 30 percent (see Chapter II.C.). More about the similarities with antiplasticizers will be mentioned later in this chapter. Other enhancements² in the modulus have been observed in some rubbery blends, for example of PVC blended with Butadiene-Acrylonitrile elastomers [1,2] and metallic glassy alloys [3]. In the case of rubbery blends, enhancements are often not found over the entire range of composition as is the case for the glassy PPO-PS blends.

Another noteworthy feature contained in Figures 4.1 through 4.8 is that the enhancement observed in each of the moduli as a function of composition curves becomes less sharp (flattens out) as the \bar{M}_w of aPS in the blend increases. In other words, the excess modulus becomes less as the \bar{M}_w of the PS in the blend increases. The excess modulus can be defined as that portion that deviates from linearity, i.e.,

$$E^E = E_{\text{Blend}} - (\chi_1 E_1 + \chi_2 E_2) \quad (94)$$

²Enhancements need not be observed as absolute maxima in the modulus—composition relationship. They may be just moduli which are higher than those calculated assuming additivity of the components.

where χ is the composition and the subscripts 1 and 2 refer to the property (modulus) of PS and PPO respectively.

A final noteworthy feature is that for any given blend composition, the modulus is more or less independent of molecular weight, except in the case of low molecular weight PS (see Figure 4.9). The low molecular weight polystyrenes were also very difficult to test. In fact, aPS-4000 was too brittle to mold, while aPS 10000 and aPS 37000 were just moldable, hence the error bars are quite a bit larger than for the other homopolymers and blends.

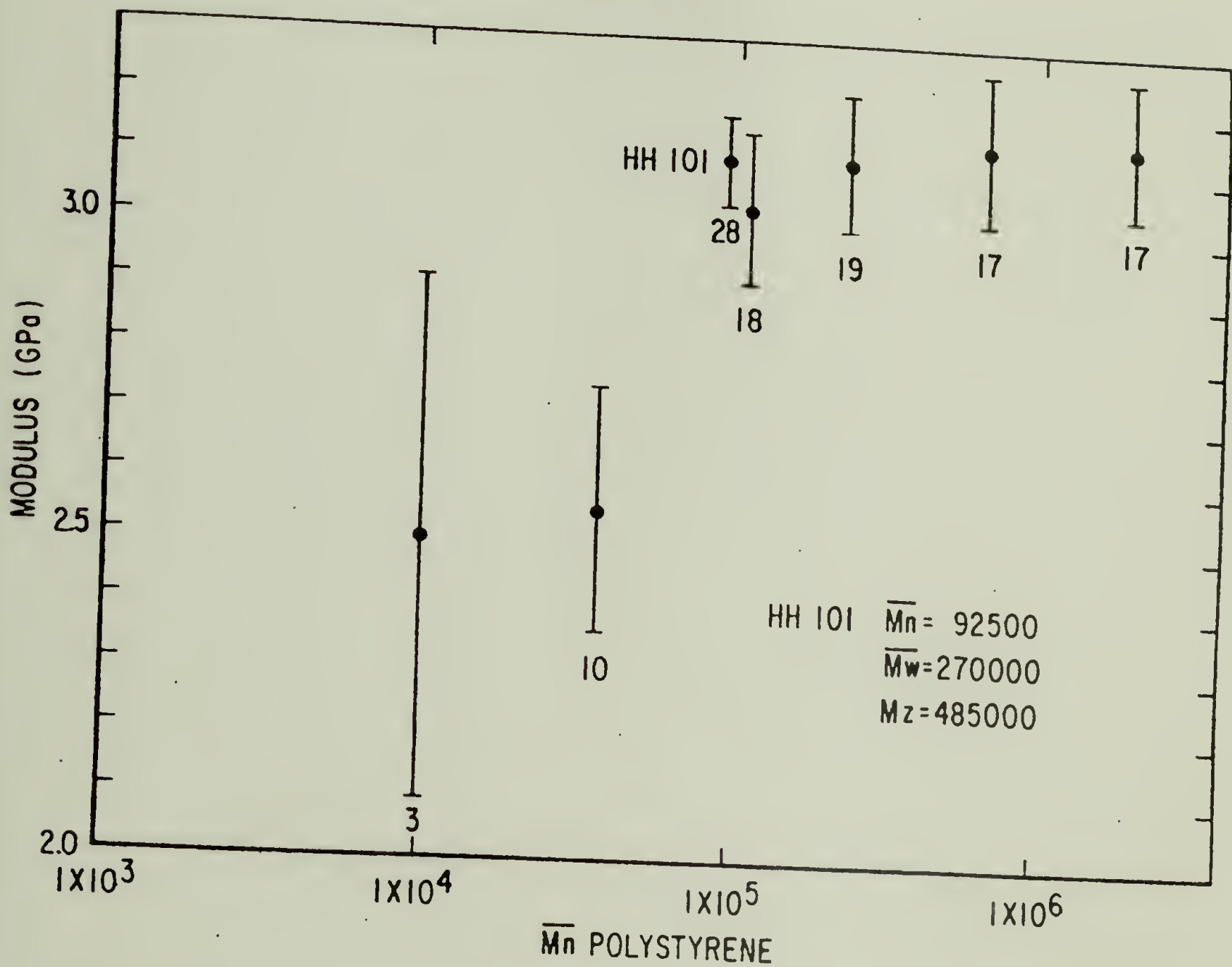
With the qualitative description of the modulus data complete, the logical progression would be a reasonable interpretation of these results. To obtain this goal it will be necessary to refer quite often to Chapter II, particularly the sections dealing with antiplasticizers, density, modulus, and secondary relaxations. Also, Figure 4.6, which features the modulus of HH 101-PS blends will receive the weight of the interpretation and discussion. Extrapolation to the other series of blends can then be readily made.

In correlating the modulus with molecular structure, it is useful to recall some of the theoretical background of Chapter II. A survey of the literature indicates that packing density, $\rho_B^* = \frac{V_w}{V}^3$, cohesive energy density, H_s/V_w , and the

³The subscript B for the packing density is to indicate that the notation of Bondi is being used. No subscript on ρ^* will indicate that the packing density of the lattice fluid is being used, which has dimensions of g/cm³.

FIGURE 4.9

VARIATION OF THE MODULUS OF POLYSTYRENE
WITH \bar{M}_n



glass transition temperature are, in the order given, the major factors that determine the numerical magnitude of the modulus. All three factors are interrelated.

It is also reported that the reducing parameter for the modulus, H_s/V_w , is not as much in evidence for glassy polymers as for highly crystalline polymers [4]; however, inconsistencies in data may be related to the exploratory nature of the work rather than in the weakness of the theory. Additionally, it is important to consider the effect of secondary relaxations, at each of which the moduli make a step change, and the effect of the time scale of the imposed deformation used in calculating the moduli. These phenomena will always exercise a blurring effect on correlation attempts.

The type of correlations for modulus with molecular structure one should attempt are easier to visualize if one recognizes that the elastic modulus at a particular temperature is composed essentially of two terms. The first term is the zero-point modulus, E_0 , which in reduced form depends primarily upon the packing density, ρ_B^* . The other term consists of a negative temperature function, the magnitude of which is largely determined by the contribution of external degrees of freedom. These contributions include, among others, internal rotation, torsional oscillation and lattice heat capacity. Usually, such contributions are lumped under the single term of background mechanical energy absorption

versus time, frequency, or temperature. The modulus, however, will be altered (below T_g) only by those secondary relaxations that also affect the free volume.

From the above discussion one realizes that density and packing are the key to understanding the modulus. Moreover, in reviewing the "antiplasticizer" literature, where maxima or enhancements in modulus versus plasticizer concentration have been shown to occur (similar to the maxima or enhancements depicted in Figures 4.1 through 4.8), one finds that the packing density of the polymer is the only equilibrium property that also passes through such a maximum. Since it appears that PS and PPO in the PS-PPO system act in a manner similar to the "antiplasticization" phenomenon found in polymer-diluent systems, it is attractive to attempt various modulus versus density correlations to ascertain their validity. The correlations will be attempted for the system HH 101-PPO. It will be useful to refer to Table 4.1 for the "Bondi" approach and later to Table 4.2 for the "lattice fluid" approach. Theoretical values listed in Table 4.1 were calculated according to methods described in references [4] and [5] of this chapter while references [129], [130], [131], and [176] of Chapter II were used for Table 2.

In Figure 4.10, the modulus (curve A) and the density (curve C) are both plotted as a function of PPO composition. Additionally, curves B and D illustrate the relationship one

TABLE 4.1

SUMMARY OF MOLECULAR PARAMETERS FOR PS (HH 101)-PPO BLENDS
UTILIZING A CORRESPONDING-STATES PRINCIPLE ACCORDING TO BONDI

w_1	ϕ_1	x_1	w_1'	E	ρ	Vw	V	Hs	E*	ρ_B^*
1.000	1.000	1.000	1.000	3.11	1.0476	62.85	99.4	9.20	5.08	0.632
0.800	0.803	0.822	0.810	3.15	1.0564	63.91	101.3	9.84	4.89	0.631
0.600	0.604	0.634	0.615	3.10	1.0628	65.04	103.5	10.52	4.58	0.628
0.400	0.404	0.435	0.415	2.99	1.0668	66.22	106.1	11.23	4.21	0.628
0.200	0.203	0.224	0.210	2.84	1.0696	67.48	109.0	11.99	3.82	0.619
0.000	0.000	0.000	0.000	2.66	1.0656	68.82	112.7	12.80	3.42	0.611

Nomenclature:

- w_1 weight fraction of PS; $w_1 + w_2 = 1$; w_2 is weight fraction of PPO
 ϕ_1 volume fraction of PS; $\phi_1 + \phi_2 = 1$
 x_1 mole fraction PS (based on monomer m.w. of 104 g/mole for PS and 120 g/mole for PPO; i.e., M_1 and M_2 respectively)

TABLE 4.1 (continued)

w_1'	w_1 when blending losses are considered
E	tensile modulus in GPa (experimental)
ρ	experimentally measured density in g/cm ³
V_w	van der Waals volume in cm ³ /mole calculated by summation of group increments
V	molar volume in cm ³ /mole = M/ρ
H_s	heat of sublimation increment per unit in kcal/mole and calculated by summation of group increments
E^*	reduced modulus, E_v/H_s , dimensionless
ρ_B^*	packing density, V_w/V , dimensionless

Mixing Rules for Blends:

1. For H_s , mole fractions were used ($H_s = X_1 H_{s1} + X_2 H_{s2}$)
2. V was calculated by M/ρ . M was calculated using mole fractions
($M = X_1 M_1 + X_2 M_2$)
3. V_w was calculated using mole fractions ($V_w = X_1 V_{w1} + X_2 V_{w2}$)

TABLE 4.2

SUMMARY OF MOLECULAR PARAMETERS FOR PS (HH 101)-PPO BLENDS
UTILIZING LATTICE FLUID THEORY ACCORDING TO SANCHEZ

w_1	ϕ_1	ϕ_1°	E	ρ	P^*	ρ^*	v^*	T^*	ϵ^*
1.00	1.00	1.00	3.11	1.0476	0.406	1.0820	16.40	803	1.596
0.80	0.811	0.766	3.15	1.0564	0.428	1.0969	15.49	798	1.586
0.60	0.617	0.551	3.10	1.0628	0.450	1.1123	14.65	793	1.576
0.40	0.417	0.353	2.99	1.0668	0.472	1.1281	13.88	788	1.565
0.20	0.212	0.170	2.84	1.0696	0.488	1.1443	13.33	782	1.555
0.00	0.00	0.00	2.66	1.0656	0.517	1.1610	12.50	777	1.544

w_1	\tilde{E}	$\tilde{\rho}$	\tilde{T}	T_g (°C)	T_g (°K)	T_f	τ_{TS}	$\bar{\tau}_{TS}$
1.00	7.66	0.9682	0.3673	105	378	0.780	45.1	0.111
0.80	7.36	0.9631	0.3697	121	394	0.749	60.8	0.142
0.60	6.89	0.9555	0.3720	140	413	0.714	71.0	0.158
0.40	6.33	0.9457	0.3744	158	431	0.684	76.5	0.162
0.20	5.82	0.9347	0.3772	185	458	0.644	77.0	0.158
0.00	5.14	0.9178	0.3797	216	489	0.603	70.7	0.137

Nomenclature:

w_1 weight fraction of PS

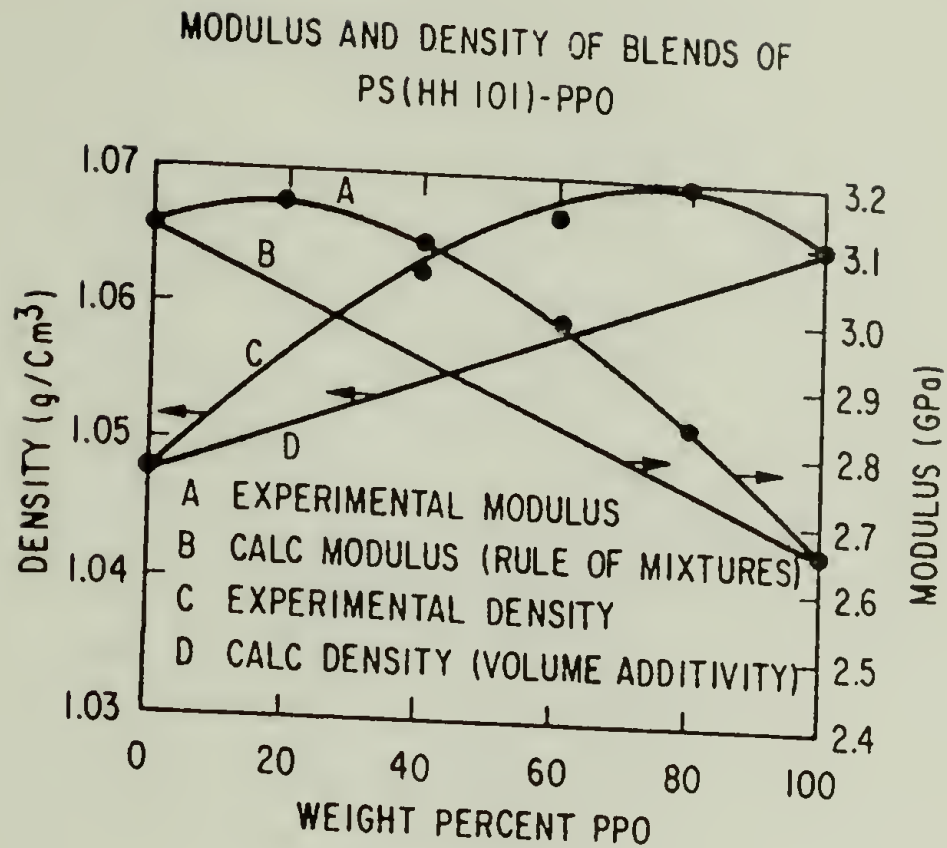
ϕ_1 see Chapter II.K. for mixing rules of blends.

ϕ_1° see Chapter II.K. for mixing rules of blends.

TABLE 4.2 (continued)

E	tensile modulus in GPa (experimental)
ρ	density in g/cm ³ (experimental)
P*	cohesive energy density in close-packed state in GPa (P* = ϵ^*/v^*)
ρ^*	packing density at absolute zero (close to crystalline density) in g/cm ³
V*	close-packed molar volume (per mer) in cm ³ /mole
T*	interaction energy per mer in close-packed state (T* = ϵ^*/k) in °K
ϵ^*	interaction energy per mer in close-packed state (hole energy) in kcal/mole
\tilde{E}	reduced modulus, E/P*, dimensionless
$\tilde{\rho}$	reduced density, ρ/ρ^* ; measure of occupied lattice, dimensionless
\tilde{T}	reduced temperature, T/T*, dimensionless
T _g	glass transition temperature
T _r	reduced temperature based on T _g , (T _r = T/T _g), dimensionless
τ_{TS}	tensile strength at break for brittle polymers or tensile strength at yield for ductile polymers, in MPa
$\tilde{\tau}_{TS}$	reduced tensile strength, $\tilde{\tau}_{TS} = \tau_{TS}/P^*$, dimensionless

FIGURE 4.10



DENSIFICATION AND EXCESS MODULUS FOR BLENDS OF PS (HH 101)-PPO

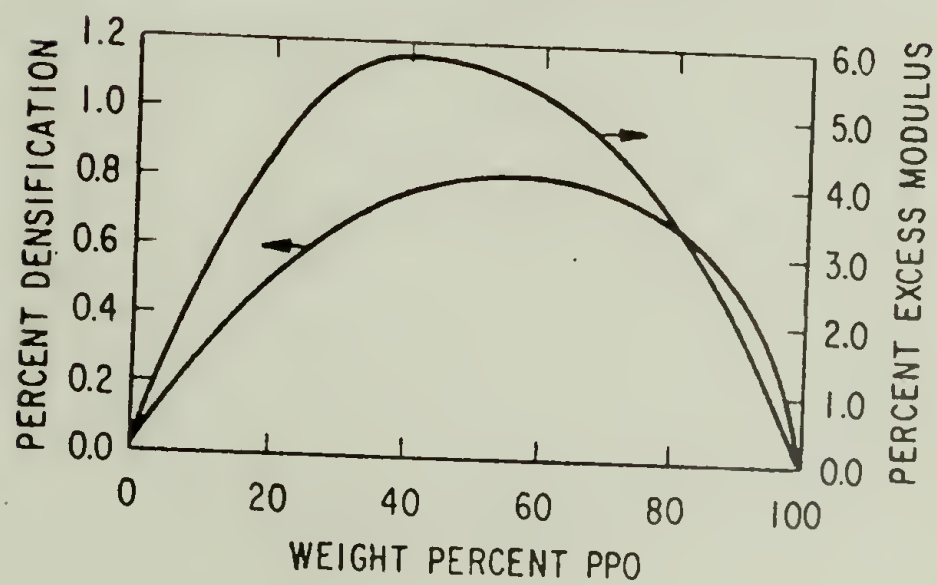


FIGURE 4.11

would expect for the modulus and density respectively, if they conformed to the "rule of mixtures". The broad maximum in the modulus occurs in the PPO composition range of 15-25 percent by weight while the maximum in density occurs somewhere between 70 and 80 percent. Because the location of the maximum of each of these two properties does not coincide, one might incorrectly conclude that there is no simple correlation between modulus and density. That is because one should not compare blend moduli and densities on an absolute scale, but rather one should compare for each particular composition the percent increase in density and modulus over that which would be calculated by assuming additivity of the homopolymer values. The additivity relationship for density is

$$\frac{1}{\rho_{\text{blend}}} = \frac{w_1}{\rho_1} + \frac{w_2}{\rho_2} \quad (95)$$

while that for the modulus is

$$E_{\text{blend}} = E_1\phi_1 + E_2\phi_2 \quad (96)$$

recalling that the subscripts 1 and 2 refer to the homopolymers properties of PS and PPO respectively.

The percent increase in density and modulus (above that calculated from equations 95 and 96) as a function of composition is depicted in Figure 4.11. This figure indicates that there is a good correlation between densification and the observed blend modulus. It is strongly suspected that there

would be even better agreement with higher precision density and modulus measurements, since even at the present level of precision the two curves could be made to almost coincide with an appropriate enlargement of the density scale or contraction of the modulus scale.

In view of the similarities with "antiplasticizers" as far as modulus behavior is concerned for these glassy-glassy polymer blends, it is desirable to give the possible modulus-density correlation even closer scrutiny. In particular, it has been mentioned that packing density, ρ_B^* , is the only equilibrium property that reveals enhancement behavior similar to that found for modulus versus plasticizer concentration. Can similar behavior be found in compatible glassy polymer systems? At this point it is useful to recall that the packing density, $\rho_B^* = V_w/V$, is a kind of measure of occupied volume. The van der Waals volume is the space occupied by the polymer molecule, which is impenetrable to other molecules with normal thermal energies [5]. Figure 4.12 verifies, within theoretical and experimental error, the strong correlation between blend packing density and the blend modulus. Hence, it can be seen that percent densification and packing density, ρ_B^* , are the important parameters (rather than the measured experimental density) in determining the modulus of the blend.

In Figure 4.13 a plot analogous to Figure 4.11 is presented. It is interesting to note the striking similarity

FIGURE 4.12

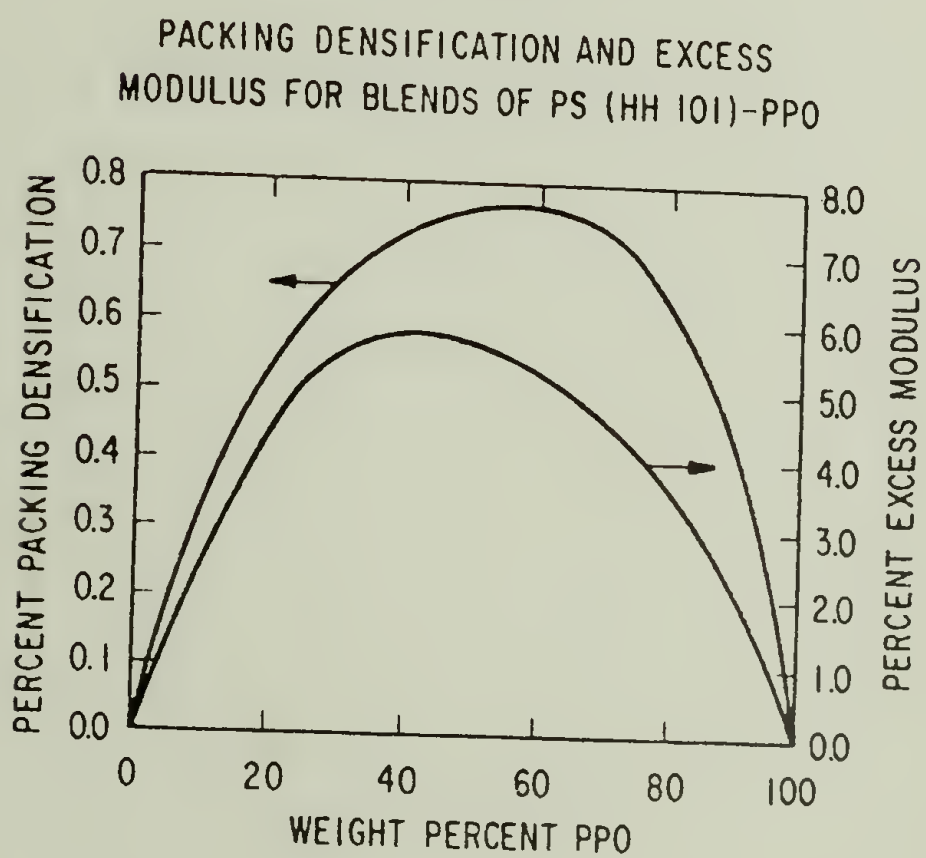
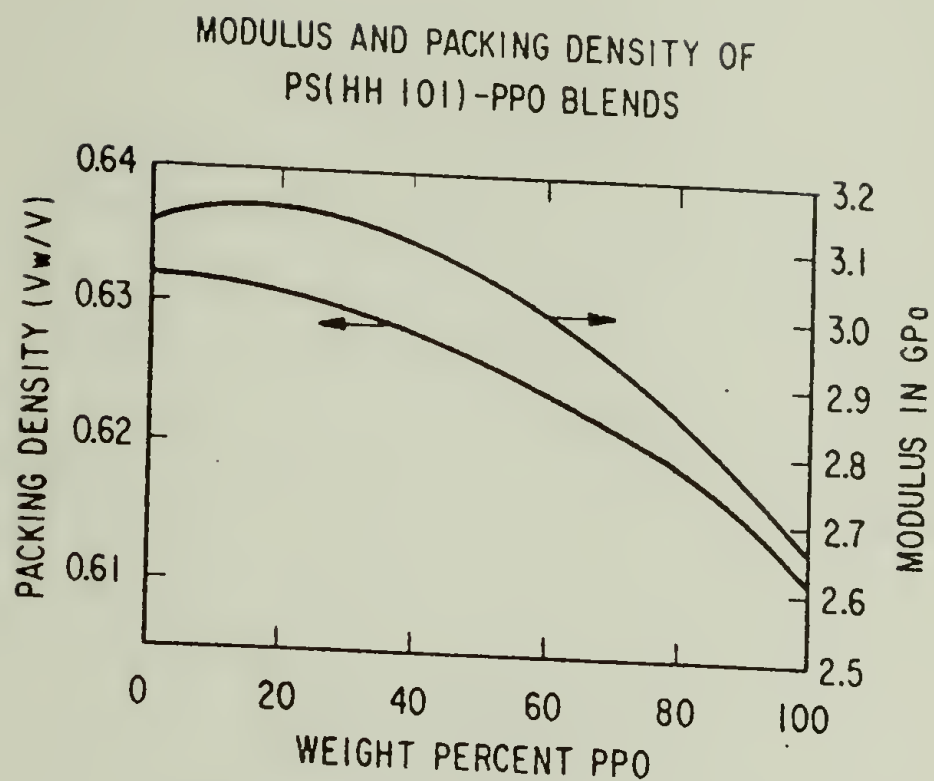


FIGURE 4.13

between the percent densification (Figure 4.11) and the percent packing densification (Figure 4.13) after taking into account that the scale in the latter case has been enlarged by a factor of two. In both cases, the maximum occurs at around 60% PPO at a densification value of 0.8%. Additionally, there is a striking similarity with "antiplasticizers" with regard to densification. For example, the addition of 6% benzophenone to PS increases the modulus by 5% and densifies the blend by 0.6% [6] (over that calculated by assuming volume additivity); while the addition of 25% PPO to PS also increases the modulus by 5% and densifies the blend by 0.6%. On the other hand, only 15% PS has to be added to PPO to obtain a 0.6% densification. Clearly the advantage that these compatible polymers have over antiplasticizers is that the entire compositional range is available in the obtaining of desirable pre-determined properties, while for antiplasticizers the upper useful limit is approximately 30% plasticizer.

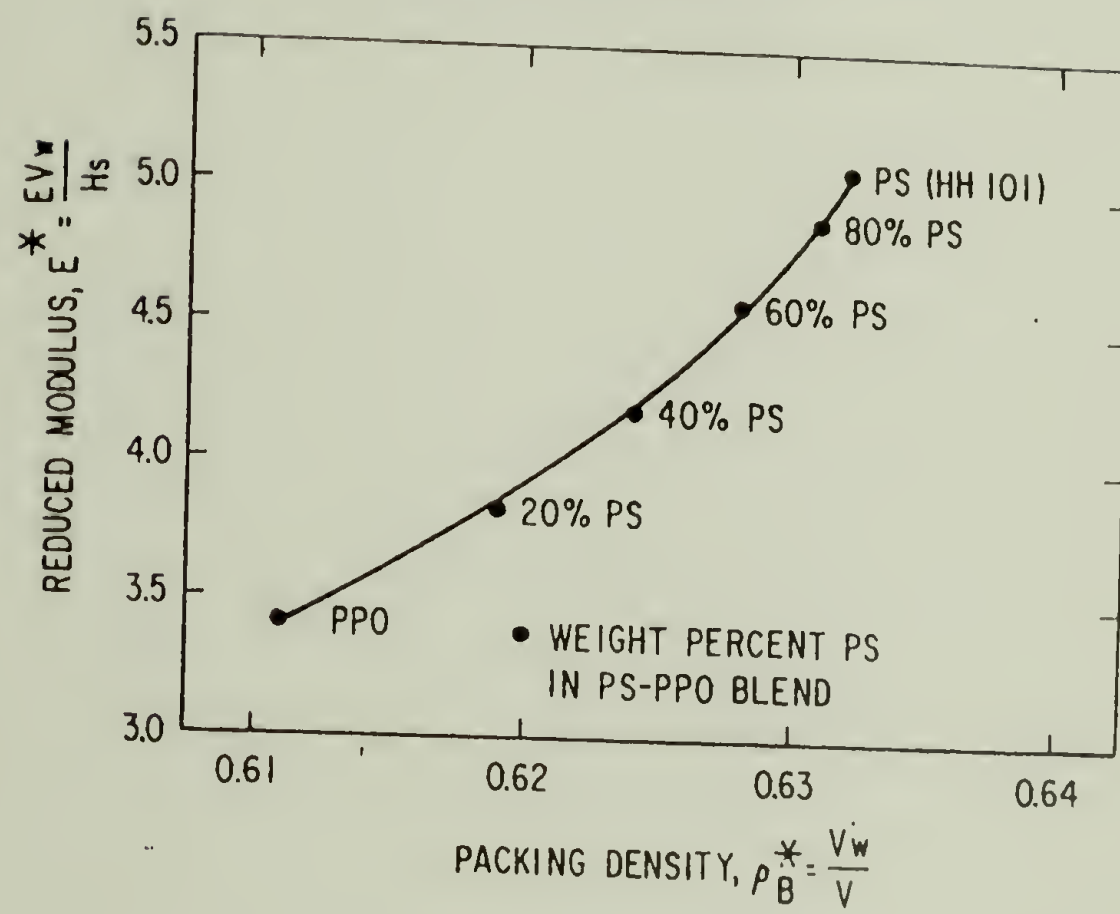
The ultimate goal of any theory pertaining to physical properties of substances is to be able to predict a desired property by a direct calculation. In many cases the theories are too complicated and/or too inaccurate to be useful for a direct calculation. This difficulty is circumvented by arranging the dependent and independent variables occurring in the differential equations (often having no analytical solution) in the form of dimensionless variables. Substitution of available experimental data into dimensionless groups and plotting

the resultant numbers in effect allows for a natural evolution of a result that theory might have supplied if it were either accurate enough or tractable. To this end the modulus can be generalized (and nondimensionalized) in terms of fundamental parameters: the heat of sublimation, H_s , and the van der Waals volume, V_w , which are measures of lattice energy and molecule geometry respectively. Now a reduced modulus is calculated from the following relationship:

$$E^* = E \frac{V_w}{H_s} \quad (97)$$

The effect of molecular structure on the modulus of isotropic polymer glasses below the glass transition is quite well represented by the reducing parameter H_s/V_w indicating that the modulus reflects primarily the van der Waals interaction between molecules [4]. In Figure 4.14, the relationship of the reduced modulus is presented as a function of the packing density, ρ_B^* , of the blend. As expected, the reduced modulus strongly depends upon packing density. In fact, a 3.4% increase in packing density results in a 49% increase in the reduced modulus. The power of the packing density lies in its predictive capabilities. For a glassy polymer or a glassy compatible polymer blend one should be able to predict the modulus given that the packing density is known and that H_s can be calculated from group increments. The predictive power should be best near absolute zero. Near this temperature one does not have to cope with the blurring effects of secondary relaxations

FIGURE 4.14

VARIATION OF REDUCED MODULUS WITH
BLEND PACKING DENSITY

that influence the free volume. Additionally, one should be able to extrapolate the reduced modulus versus packing density curve to include polymers that have packing densities outside of the range shown in Figure 4.14. It should be noted that semi-crystalline polymers are not expected to follow this particular curve because their packing structure cannot be predicted a priori.

Without more experimental data, it is difficult to assert whether the curve depicted in Figure 4.14 is universal for glassy homopolymers and polymer alloys. Theory indicates that it should be universal at least for simple systems, i.e., those that exhibit no major secondary relaxational effects. Universal or not, there are still some rather satisfying aspects indicated in this particular E^* versus ρ_B^* correlation. First, the reduced modulus of PS is greater than that of PPO, indicating PS is a stiffer molecule. Second, the packing density of PPO is less than that of PS even though the experimental density of PPO is higher. These observations are in accordance with expected results. A material with a higher packing density (but not necessarily higher density) is anticipated to exhibit a higher reduced modulus. Finally, since the packing density, ρ_B^* , is a type of measure of occupied volume, it may also be the key to explaining the high impact strength of PPO (twice that of PC at -200°C !). Although PPO has secondary relaxations, none of them are pronounced ($\tan \delta$

remains below 10^{-2} until near the glass transition) [7,8]. Therefore, secondary relaxations alone would not be expected to account for PPO's remarkably high impact strength. Perhaps the high unoccupied volume of PPO is responsible for this unusual behavior. A cataloging of impact strength versus packing density would clarify this possible relationship⁴.

In the previous discussion it was shown that the modulus could be generalized and non-dimensionalized in terms of lattice energy and molecule geometry (H_s and V_w respectively). The resulting reduced modulus is not unique. Now it will be shown that the modulus can also be generalized using the formalism developed in Chapter II.K. Since the modulus is related to the cohesive energy density and recalling from

⁴Litt and Tobolsky [6] have attempted such a correlation. They define fractional unoccupied volume as follows:

$$\bar{f} = 1.0 - (\rho_a / \rho_c) \quad (98)$$

where ρ_a is the amorphous density and ρ_c is the theoretical crystalline density as measured by x-rays on a well-annealed sample. In the case of packing density, ρ_B^* , the fractional unoccupied volume is simply:

$$\bar{f}_B = 1 - \rho_B^* \quad (99)$$

Table 4.2 that P^* is the cohesive energy density in the close-packed state, it would seem natural to define a reduced modulus, \tilde{E} , as follows:

$$\tilde{E} = E/P^* \quad (100)$$

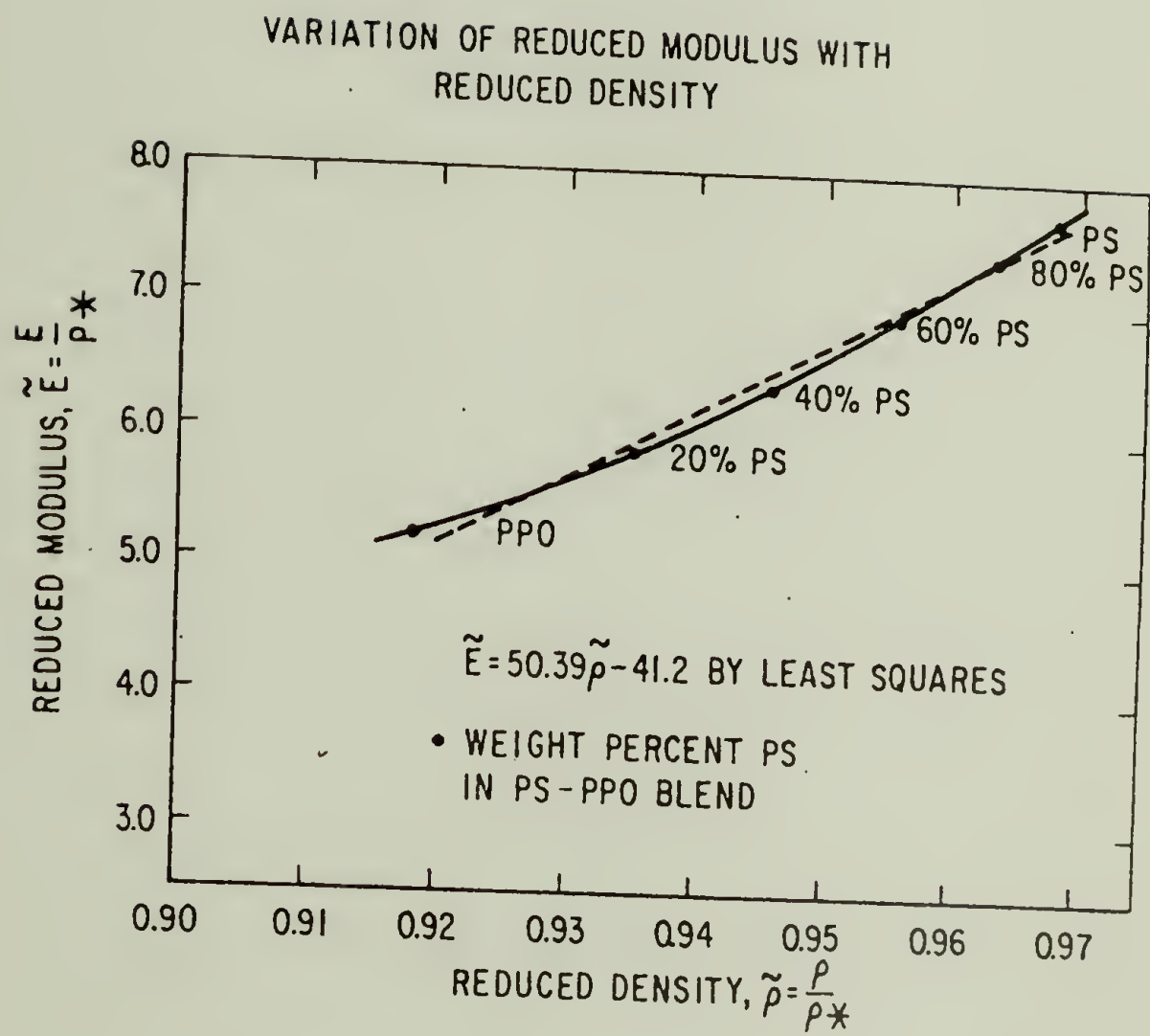
P^* is equivalent to ϵ^*/v^* . Besides its usual meaning, ϵ^* is also equal to the energy required to create a "hole" in the lattice. In terms of experimentally accessible quantities,

$$P^* = T\alpha/\tilde{\rho}^2\beta \quad (101)$$

where α , β , and $\tilde{\rho}^2$ are the thermal expansion coefficient, isothermal compressibility, and the reduced density, respectively. These definitions should justify using P^* as a reducing parameter for E .

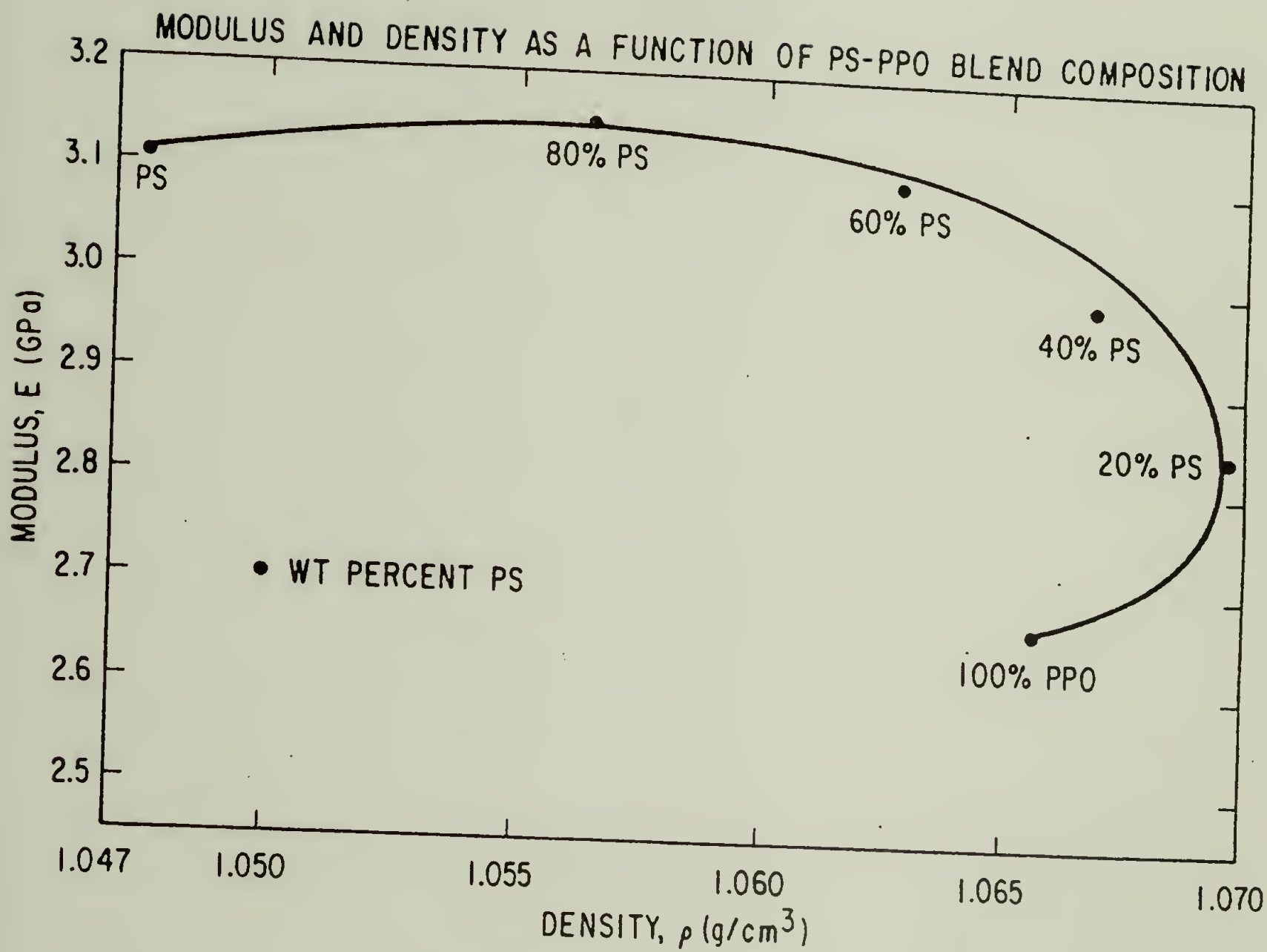
In Figure 4.15, the relationship between the reduced modulus and the reduced density utilizing lattice fluid theory is presented. As can be seen, this curve appears quite similar to the one presented in Figure 4.14. That is not surprising since both theories make use of measures of lattice energy (H_s or P^*) and molecule geometry or packing (ρ_B^* or $\tilde{\rho}$). Again, as in the corresponding states theory according to Bondi, the strong dependence of reduced modulus upon the reduced density can be noted in that a 5.5% increase in $\tilde{\rho}$ results in a 49% increase in \tilde{E} . The power of the reduced density, $\tilde{\rho}$, (just like ρ_B^*) could lie in its predictive capability. $\tilde{\rho}$, which is a measure of the occupied

FIGURE 4.15



volume (technically it is a measure of the fraction of occupied lattice sites), could be used to predict the modulus of a glassy homopolymer or compatible polymer blend. Without considerably more data, it is difficult to determine at this point whether the correlation depicted in Figure 4.15 is universal for all glassy isotropic polymer systems. For the same reason, it is also difficult to know whether extrapolation of the curve shown in Figure 4.14 to include polymer systems outside of the recorded range is justified. Certainly universality is a most desired feature of any theory; however, universal or not, this particular E versus $\tilde{\rho}$ correlation has the same satisfying aspects that were attributed to the E^* versus ρ_B^* correlation. One additional satisfying aspect is that P^* can be calculated directly from experimental quantities; however, H_s cannot. At the very least, both theories allow one to predict the moduli of the blend at any composition given only the packing density or the reduced density of each homopolymer. Additionally, Figures 4.14 and 4.15 are actually three-dimensional plots that define a unique surface in space. Therefore, any given packing density or reduced density immediately defines a unique blend composition and reduced modulus. Without resorting to parameters that result in dimensionless groups, unique values cannot be defined in three-dimensional space for polymer systems that exhibit excess moduli and densification. Figure 4.16 illustrates this

FIGURE 4.16



point in that a particular density does not necessarily define a unique modulus or blend composition.

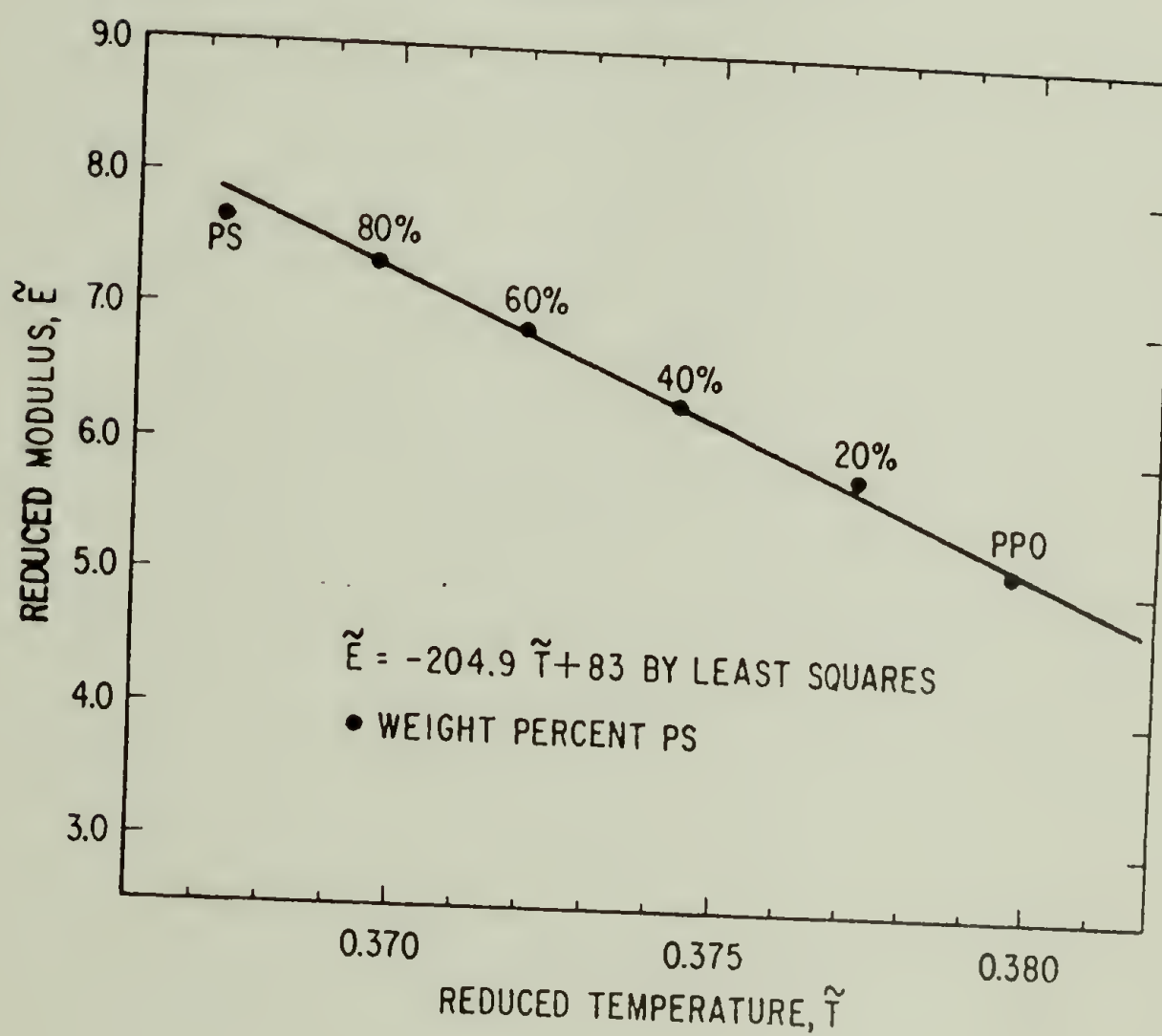
The lattice fluid theory also allows the modulus to be generalized with respect to a reduced temperature, \tilde{T} , as is shown in Figure 4.17. The reduced temperature, \tilde{T} , is directly proportional to the ambient temperature, T , and inversely proportional to the energy required to create a hole in the lattice, T^* . The negative temperature coefficient ($\frac{\partial \tilde{E}}{\partial \tilde{T}} = -204.9$) is expected. The modulus should decrease with increasing temperature due to a weakening of intermolecular forces and a decrease in packing density. Moreover, the modulus should increase with increasing T^* because of its direct relationship to the interaction energy in the close-packed state. In Figure 4.17, a unique modulus and blend composition is defined at any particular reduced temperature. \tilde{E} is very sensitive to \tilde{T} in that an increase in \tilde{T} of 3.4% results in a decrease in \tilde{E} of 33%. Once again it would gratifying if the developed correlation

$$\tilde{E} = -204.9 \tilde{T} + 83 \quad (102)$$

would hold for other glassy polymer alloys as well or at least for the PS-PPO system over a wider range of reduced temperatures. More data is necessary to verify the predictive power of this relationship. If it does hold for a much wider range of temperatures, the number of experiments necessary to

FIGURE 4.17

VARIATION OF REDUCED MODULUS WITH
REDUCED TEMPERATURE AND BLEND
COMPOSITION



evaluate the modulus of a polymer system under a variety of conditions would be markedly reduced.

Inspection of Tables 4.1 and 4.2 indicate that quite a few more correlations could be developed; for example, $\tilde{\rho}$ as a function of \tilde{T} , which incidentally shows a trend similar to that recently reported in the literature for homopolymers [9]. The numerous potential correlations will be omitted since they do not directly contribute to any new knowledge leading to an understanding of the moduli of compatible polymer blends. In this paragraph it should also be noted that a correlation often attempted for homopolymers is reduced modulus, $E^* = \frac{EV_w}{H_s}$, as a function of reduced temperature, $T_r = T/T_g$. While such a correlation may be adequate for many homopolymers, it fails for the PPO-PS system. In fact, the correlation yields a positive temperature coefficient with respect to the reduced modulus. The failure of this correlation is not surprising since T_g is not a corresponding state. Why the E^* versus T_r correlation yields a surprisingly correct temperature coefficient for homopolymers is unknown.

Before leaving the Bondi approach or the Sanchez approach, it would be useful to briefly discuss their shortcomings. Aside from needing extremely accurate experimental and theoretical data to apply both of these approaches, the major shortcoming of each is involved with the blending rules

used. Even though the modulus and density of compatible polymer blends as a function of composition deviates somewhat from the "rule of mixtures", most mixing rules used for the reducing parameters (e.g., H_s , v^* , etc.) at a particular PS-PPO composition were based upon simple molar, volume, or weight additivity. Only the equation for ϵ^* contained an interaction term (see equation (79)). It would not be surprising if all the reducing parameters in reality also deviated from linearity (perhaps by one or two percent) when considering these parameters as a function of blend composition. One way to make progress in this area is to obtain highly accurate experimental data for density and modulus and then work backwards; i.e., see what additional term is required in the reducing parameter to allow theory and experiment to agree more precisely. Success with such an endeavor appears highly unlikely since density must be known to at least 0.1% and the modulus to 0.3%. Moreover, it is difficult to refine a parameter such as H_s for a blend when it can be calculated to within only ~4% for the homopolymer. It is highly unlikely that simple additivity would apply for a parameter such as H_s since, for a blend, its value can be greatly influenced by molecular environment.

A final shortcoming applies only to the lattice fluid approach. This approach was developed for polymers above their respective glass transitions. In this work the theory

was extended to polymers far below their respective glass transition temperatures. At this point, it is difficult to ascertain how justified such an extrapolation is.

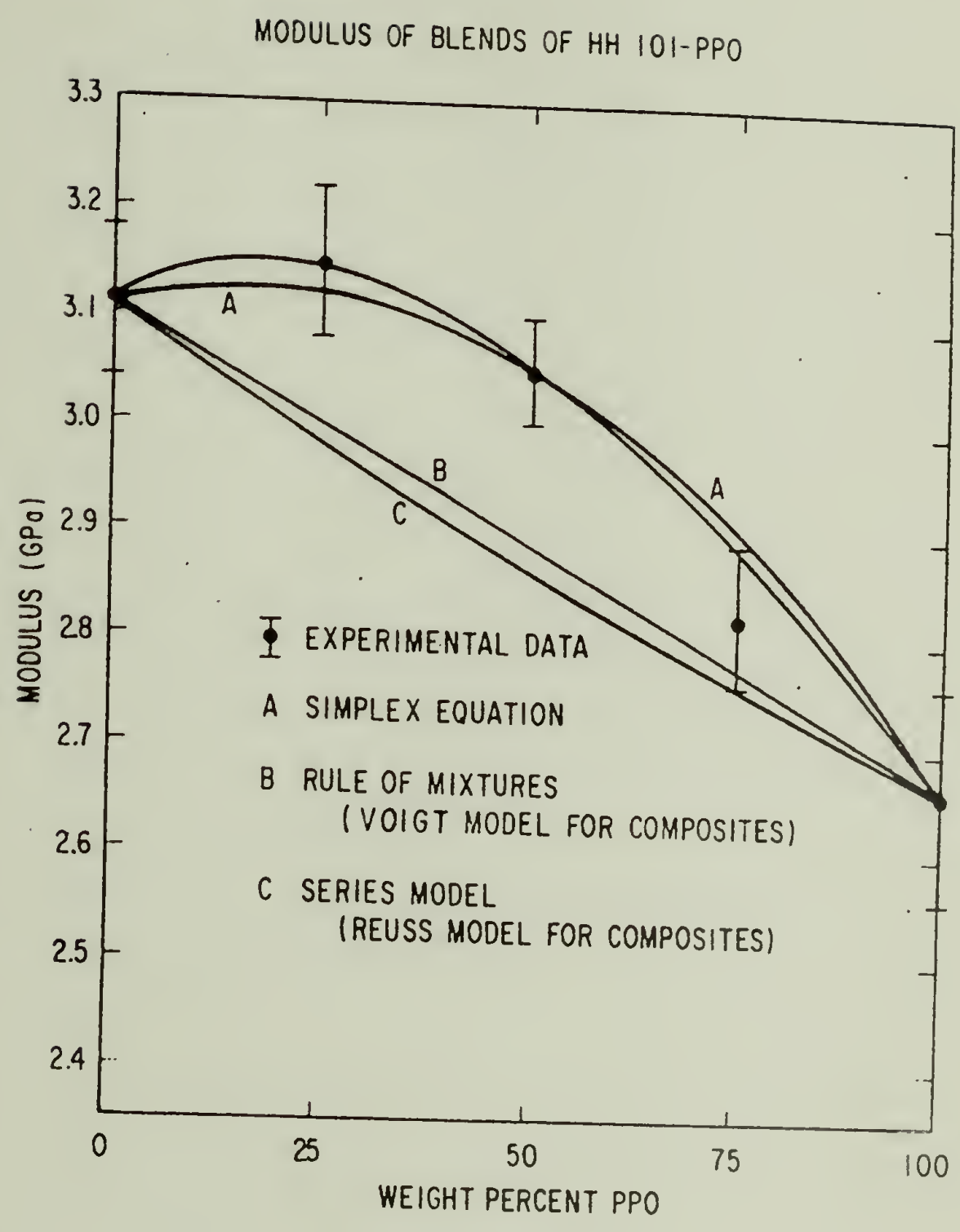
In spite of these shortcomings, it is surprising how well both of these theories seem to apply to PPO-PS blends. Their usefulness have already been demonstrated in the literature for some homopolymer properties. This marks the first time these approaches have been extended to the moduli of glassy polymer alloys.

Another approach that may be useful in modeling the modulus of glassy alloys as a function of composition is composite theory. That is, it will now be determined whether homogeneous mixtures can be treated using theories developed for heterogeneous mixtures (composites). Emphasis will be placed upon the HH 101-PPO system in this discussion. A subscript 1 will represent the PS while 2 will represent the PPO. As was explained in Chapter II.F., the maximum possible modulus for a two component composite system is represented by the "rule of mixtures" and results when the two materials comprising the composite are connected in parallel:

$$E = \phi_1 E_1 + \phi_2 E_2 \quad (24)$$

Equation (24) is represented by Curve B in Figure 4.18. Curve B is the closest any composite theory can approach the experimental data. On the other hand, the lowest possible modulus is obtained when the two materials comprising the

FIGURE 4.18

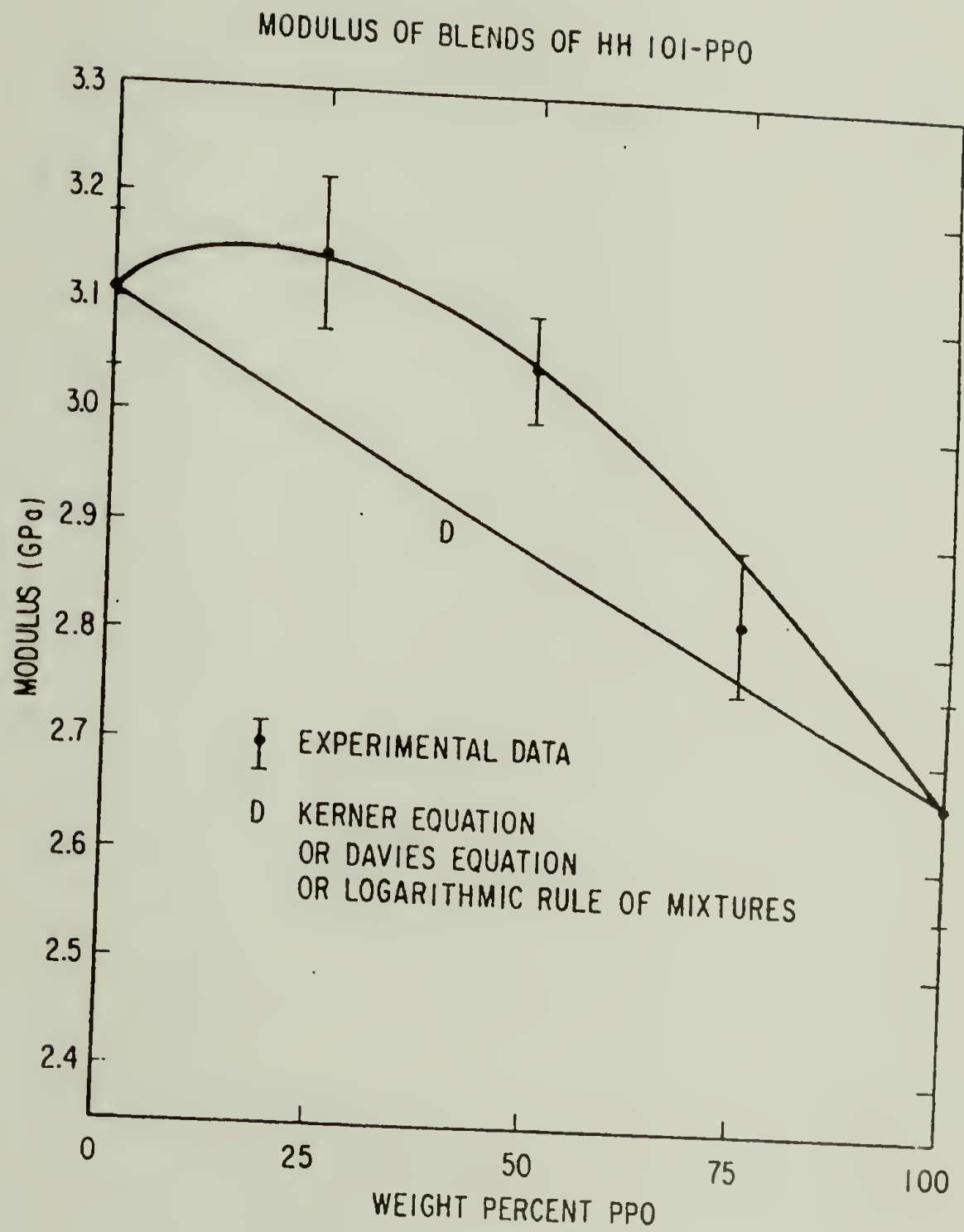


composite are connected in series. The equation then becomes:

$$\frac{1}{E} = \frac{\phi_1}{E_1} + \frac{\phi_2}{E_2} \quad (25)$$

Equation (25) is represented by Curve C in Figure 4.18. Since Equation (24) (a representation of the maximum possible modulus for a two component system) fails to represent the modulus as a function of compatible blend composition, it is safe to say that no other composite equation could possibly be valid either. The modulus for any composite will never be higher than either of its constituents. For the sake of completeness, Figure 4.19 depicts Curve D which is a representative of the Kerner equation (see Equation 26). The Kerner equation or the Halpin-Tsai equations (which are actually generalized Kerner equations) are the most common composite equations and are applied to model either moduli of glassy or rubbery filled systems. In this particular case, the Davies equation (see Equation 44) or the logarithmic rule of mixtures (see Equation 42) supply numerical values (within three significant figures) identical to the Kerner equation. As expected, the numerical values of these equations (Curve D) lie midway between Curves B and C in Figure 4.18. The Davies equation is sometimes used to model interpenetrating networks, while the logarithmic rule of mixtures can be applied to semi-crystalline polymers. The numerical values obtained by

FIGURE 4.19



the application of these composite equations (Curves B and C in Figure 4.18 and Curve D in Figure 4.19) were identical regardless whether PPO or PS was considered to be the filler in the continuous polymer matrix.

In these composite equations, Curves B and C are actually represented by the following equations respectively:

$$E = 3.11 \phi_1 + 2.66 \phi_2 \quad (103)$$

and

$$E = \frac{\phi_1}{3.11} + \frac{\phi_2}{2.66} \quad (104)$$

Although composite equations require volume percent for their compositional functionality, weight percentages were retained in Figures 4.18 and 4.19. Since the densities of both components are nearly identical, volume or weight percentages are also nearly identical and so can be used interchangeably in this case without introducing any appreciable error. In the case of Curve D, the Poisson's ratio was taken to be 0.33 and 0.35 for PS and PPO respectively [4, 10].

Although composite equations fail to model the modulus for these blends, Simplex equations can be generated which agree with the empirical data over the entire compositional range, as can be seen by noting Curve A in Figure 4.18. Curve A is a representation of a second order polynomial for a two component system (see Chapter II.J.). In terms of the modulus, the equation has the following form:

$$E = E_1 X_1 + E_2 X_2 + \beta_{12}^E X_1 X_2 \quad (67)$$

In this case E_1 , E_2 , χ_1 , and χ_2 represent the moduli and composition of PS and PPO respectively. The superscript E has been placed on the interaction term, β_{12} , to emphasize that this term goes with the modulus. As equation (65) of Chapter II.J. indicates, the solution to Equation (67) is:

$$\beta_{12}^E = 4E_{12} - 2E_1 - 2E_2 \quad (105)$$

It is useful to recall that E_{12} represents the response of the 50:50 mixture. Moreover, the first two terms of Equation (67) correspond to the linear rule of mixtures, while the magnitude of β_{12}^E expresses the extent of deviation from non-linearity. A positive β_{12}^E represents a non-linear synergism (criterion for compatibility?) while a negative β_{12}^E expresses a non-linear antagonism (criterion for incompatibility?).

Table 4.3 provides a summary of the equations that represent the moduli as a function of composition for PS-PPO blends, while Figure 4.20 depicts the variation of β_{12}^E as a function of \bar{M}_w of PS in the PS-PPO blend. As can be noted, β_{12}^E decreases with increasing PS molecular weight. If β_{12}^E has some relationship with level of compatibility, the trend depicted in Figure 4.20 is correct. Compatibility decreases for compatible systems when the molecular weight of any of the blend's constituents is increased. Although most investigators ignore the effect of molecular weight, it is extremely important. For example, high molecular weight poly (α -methyl

TABLE 4.3

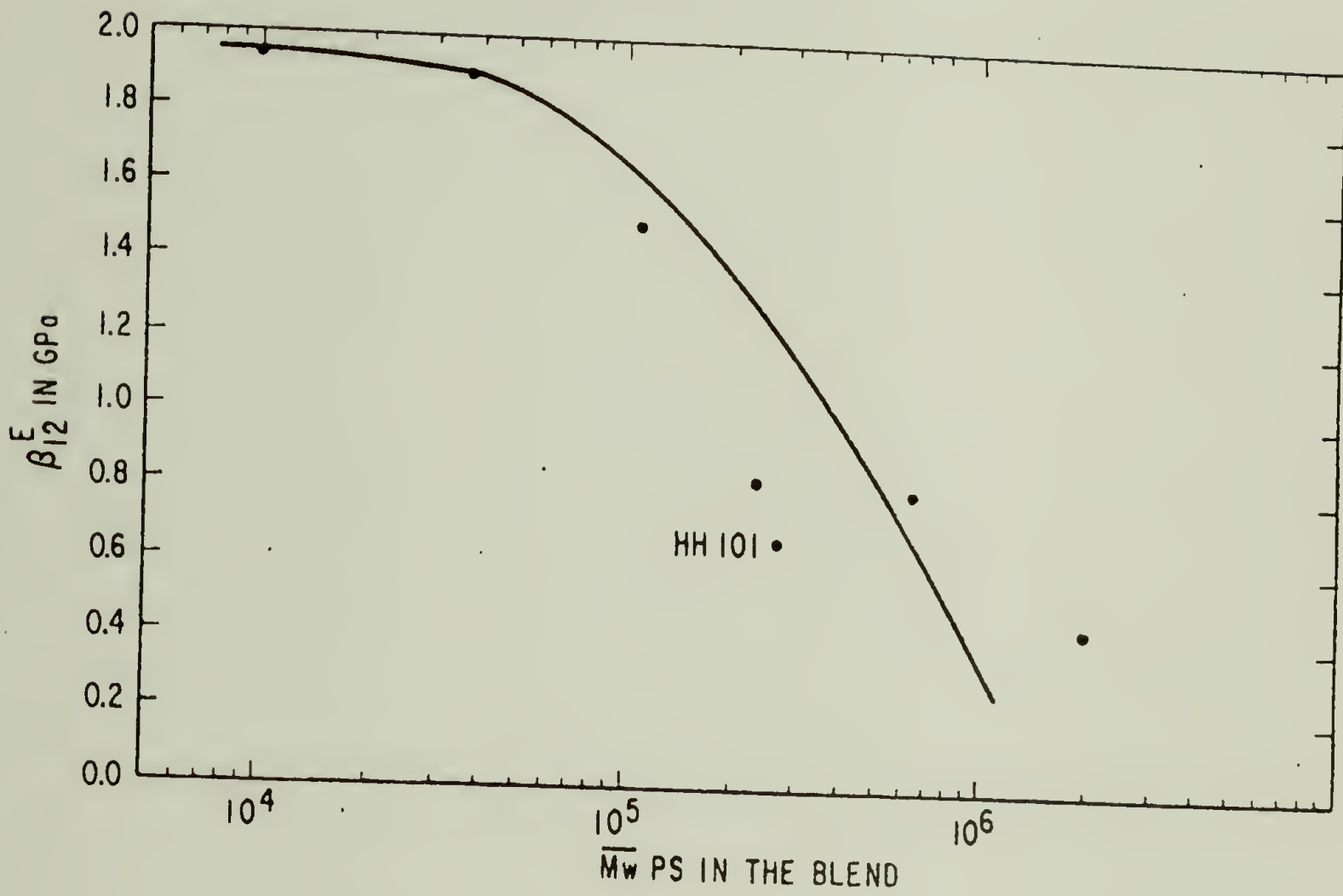
SUMMARY OF SIMPLEX EQUATIONS REPRESENTING
THE MODULI OF PS-PPO BLENDS

BLEND	EQUATION
GENERAL	$E = E_1x_1 + E_2x_2 + \beta_{12}^E x_1x_2$
aPS-4000/PPO	no value could be obtained experimentally for E_1
aPS-10000/PPO	$E = 2.50x_1 + 2.66x_2 + 1.94x_1x_2$
aPS-37000/PPO	$E = 2.55x_1 + 2.66x_2 + 1.90x_1x_2$
aPS-110000/PPO	$E = 3.03x_1 + 2.66x_2 + 1.50x_1x_2$
aPS-233000/PPO	$E = 3.11x_1 + 2.66x_2 + 0.82x_1x_2$
aPS-HH101/PPO	$E = 3.11x_1 + 2.66x_2 + 0.66x_1x_2$
aPS-670000/PPO	$E = 3.14x_1 + 2.66x_2 + 0.80x_1x_2$
aPS-2000000/PPO	$E = 3.15x_1 + 2.66x_2 + 0.46x_1x_2$

Nomenclature:

E_1	modulus of PS in GPa
E_2	modulus of PPO in GPa
x_1	weight or volume percent PS
x_2	weight or volume percent PPO
β_{12}^E	interaction term (compatibility coefficient) in GPa

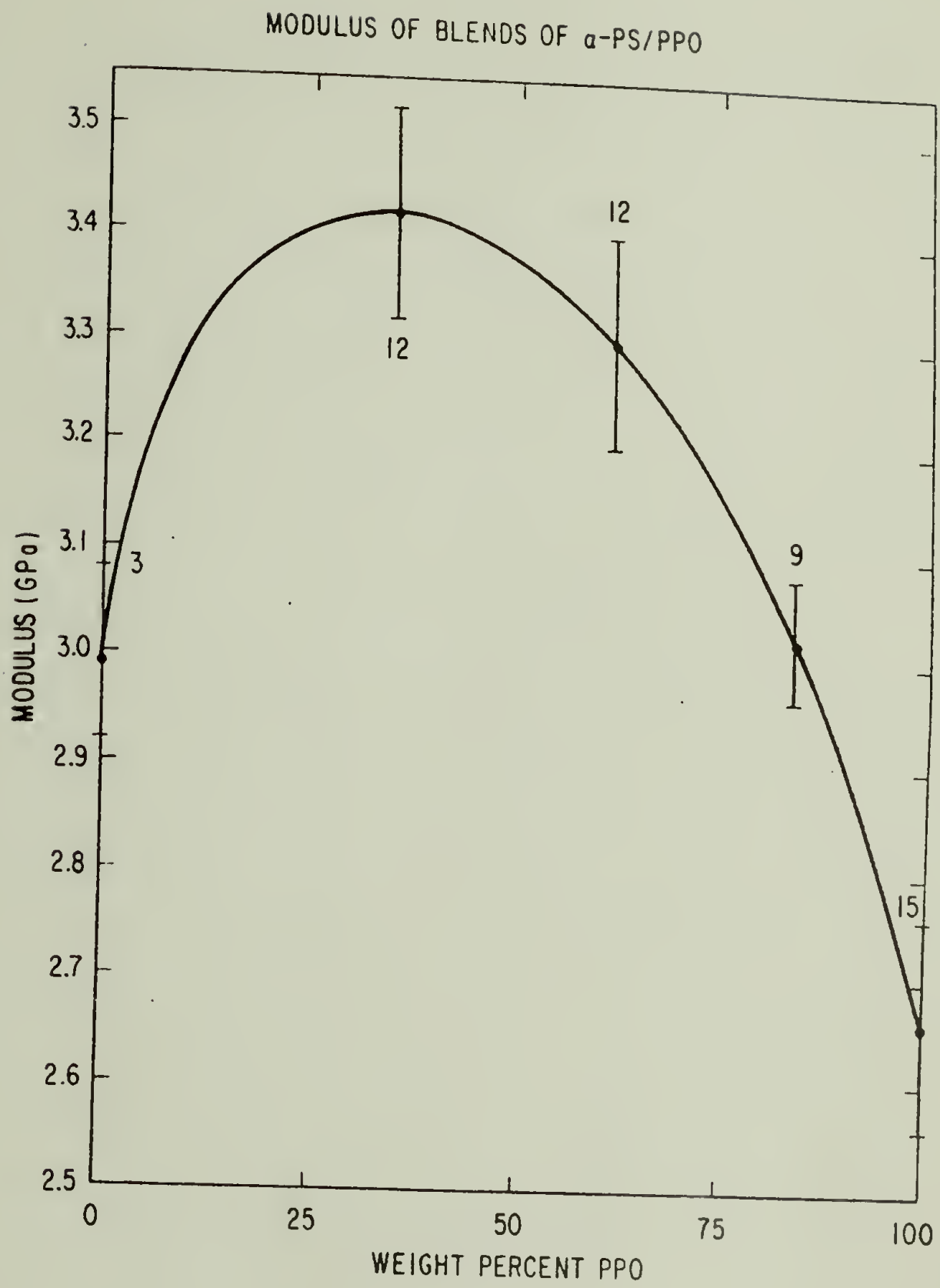
FIGURE 4.20

 β_{12}^E FOR PS-PPO BLENDS

styrene) (α -PS) is incompatible with PS. These polymer blends exhibit two Tg's by dynamic mechanical measurements and compression molded films appear cloudy [11]. However, when the molecular weight of α -PS becomes sufficiently low, α -PS/PS blends become compatible. These blends then exhibit a single glass transition (see Appendix) and yield clear films upon compression molding [12].

A valid question at this point would be: is it possible to establish a compatibility criterion based upon the modulus data? Specifically, is a positive β_{12}^E indicative of compatibility? The discussion of this aspect will be confined to polymer blends below their Tg throughout their entire compositional range. Compatible mixtures of glassy-rubbery polymers also exhibit moduli above additivity [13], however, these mixtures cannot be modeled by the Simplex equation since at a particular composition (at Tg) the modulus undergoes a catastrophic decrease (glass to rubber transition). However, all compatible glassy-glassy polymer systems exhibit a positive β_{12}^E . For example, the compatible blend, α -PS/PPO exhibits such behavior, as can be observed in Figure 4.21. This glassy alloy has a relatively high β_{12}^E ($\beta_{12}^E = 2.22$ GPa), qualitatively indicating a high "level of compatibility". All examples of glassy alloys considered so far, consisted of a ductile polymer and a brittle polymer. A glassy alloy comprised of two brittle polymers is low molecular weight α -PS

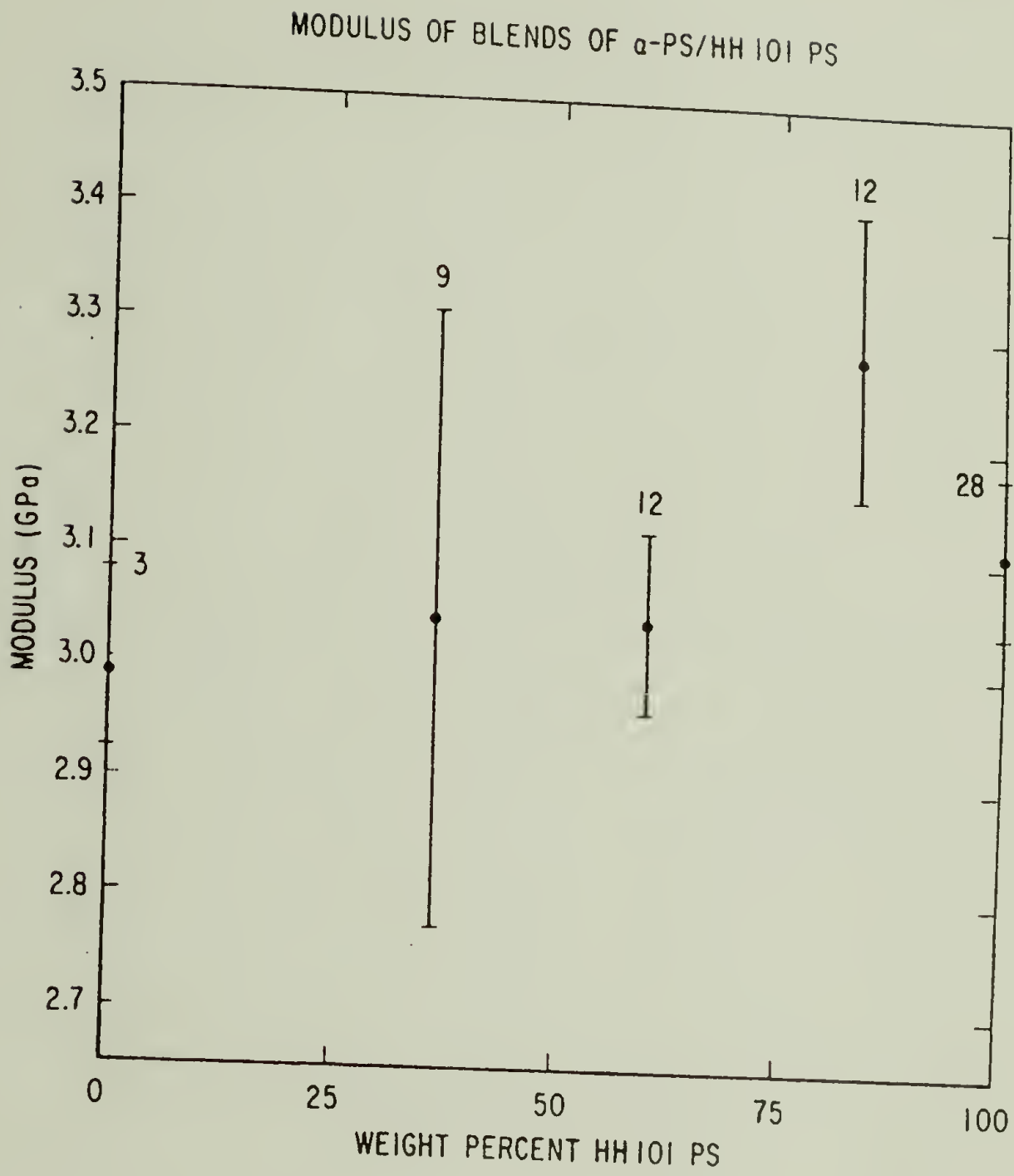
FIGURE 4.21



and high molecular weight PS. These blends do not conclusively show a positive β_{12}^E (see Figure 4.22). There are two reasons for this behavior. First, it was very difficult to obtain accurate modulus data due to the extreme brittleness of the blend; and second, the "level of compatibility" is rather low anyway, leading to a relatively low positive β_{12} . The latter assertion is supported by the Flory-Huggins theory [14] which can be used to calculate the limit of molecular weight at which a mixture of homopolymers with an interaction parameter of 0.002 is miscible in all proportions. This occurs at a degree of polymerization of 1000 [15]. So, if the molecular weight of both homopolymers exceeds 100,000, phase separation is to be expected.

In all cases of two component polymer alloys examined, a positive β_{12}^E was or could be calculated. Incompatible glassy polymer-polymer systems such as those based upon para-chlorostyrene (p-CIPS) and PPO show more complicated modulus composition behavior [16]. However, in not one of the many incompatible systems studied could a positive β_{12}^E be calculated. For these incompatible systems, there is no modulus enhancement (modulus greater than that calculated from the rule of mixtures) throughout the entire range of composition. Based upon the amount of evidence presented, it can be stated that all glassy alloys exhibit a positive β_{12}^E throughout their entire range of composition, while incompatible systems do not.

FIGURE 4.22



Clearly, it would be desirable to examine a greater number of glassy alloys to ascertain the universality of the previous statement.

Because of considerable favorable evidence and the lack of any refutative manifestation, it will now be proposed that the magnitude of β_{12}^E for a given glassy compatible system could be a measure of the "level of compatibility". Supportive evidence is presented in Figure 4.20. As previously mentioned, such a trend is expected, if indeed β_{12}^E can be considered a type of measure of the compatibility. Verification of the significance of β_{12}^E unfortunately depends considerably upon the accuracy of the data. For example, in the case of aPS-HH101/PPO, just a one percent increase in E_{12} (see Equation 105 and Table 4.3) will result in an 18.8% increase in β_{12}^E (from 0.66 to 0.78). In this example, E_1 and E_2 were allowed to retain their values. Because of the nature of Equation 105, β_{12}^E is extremely sensitive to the accuracy of the experimental data. Such is always the case for any equation which involves the subtraction of numbers of equal magnitude. Since it is not possible to obtain modulus data from tensile tests within one percent accuracy, one can assume that the values for β_{12}^E could easily be in error by 20 percent. In spite of this problem, the trends shown in Figure 4.20 are significant because β_{12}^E is greater for aPS-4000/PPO than for aPS-2000000/PPO even when one allows for a 50 percent error.

If more accurate data could be obtained, the task of truly attaching some significance to β_{12}^E would be considerably easier.

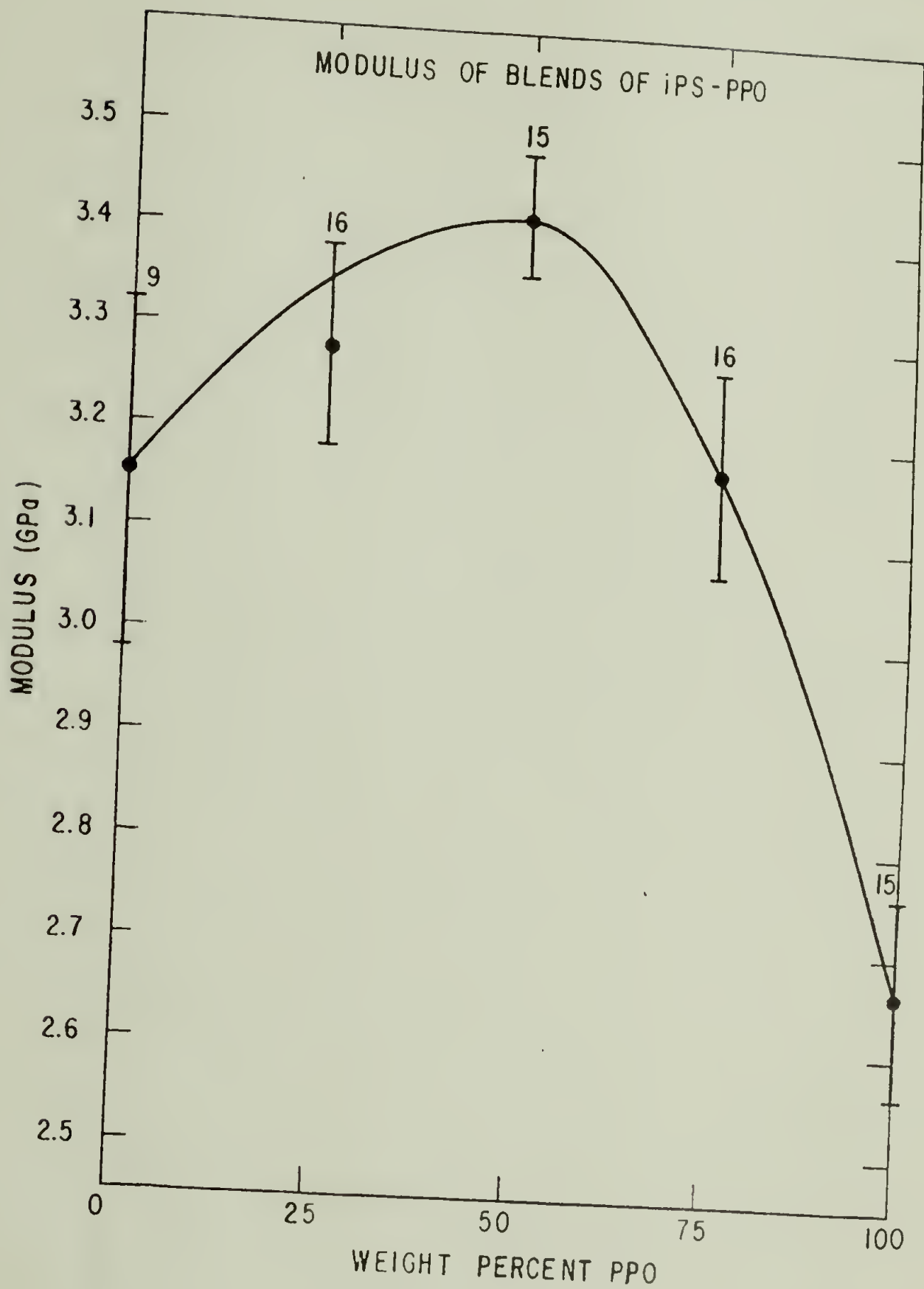
In spite of the lack of availability of more accurate data, it would still be useful to observe some trends in order to do some additional speculation concerning the level of compatibility as measured by the magnitude of β_{12}^E . Referring to Figure 4.23, one observes the modulus of i-PS/PPO alloys as a function of composition. The equation describing this relationship is

$$E = 3.15 X_1 + 2.66 X_2 + 2.06 X_1 X_2 \quad (106)$$

where the subscripts 1 and 2 refer to iPS and PPO respectively. 3.15 is the modulus of pure iPS, 2.66 is the modulus of PPO and 2.06 represents the interaction term β_{12}^E . If the previous significance attached to β_{12}^E is borne out, then iPS must be more compatible than aPS with PPO at equivalent PS molecular weights. In fact, the iPS (Mw = 724,000) appears to be as compatible as aPS-10000 (see Table 4.3) is with PPO.

Some supportive evidence can be found both in the literature and in this work. A comparison of the dynamic mechanical measurements of blends of iPS-PPO [17] with those of blends of aPS-PPO [8] indicates that iPS is somewhat more efficient at suppressing the broad β relaxation of PPO. Only 15 weight percent iPS is necessary to suppress the low temperature β peak of PPO. Generally, the same amount of low molecular weight antiplasticizer suppresses the β relaxation of PC and

FIGURE 4.23



PVC, suggesting that iPS is mixing to the same extent as these low molecular weight additives [17]. In the case of high molecular weight aPS, even as much as 50 weight percent does not completely suppress the β relaxation of PPO [8]. Suppression of the secondary relaxation embrittles the polymer and raises the modulus. The iPS is more efficient than aPS in the embrittlement of PPO. A 25/75 PS-PPO blend will always reveal brittle failure when the PS component is isotactic, but will show predominantly ductile failure when the PS is atactic. Moreover, the elongation to break curves for these blends exhibit a sharper decrease when iPS is added to PPO than when the additive is aPS (see elongation to break curves in Section D of this chapter). Finally, the differences in the increase in modulus should be noted for 25/75 PS-PPO blends. While 25% aPS-670000 increases the modulus of PPO by 14%, 25% iPS-724000 increases the modulus of PPO by 20%. Even aPS-4000 is not as efficient as iPS in its action to embrittle PPO and increase its modulus. These remarks all lend support to the premise that the magnitude of β_{12}^E (a measure of deviation of the modulus from non-linearity) is also an indication of the "level of compatibility" or the "extent of mixing".

The iPS-PPO modulus-composition relationship presented in Figure 4.23 may possibly be explained on the basis of density and packing density, ρ_B^* (similar to the HH101 PS-PPO relationships depicted in Figure 4.12). There is some

indication in the literature [6,18] that the density and therefore the packing density is somewhat greater for iPS than aPS. Common values for the density of equal molecular weight aPS and amorphous iPS are 1.047 and 1.053 g-cm⁻³ respectively. The packing density for the iPS-PPO blends could very well also be somewhat higher. Unfortunately, density measurements were not performed for the iPS-PPO blends in order to verify this speculation.

The conclusions that can be stated regarding the moduli of glassy alloys are:

1. All the criteria for antiplasticizers, as summarized in Chapter II.C. are met for the PS-PPO system.
2. Packing density is the key to understanding the moduli of glassy alloys. It is also useful for explaining antiplasticization and compatibility. The packing density is the only equilibrium quantity which passes through a maximum similar to the modulus. The results in this section suggest that compatibility can be handled without resorting to specific molecular interactions.
3. An interaction term, β_{12}^E , is useful in the modeling of the moduli of glassy alloys as a function of composition. It is proposed that β_{12}^E be further evaluated for its ability to gauge compatibility and level of compatibility.
4. Composite theory can not be applied to model the moduli of glassy alloys as a function of composition; however, a second order Simplex equation has been shown to be entirely satisfactory.

IV.C. TENSILE STRENGTHS OF THE GLASSY HOMOPOLYMERS AND COMPATIBLE POLYMER BLENDS

As was the case for the modulus, the tensile strengths for PPO-aPS blends were also evaluated as a function of composition and aPS molecular weight. Representative tensile

strength - composition relationships are presented in Figures 4.24 through 4.28 (see the Appendix for a more complete tabulation). Again, in each of these figures, the PPO had the same molecular weight and molecular weight distribution, while aPS's of progressively higher molecular weight were blended with the PPO (see Table 3.1 of Chapter III).

The features of these curves (Figures 4.24 through 4.28) are strikingly similar to those found in the modulus — composition curves (see Figures 4.1 through 4.8). In particular, the tensile strength, τ , at each blend composition, χ , is greater than that which would be calculated from the additivity relationship: $\tau = \tau_1\chi_1 + \tau_2\chi_2$, where 1 and 2 refer to PS and PPO, respectively. This rule of mixtures represents the highest tensile strength achievable in a two-phase composite.

Another feature of Figures 4.24 through 4.28 is that the enhancement observed in each of the tensile strength as a function of composition curves becomes less sharp as the molecular weight of the aPS in the blend increases. In other words, the "excess tensile strength" becomes less as the

$$\tau^E = \tau_{\text{blend}} - (\tau_1\chi_1 + \tau_2\chi_2) \quad (107)$$

molecular weight of the aPS in the blend increases.

The enhancements observed in Figures 4.24 through 4.28 are characteristic for polymer mixtures which are compatible throughout their range of composition and have been observed

FIGURE 4.24

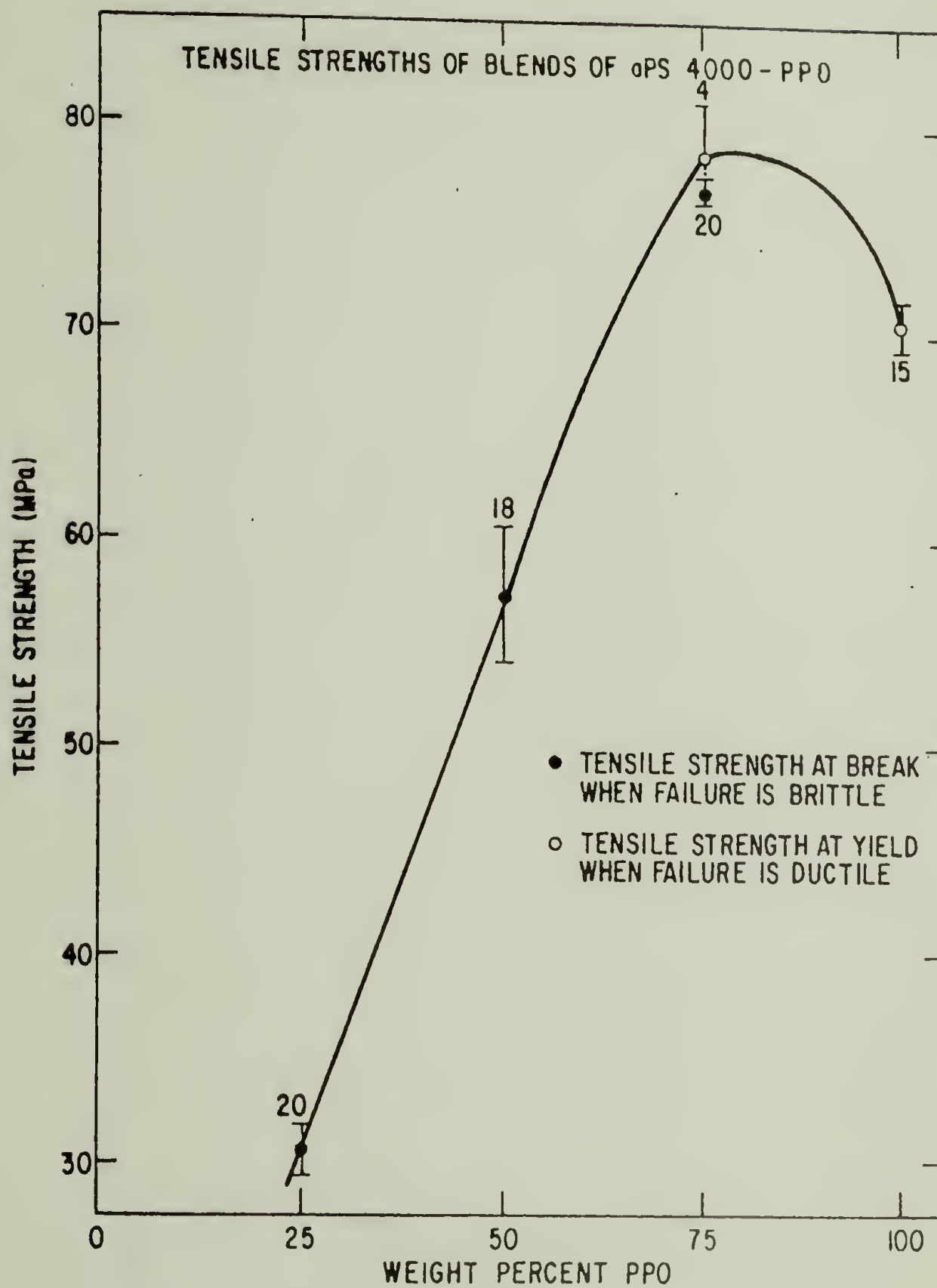


FIGURE 4.25.

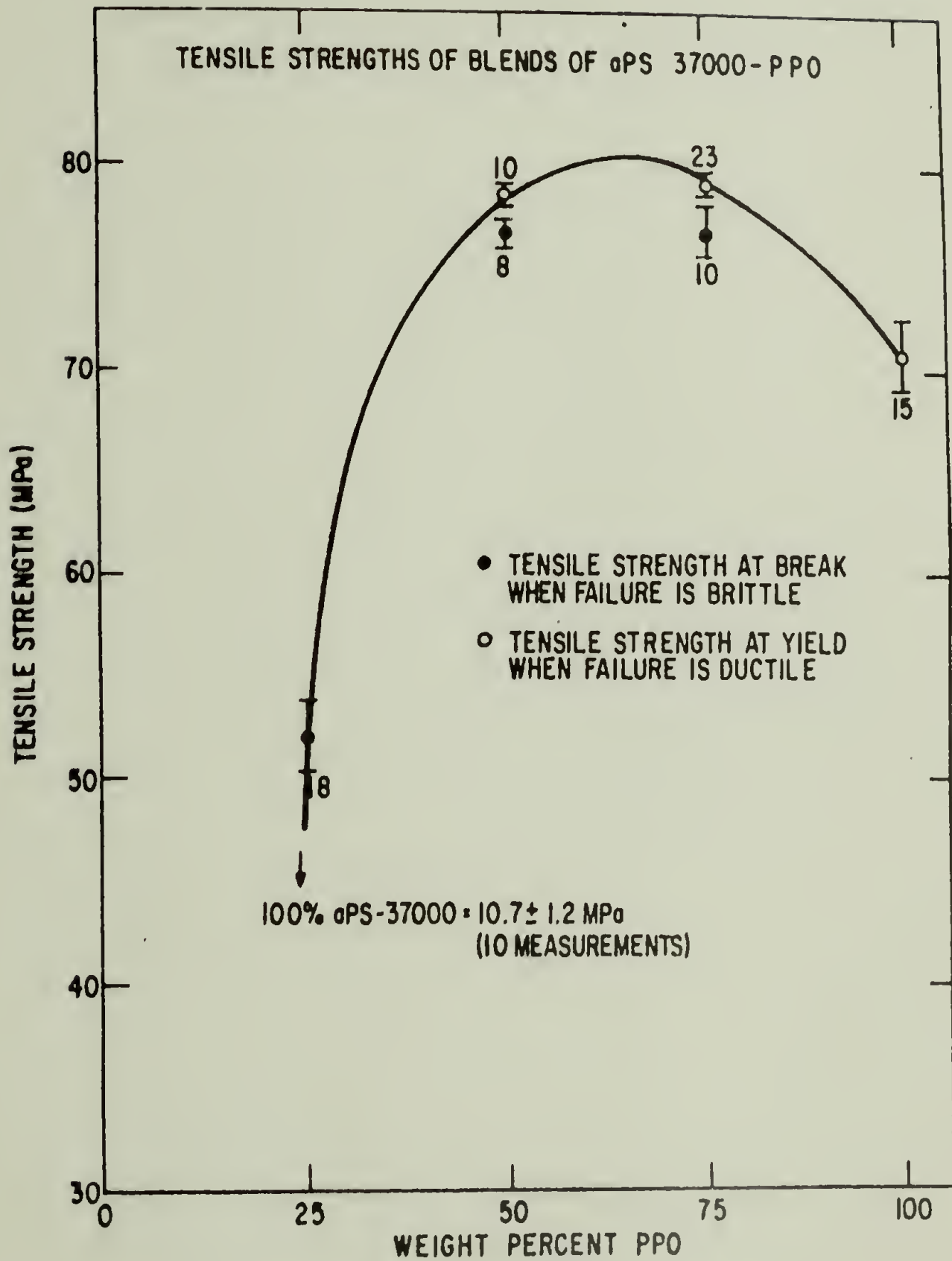


FIGURE 4.26

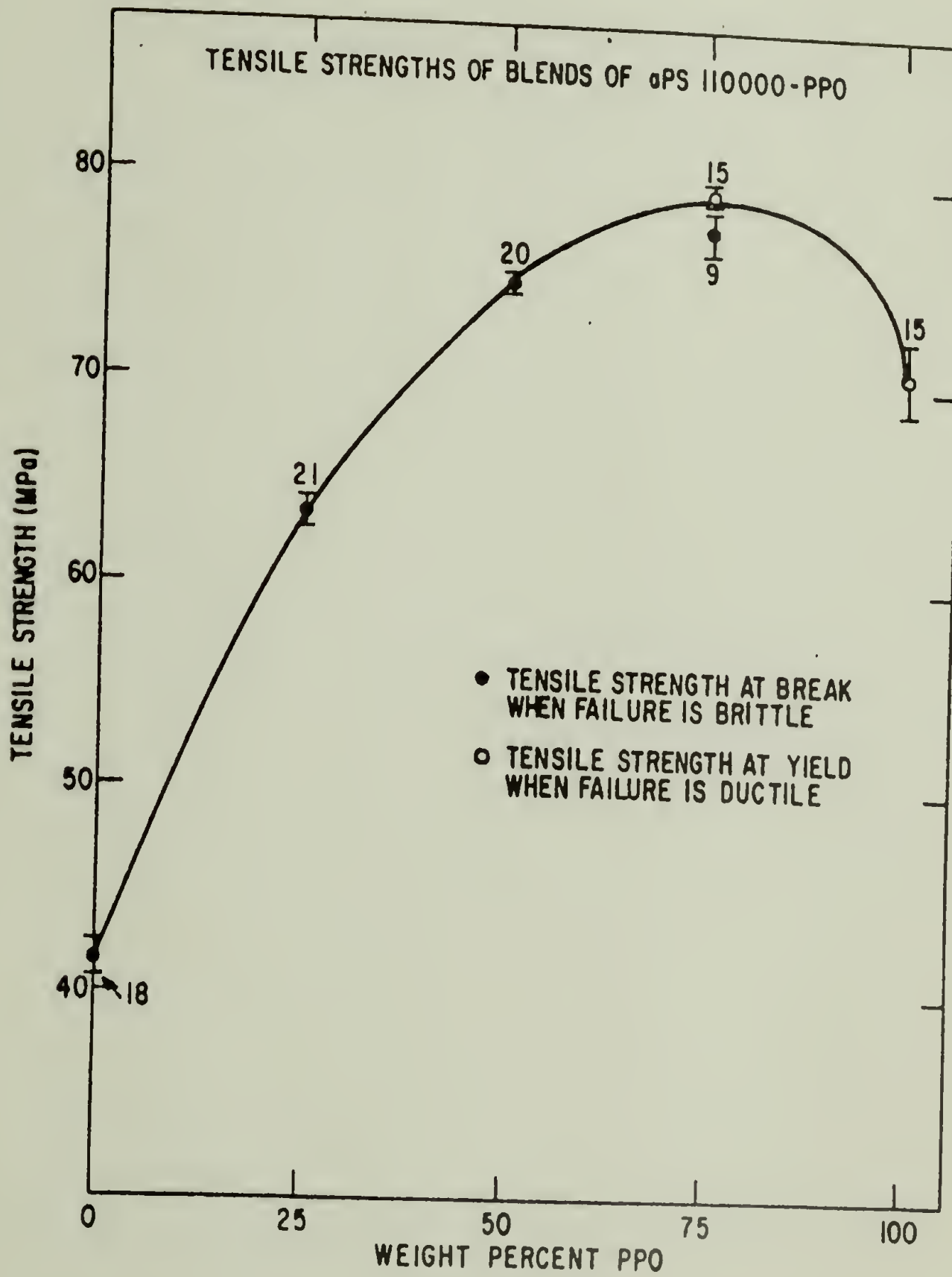


FIGURE 4.27

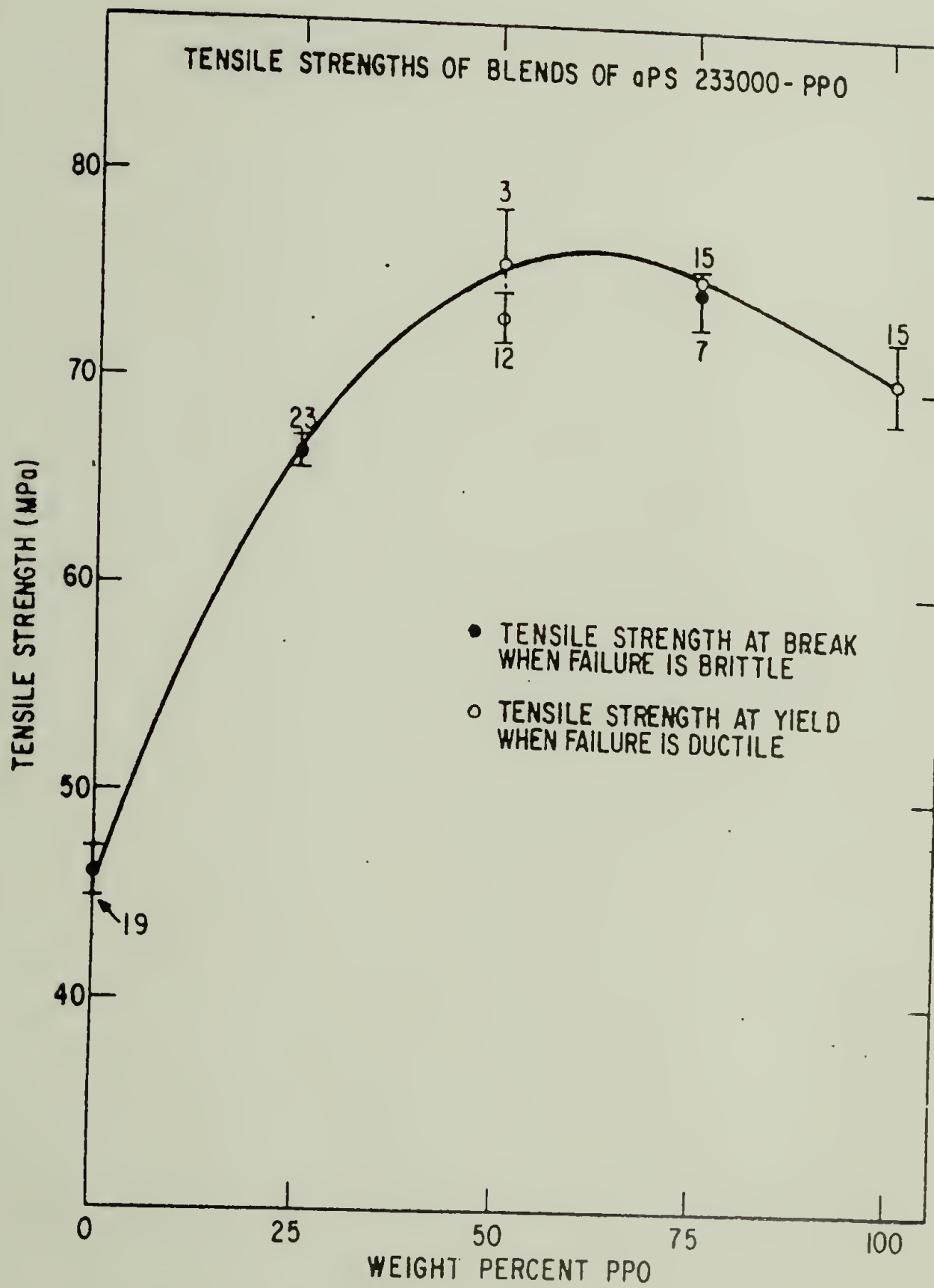
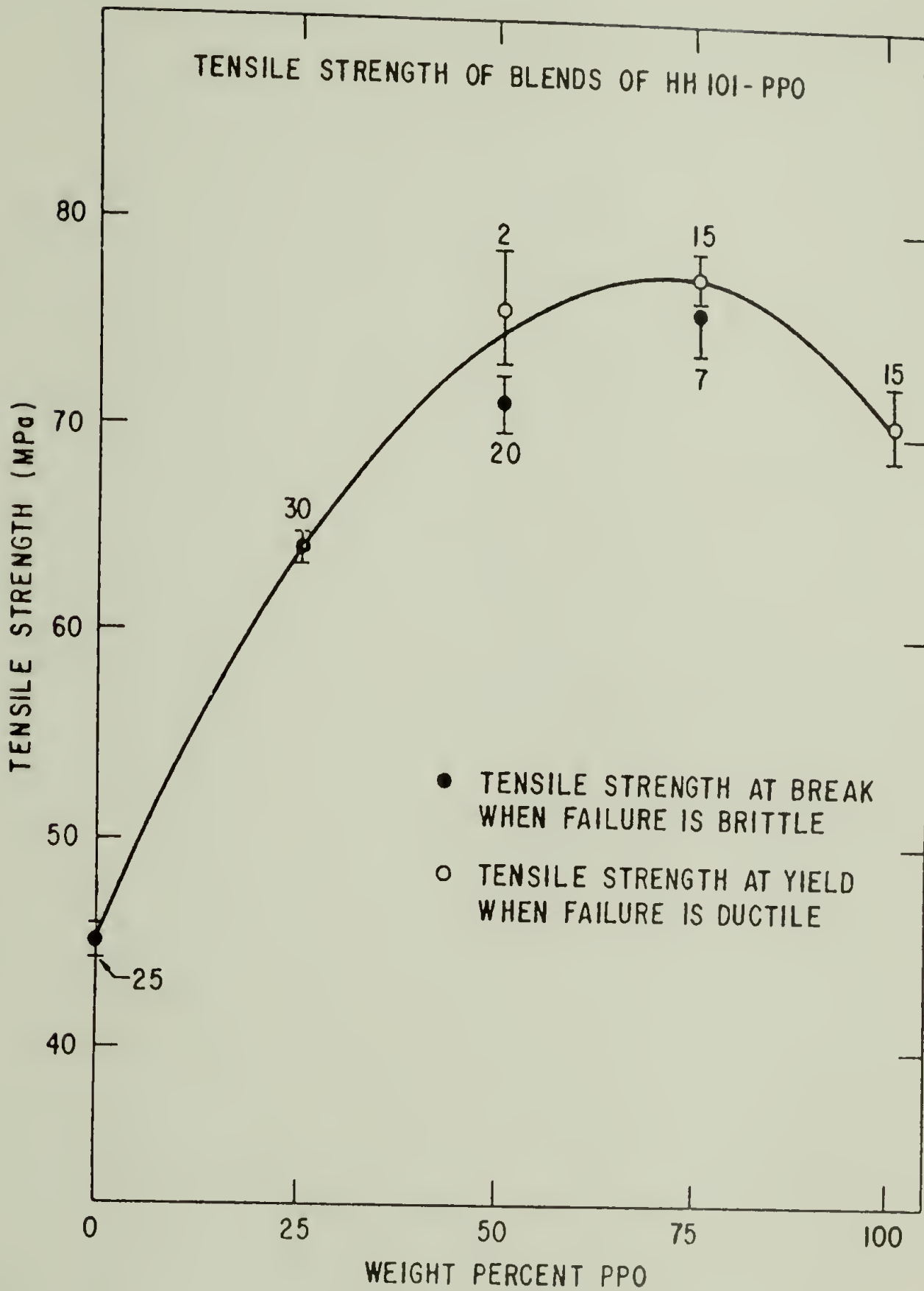


FIGURE 4.28



for several such systems [12,13,16]. In spite of the similarity in features between modulus and tensile strength data as presented in this chapter (Figures 4.1 through 4.8 and 4.24 through 4.28, in particular), a similar interpretation of results is unjustified at this stage of development. It should be remembered that the modulus and tensile strength values are derived from entirely different conditions: from condition of the undamaged blend (low extension) on one hand, and from catastrophic failure (high extension) on the other. As discussed in Chapter II.G., the tensile strength of polymers is not nearly as well understood as the modulus.

It might be expected that blend tensile strength (as depicted in Figure 4.28) can be correlated with the blend density (as depicted in Figure 4.10) since these physical properties exhibit remarkably similar behavior. A synergistic improvement can be ascribed to both properties in relationship to the properties of the base resin. Also, in each case the broad maxima appear at more or less identical blend composition. Indeed, a plot of the percent increase in density and tensile strength as a function of composition would show trends similar to those depicted in Figure 4.11. Similar increases have been observed for unblended polymers either by annealing below the glass transition or by cooling through the glass transition while maintaining a hydrostatic pressure (see Chapter II.D. for a list of references). In

the case of blends, such behavior is most frequently observed for polymer-diluent systems exhibiting antiplasticization (see Chapter II.C.) and least frequently for polymer-polymer systems [2,19-21].

Unfortunately, stress-strain property data taken after densification treatments are rarely found in the literature. The reverse is also true; i.e., little density data can be found for those blends whose stress-strain properties were described. Such data is necessary in order to answer the question: can the increase in density alone account for the increase in tensile strength of compatible glassy polyblends? Tensile strength and concomitant density data were found in the literature for a densified amorphous PS (Dylene KPD-1037; $\bar{M}_n = 110,000$ and $\bar{M}_w = 274,000$) [22] whose molecular weight and polydispersity was quite similar to the HH101 PS used in this study. The PS was densified by cooling it through the glass transition while experiencing a high hydrostatic pressure. For example, this PS sample had a density of 1.050 and 1.067 g-cm⁻³ for vitrification pressures of 1.0 and 4000 atmospheres, respectively. A densification of 1.6% resulted in a tensile strength increase of 50%. A 60 weight percent PPO blend with HH101 PS also has a density of 1.067. Its tensile strength is 70% higher than pure HH101 PS. Therefore, such a direct correlation between density and tensile strength is unjustified. Perhaps, part of the increase in tensile strength for these blends may be attributed to densification

and part to stronger intermolecular attractions.

It was also found that the reducing parameters (cohesive energy densities) H_s/V_w or P^* which were so well suited for the blend moduli are unsuited for reducing the tensile strength. Therefore, correlations for the modulus of the type depicted in Figures 4.14 and 4.15 simply cannot be generated for the tensile strength. Again these findings are not surprising when one considers the macroscopic alteration a sample experiences in the determination of its tensile strength.

IV.D. ELONGATION AT BREAK AND YIELD OF THE GLASSY HOMOPOLYMERS AND COMPATIBLE POLYMER BLENDS

The elongations at break when the tensile failure was brittle and the elongations at yield when the failure was ductile were evaluated as a function of composition and aPS molecular weight. Representative elongation -- aPS composition relationships are presented in Figures 4.29 through 4.33. Again, in each of these figures, the PPO had the same molecular weight and molecular weight distribution, while aPS's of progressively higher molecular weight were blended with the PPO.

Two features of these curves are particularly noteworthy. First, the elongation increases with aPS molecular weight at any set composition until 75 weight percent PPO is reached. The elongations are identical (independent of molecular weight) in the 75 to 100 weight percent PPO compositional

FIGURE 4.29

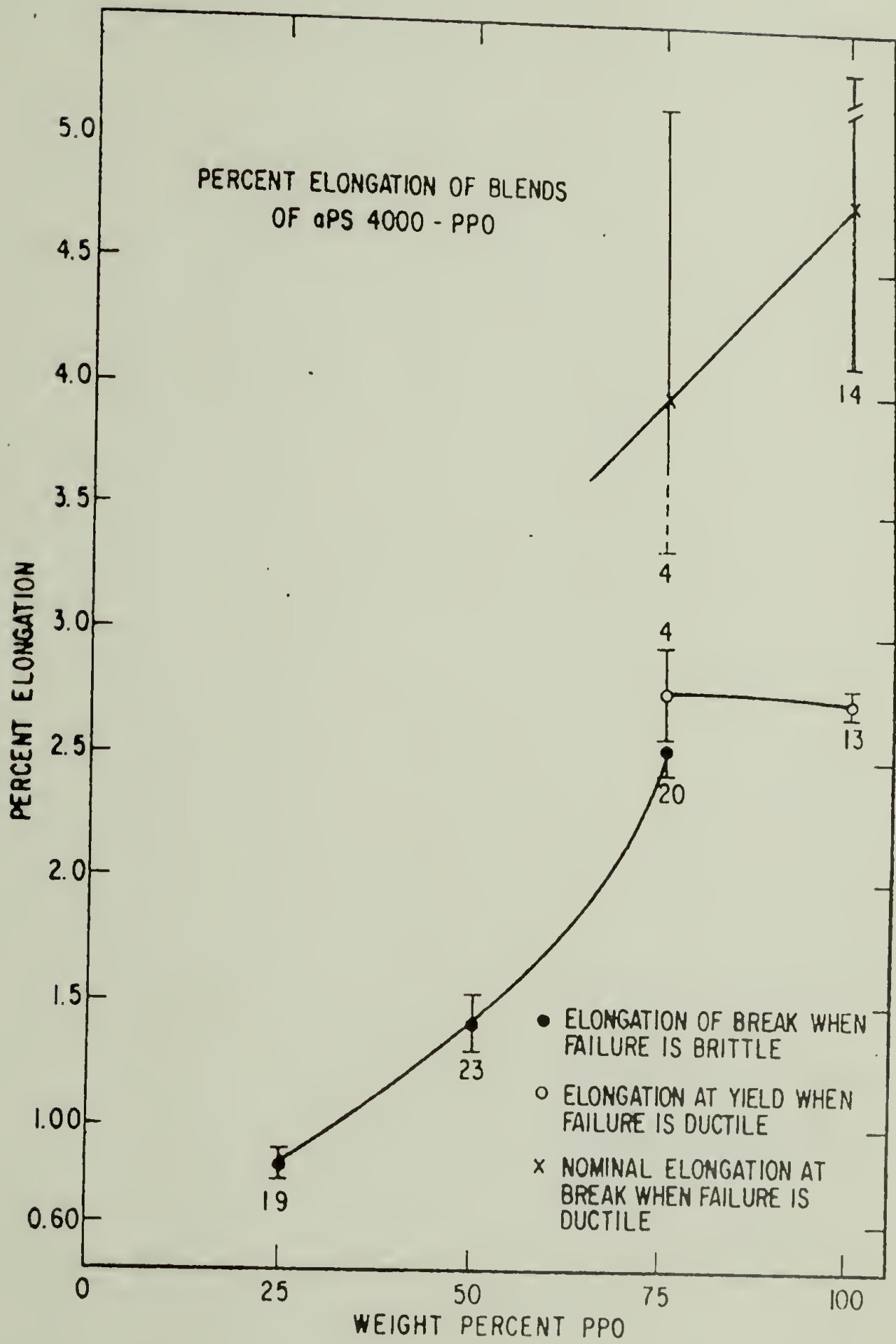


FIGURE 4.30

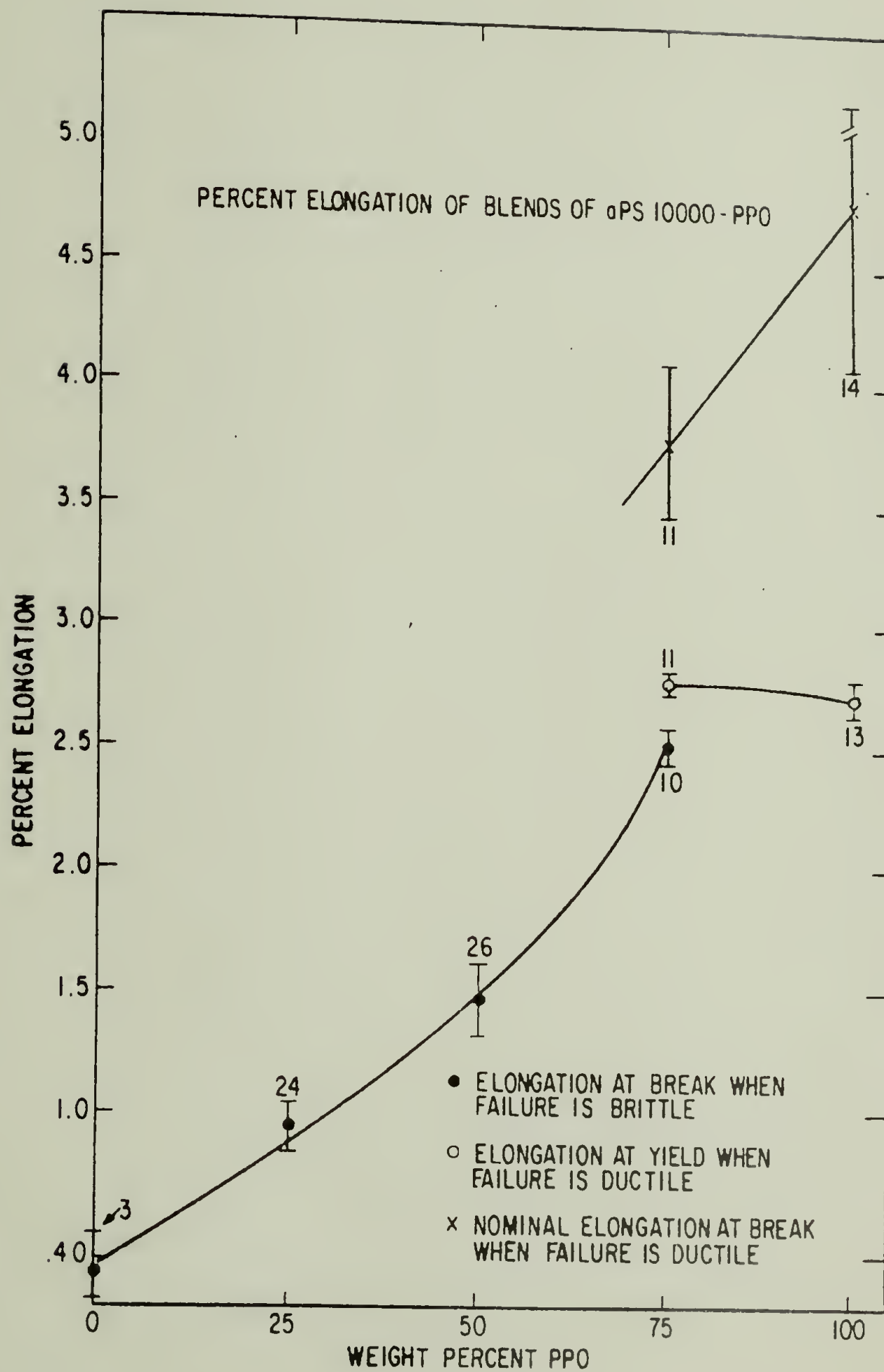


FIGURE 4.31

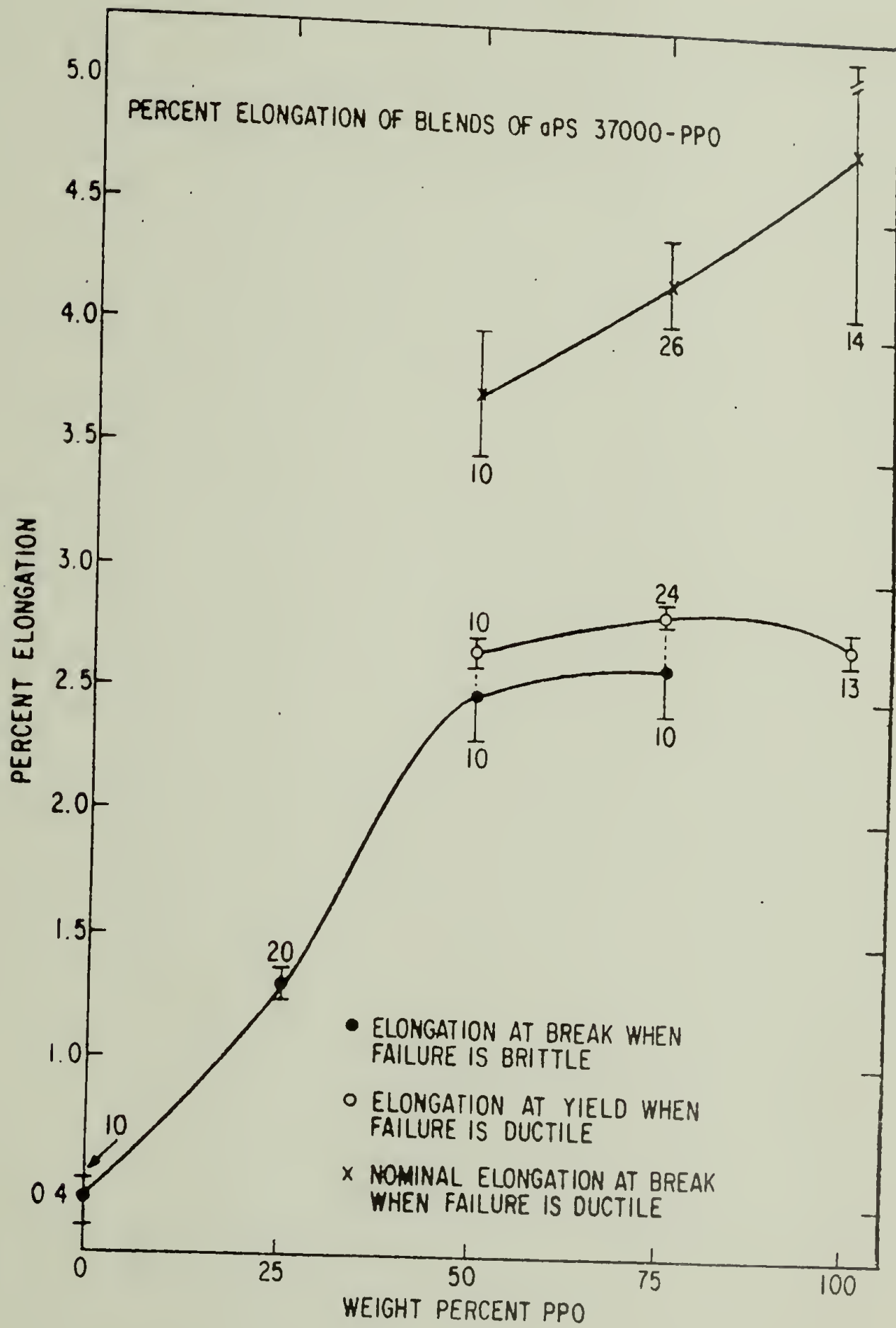


FIGURE 4.32

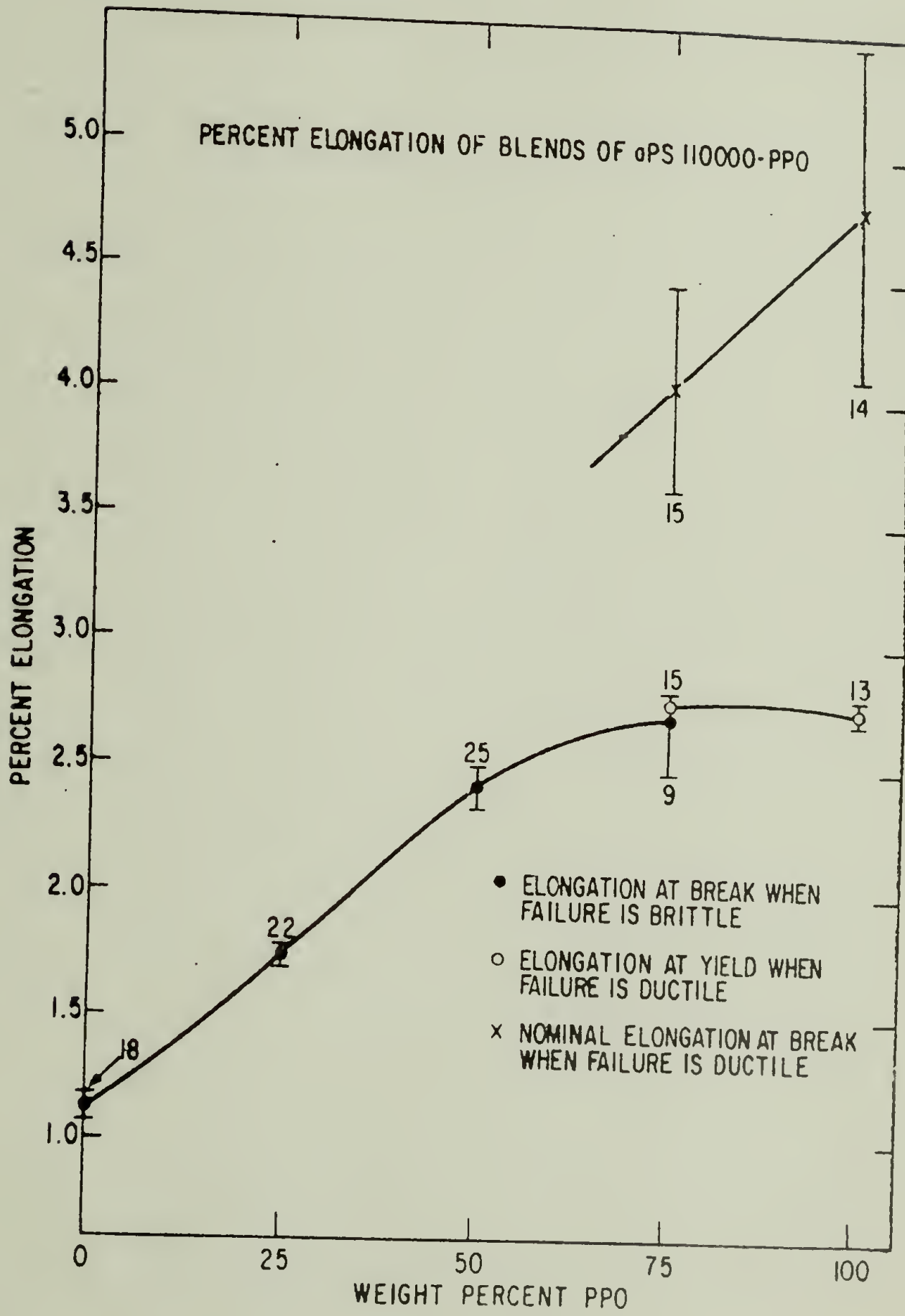
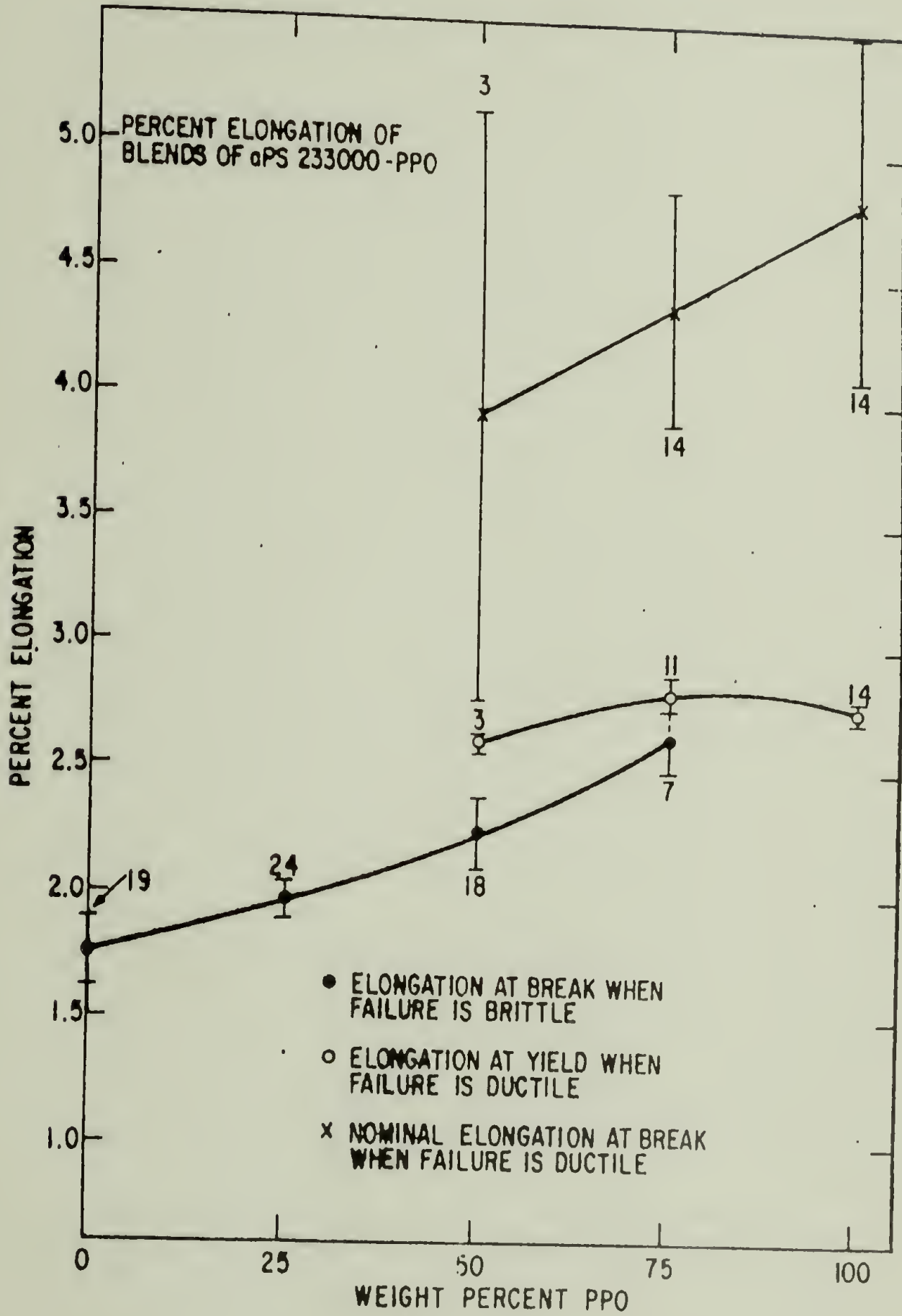


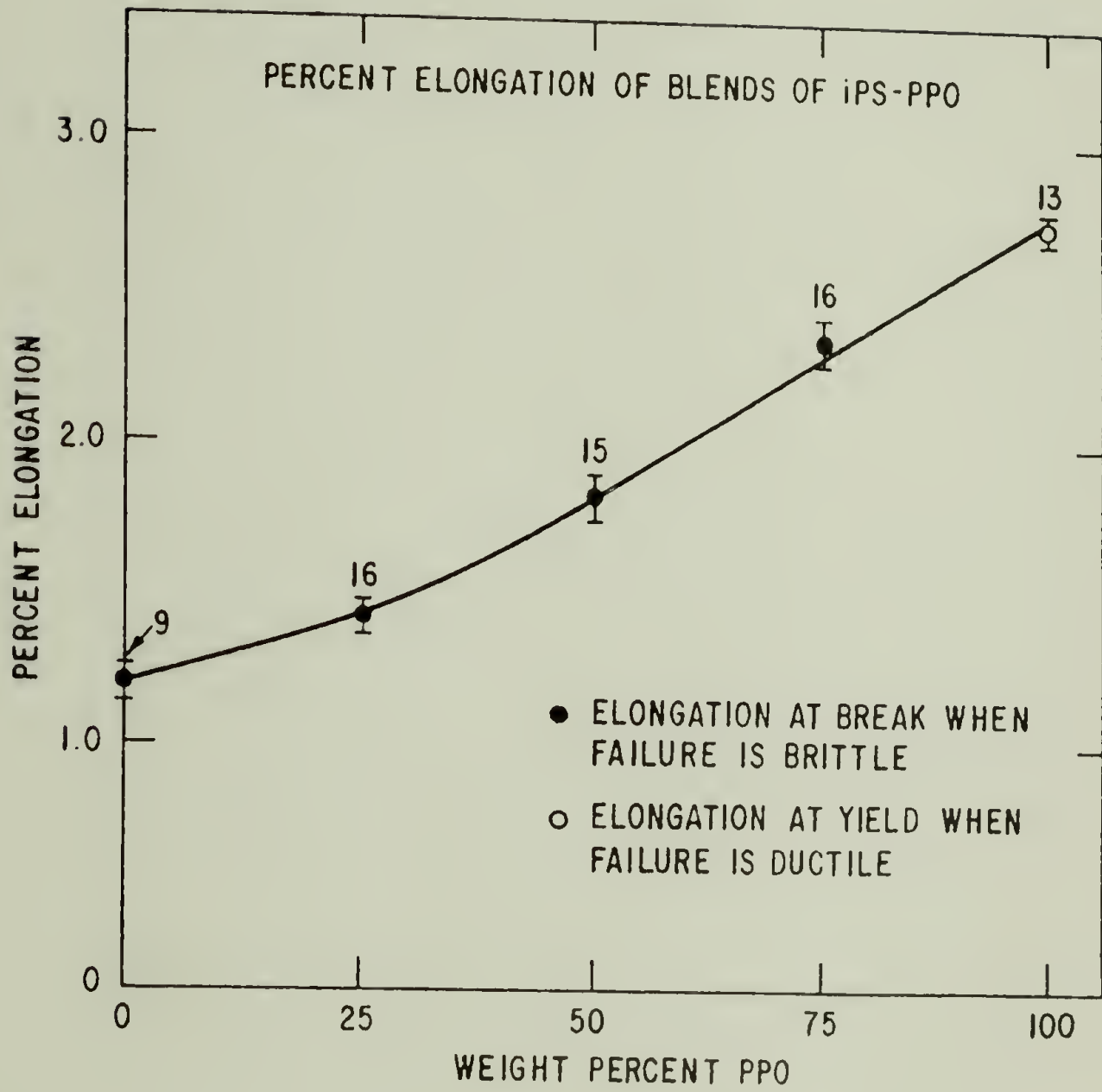
FIGURE 4.33



range. Second, there is a broad brittle to ductile transition centered about 75 weight percent PPO. These trends can be qualitatively explained upon realizing that the PS in the PS-PPO blend is behaving like a high molecular weight "antiplasticizer". The PS, like the low molecular weight antiplasticizer (diluent), serves to embrittle the PPO. The embrittlement occurs at blend compositions at which the suppression of the β relaxation of PPO is observed [8,17]. Apparently, the efficiency of these high molecular weight antiplasticizers is independent of molecular weight until more than 25 percent PS is added to the PPO.

A more efficient high molecular weight antiplasticizer for PPO is iPS. Only 15 weight percent iPS is necessary to almost completely eliminate the β peak of PPO [17]. The efficiency of iPS in embrittling PPO is mechanically verified in Figure 4.34. No brittle-ductile transition is observed at 75 weight percent PPO and all elongations to break are markedly lower than for aPS-PPO blends at all compositions of similar molecular weight. As previously noted, the brittle-ductile transition occurs at 85 weight percent PPO and coincides with the suppression of PPO's β peak. It should also be noted that the iPS minor secondary relaxations are less pronounced than those of aPS [23] and that the packing density of amorphous iPS is greater than aPS [18]. All these factors could account for the observed trends in elongation.

FIGURE 4.34



REFERENCES

1. E. F. Jordan, B. Artymyshyn, G. R. Riser, and A. N. Wrigley, J. Appl. Polym. Sci., 20, 2715, 2737, 2757 (1976).
2. Y. J. Shur and B. Ranby, J. Appl. Polym. Sci., 19, 2143 (1975).
3. H. S. Chen, J. T. Krause, and E. Coleman, J. Non-Cryst. Solids, 18, 157 (1975).
4. A. Bondi, "Physical Properties of Molecular Crystals, Liquids, and Glasses," John Wiley, New York, 1968.
5. D. W. Van Krevelen, "Properties of Polymers-Correlations with Chemical Structure", Elsevier, New York, 1972.
6. M. H. Litt and Tobolsky, J. Macromol. Sci., B1(3), 433 (1967).
7. R. F. Boyer, Polym. Eng. and Sci., 8, 161 (1968).
8. A. F. Yee, Polym. Eng. and Sci., 17, 213 (1977).
9. I. C. Sanchez and R. H. Lacombe, J. Polym. Sci., Letters Ed., 15, 71 (1977).
10. L. Nicolais and A. T. DiBenedetto, J. Appl. Polym. Sci., 15, 1585 (1971).
11. M. Baer, J. Polym. Sci., Part A, 2, 417 (1964).
12. L. Kleiner, unpublished results.
13. C. G. Seefried, J. V. Koleske, and F. E. Critchfield, Polym. Eng. and Sci., 16, 771 (1976).
14. P. J. Flory, "Principles of Polymer Chemistry", Cornell University Press, Ithaca, N.Y., 1953.
15. S. Krause, in "Block and Graft Copolymers", J. J. Burke and V. Weiss, eds., Syracuse University Press, 1973.
16. J. Fried, PhD Dissertation, University of Massachusetts, 1976.
17. S. Wellinghoff and E. Baer, Coatings and Plastics Pre-Prints, 36(1), 140 (1976).

18. F. E. Karasz, H. E. Bair, and J. M. O'Reilly, J. Phys. Chem., 69, 2657 (1965).
19. G. A. Zakrzewski, Polymer, 14, 347 (1973).
20. B. G. Ranby, J. Polym. Sci., Polym. Symp., 51, 89 (1975).
21. T. K. Kwei, T. Nishi, and R. F. Roberts, Macromolecules, 7, 667 (1974).
22. J. B. Yourtee and S. L. Cooper, J. Appl. Polym. Sci., 18, 897 (1974).
23. G. E. Roberts and E. F. T. White in "The Physics of Glassy Polymers", R. N. Haward, ed., Halsted Press, New York, 1973.

CHAPTER V

SUMMARY AND CONCLUSIONS

The main theme of this work was to examine large deformation tensile properties of compatible PPO based blends. It was desired to assess the influence of composition, molecular weight and molecular weight distribution upon blend tensile properties. With this goal achieved, the next step was to develop correlations with the experimentally determined properties and theory. Finally, attention was given to the development of compatibility criteria based upon the tensile measurements.

It was noted that both the modulus and the tensile strength at each blend composition was greater in magnitude than would be predicted from the simple "rule of mixtures." It was not possible to correlate these empirical trends with composite theory; however, a second order Simplex equation could be generated which served to adequately model the modulus-compositional relationship of all glassy alloys studied: aPS/PPO, iPS/PPO, α -PS/PPO and α -PS/aPS. Moreover, there were strong indications that the magnitude of the interaction term, β_{12}^E , could serve as a useful gauge for "level of compatibility." This term was

found to decrease for aPS/PPO blends as the molecular weight of the aPS component was increased, suggesting a decrease in the "level of compatibility." With this line of reasoning it was suggested that both α -PS and iPS are more compatible with PPO than aPS (at equivalent molecular weights).

A review of the "antiplasticizer" literature indicates that their property behavior is similar in many ways to compatible polymer blends. Up to particular concentrations, the "antiplasticizer" in a polymer will actually raise the tensile strength and modulus of the mixture above values predicted by additivity. Embrittlement occurs concomitantly. In addition, similar to a plasticizer, the "antiplasticizer" decreases the glass transition temperature. These results are explained on the basis of suppression of secondary relaxations. In compatible polymer blends, similar trends were noted, only that a broader range of composition was available for this phenomenon to apply.

Upon further examination of the "antiplasticizer" literature, where (as previously noted) maxima or enhancements in modulus versus antiplasticizer concentration have been shown to occur, one finds that the packing density of the polymer was the only equilibrium property that also passed through such a maximum. Since it appeared that PS and PPO in the PS-PPO system behave in a similar manner, various modulus-density correlations were attempted.

It was found that there is a strong correlation between blend packing density and modulus. It was also possible to correlate the blend modulus with lattice energy and molecule geometry through a suitable non-dimensionalization. The results indicated that packing density and cohesive energy density are the major factors that determine the magnitude of the blend moduli.

CHAPTER VI

SUGGESTIONS FOR FURTHER STUDIES

Several theoretical relationships and modeling parameters were established for the tensile properties, especially the modulus, of compatible PPO based blends. It would be highly desirable to verify if the same relationships and modeling parameters hold as well for other glassy compatible polymer systems. If they do not, the reasons have to be established. It could be that the theories presented are not entirely valid or that another system maintains larger secondary relaxations which may obscure the evaluation somewhat.

It is proposed that several other compatible glassy polymer-polymer and polymer-diluent ("antiplasticizer") systems be studied. It should first be established whether the suppression of secondary relaxations (which also affect the free volume) occurs upon the addition of either "antiplasticizer" or glassy polymer to another polymer. It would also be useful to study the effects of very low amounts of styrene monomer and oligomer upon PPO. These effects could be readily studied by dynamic mechanical means and would serve to explain the modulus and tensile strength enhancements (above those predicted by additivity) and the reduction

in elongation to break. Also, the question whether all compatible glassy polymer systems behave in a manner similar to polymer-antiplasticizer pairs needs to be answered.

Next, the universality of the predictive power of the packing density ρ_B^* , and the reduced density, $\tilde{\rho}$, needs to be verified. Specifically, do the reduced moduli for all amorphous glassy polymers and compatible polymer systems have relationships with respect to packing density or reduced density identical to those established for the PPO-PS system? This question may only be answered if accurate modulus and density data were available for a wide variety of amorphous homopolymers and compatible polyblends, having identical thermal histories.

Finally, the validity of using the magnitude of the interaction term, β_{12}^E , as a gauge for the "level of compatibility" needs to be verified for other compatible systems. One interesting pair is α -PS/PS, because the level of compatibility can be varied rather readily. Low molecular weight α -PS is compatible with PS while high molecular weight α -PS (greater than $\sim 100,000$) is incompatible. If β_{12}^E decreases with increasing α -PS molecular weight in a α -PS/PS blend, then we have additional verification that the interaction term can serve as a gauge for "level of compatibility". A glassy polymer pair must be compatible over the entire range of possible compositions in order to calculate β_{12}^E . For low levels of compatibility, β_{12}^E should approach zero.

APPENDIX

DATA TABULATION

TABLE A.1

NOMENCLATURE FOR SUBSEQUENT TABLES

E	Tensile modulus in GPA
τ_b	Tensile strength at break in MPa
τ_y	Tensile strength at yield in MPa
e	Elongation at break when failure is brittle (%)
ey	Elongation at yield when failure is ductile (%)
W	Weight fraction (%)
\pm	Confidence limits for experimental data reported as:
	$\bar{X} \pm \frac{t\sigma_s}{\sqrt{N}}$
\bar{X}	Mean of a series of experimental measurements
t	Value obtained from "Student's t" distribution at 95% confidence limit
σ_s	Standard deviation
N	Number of measurements
Tg	Glass transition temperature

TABLE A.2SUMMARY OF TENSILE PROPERTIES FOR
aPS - 4000/PPO BLENDS

W	=	100% aPS-4000	(too brittle for tensile testing)	
W	=	25% PPO		
E	=	3.17 ± 0.07		N = 19
τ_b	=	30.8 ± 1.10		N = 20
e	=	0.84 ± 0.03		N = 19
W	=	50% PPO		
E	=	3.10 ± 0.09		N = 23
τ_b	=	57.3 ± 3.30		N = 18
e	=	1.40 ± 0.13		N = 23
W	=	75% PPO		
E	=	3.04 ± 0.03		N = 24
τ_b	=	77.0 ± 0.50		N = 20
τ_y	=	78.7 ± 2.70		N = 4
e	=	2.54 ± 0.11		N = 20
ey	=	2.77 ± 0.21		N = 4
W	=	100% PPO		
E	=	2.66 ± 0.10		N = 15
τ_y	=	70.7 ± 1.80		N = 15
ey	=	2.73 ± 0.05		N = 13

TABLE A.3SUMMARY OF TENSILE PROPERTIES FOR
aPS - 10000/PPO BLENDS

W	=	100% aPS - 10000	(too brittle for accurate testing)	
E	=	2.50 ± 0.41		N = 3
τ_b	=	4.10 ± 7.50		N = 3
e	=	0.21 ± 0.15		N = 3
W	=	25% PPO		
E	=	3.18 ± 0.05		N = 21
τ_b	=	36.4 ± 1.80		N = 22
e	=	0.96 ± 0.05		N = 24
W	=	50% PPO		
E	=	2.99 ± 0.07		N = 24
τ_b	=	55.2 ± 5.00		N = 25
e	=	1.47 ± 0.15		N = 26
W	=	75% PPO		
E	=	2.92 ± 0.07		N = 21
τ_b	=	77.0 ± 0.80		N = 9
τ_y	=	79.1 ± 0.60		N = 11
e	=	2.53 ± 0.06		N = 10
ey	=	2.78 ± 0.03		N = 11

TABLE A.4SUMMARY OF TENSILE PROPERTIES FOR
aPS - 37000/PPO BLENDS

W	=	100% aPS - 37000	(too brittle for accurate testing)		
E	=	2.55 ± 0.19		N	= 10
τ_b	=	10.7 ± 2.60		N	= 10
e	=	0.42 ± 0.08		N	= 10
W	=	25% PPO			
E	=	3.03 ± 0.09		N	= 22
τ_b	=	52.2 ± 1.60		N	= 18
e	=	1.31 ± 0.05		N	= 20
W	=	50% PPO			
E	=	3.08 ± 0.05		N	= 21
τ_b	=	76.5 ± 0.80		N	= 8
τ_y	=	78.5 ± 0.30		N	= 10
e	=	2.50 ± 0.19		N	= 10
ey	=	2.67 ± 0.06		N	= 10
W	=	75% PPO			
E	=	2.94 ± 0.03		N	= 31
τ_b	=	76.7 ± 1.50		N	= 10
τ_y	=	79.0 ± 0.30		N	= 23
e	=	2.62 ± 0.19		N	= 10
ey	=	2.84 ± 0.03		N	= 24

TABLE A.5SUMMARY OF TENSILE PROPERTIES FOR
aPS - 110000/PPO BLENDS

W =	100% aPS - 110000		
E =	3.03 ± 0.12		
τ_b =	41.5 ± 1.70	N =	18
e =	1.11 ± 0.03	N =	17
		N =	18
W =	25% PPO		
E =	3.20 ± 0.07		
τ_b =	63.5 ± 0.70	N =	24
e =	1.74 ± 0.03	N =	21
		N =	22
W =	50% PPO		
E =	3.22 ± 0.05		
τ_b =	76.2 ± 0.30	N =	23
e =	2.41 ± 0.09	N =	20
		N =	25
W =	75% PPO		
E =	3.02 ± 0.05		
τ_b =	77.9 ± 1.50	N =	22
τ_y =	79.5 ± 0.50	N =	9
e =	2.70 ± 0.22	N =	15
ey =	2.76 ± 0.03	N =	9
		N =	15

TABLE A.6SUMMARY OF TENSILE PROPERTIES FOR
aPS - 233000/PPO BLENDS

W	=	100% aPS - 233000		
E	=	3.11 ± 0.11	N	= 19
τ_b	=	46.1 ± 0.90	N	= 19
e	=	1.75 ± 0.14	N	= 19
W	=	25% PPO		
E	=	3.18 ± 0.07	N	= 24
τ_b	=	66.4 ± 0.70	N	= 23
e	=	1.97 ± 0.07	N	= 24
W	=	50% PPO		
E	=	3.06 ± 0.05	N	= 21
τ_b	=	73.2 ± 1.20	N	= 18
τ_y	=	75.8 ± 2.80	N	= 3
e	=	2.24 ± 0.14	N	= 18
ey	=	2.60 ± 0.03	N	= 3
W	=	75% PPO		
E	=	2.97 ± 0.07	N	= 17
τ_b	=	74.6 ± 1.80	N	= 7
τ_y	=	75.1 ± 0.50	N	= 15
e	=	2.62 ± 0.13	N	= 7
ey	=	2.71 ± 0.06	N	= 15

TABLE A.7SUMMARY OF TENSILE PROPERTIES FOR
HH101 aPS/PPO BLENDS

W	=	100% HH101 PS		
E	=	3.11 ± 0.07	N	= 28
τ_b	=	45.1 ± 0.70	N	= 25
e	=	1.71 ± 0.12	N	= 32
W	=	25% PPO		
E	=	3.15 ± 0.07	N	= 31
τ_b	=	64.0 ± 0.70	N	= 30
e	=	1.83 ± 0.05	N	= 32
W	=	50% PPO		
E	=	3.06 ± 0.05	N	= 22
τ_b	=	71.3 ± 1.60	N	= 20
τ_y	=	75.9 ± 2.7	N	= 2
e	=	2.15 ± 0.09	N	= 21
e_y	=	2.46 ± 0.27	N	= 2
W	=	75% PPO		
E	=	2.82 ± 0.05	N	= 21
τ_b	=	75.8 ± 2.10	N	= 7
τ_y	=	77.6 ± 1.20	N	= 15
e	=	2.57 ± 0.11	N	= 7
e_y	=	2.76 ± 0.07	N	= 15

TABLE A.8SUMMARY OF TENSILE PROPERTIES
FOR aPS -670000/PPO BLENDS

W	=	100% aPS 670000		
E	=	3.14 ± 0.12	N	= 17
τ_b	=	53.1 ± 1.00	N	= 15
e	=	1.83 ± 0.10	N	= 16
W	=	25% PPO		
E	=	3.17 ± 0.09	N	= 22
τ_b	=	72.6 ± 0.50	N	= 16
e	=	2.22 ± 0.05	N	= 18
W	=	50% PPO		
E	=	3.10 ± 0.05	N	= 16
τ_b	=	70.0 ± 1.10	N	= 20
e	=	2.22 ± 0.11	N	= 20
W	=	75% PPO		
E	=	3.03 ± 0.05	N	= 20
τ_b	=	72.6 ± 1.10	N	= 6
τ_y	=	77.0 ± 0.50	N	= 15
e	=	2.36 ± 0.22	N	= 6
e _y	=	2.71 ± 0.03	N	= 15

TABLE A.9

SUMMARY OF TENSILE PROPERTIES FOR
aPS 2000000/PPO BLENDS

W	=	100% aPS - 2000000		
E	=	3.15 ± 0.07	N	= 17
τ_b	=	58.6 ± 1.80	N	= 17
e	=	1.81 ± 0.07	N	= 16
W	=	25% PPO		
E	=	3.16 ± 0.11	N	= 11
τ_b	=	73.8 ± 1.20	N	= 11
τ_y	=	76.1 ± 2.30	N	= 5
e	=	2.38 ± 0.11	N	= 11
ey	=	2.46 ± 0.25	N	= 5
W	=	50% PPO		
E	=	3.02 ± 0.15	N	= 6
τ_b	=	70.3 ± 3.60	N	= 8
τ_y	=	73.6 ± 4.30	N	= 5
e	=	2.33 ± 0.20	N	= 8
ey	=	2.92	N	= 1
W	=	75% PPO		
E	=	2.95 ± 0.12	N	= 7
τ_b	=	77.2	N	= 1
τ_y	=	77.1 ± 0.85	N	= 10
e	=	2.66	N	= 1
ey	=	2.67 ± 0.12	N	= 8

TABLE A.10

SUMMARY OF TENSILE PROPERTIES FOR
 α -PS/PPO BLENDS

W	=	100% α -PS	(\bar{M}_n = 10,000)		
E	=	2.99 \pm 0.09		N	= 3
τ_b	=	8.60 \pm 5.20		N	= 3
e	=	0.32 \pm 0.16		N	= 3
W	=	35% PPO			
E	=	3.42 \pm 0.10		N	= 12
τ_b	=	50.3 \pm 3.70		N	= 8
e	=	1.15 \pm 0.08		N	= 8
W	=	61.7% PPO			
E	=	3.30 \pm 0.10		N	= 12
τ_b	=	87.0 \pm 2.30		N	= 11
e	=	2.32 \pm 0.14		N	= 13
W	=	83.9% PPO			
E	=	3.02 \pm 0.06		N	= 9
τ_b	=	82.6 \pm 0.7		N	= 5
τ_y	=	83.3 \pm 1.2		N	= 6
e	=	2.60 \pm 0.18		N	= 5

TABLE A.11SUMMARY OF TENSILE PROPERTIES FOR
 α -PS/HH101 aPS BLENDS

W	=	36.4% HH101		
E	=	3.04 \pm 0.28	N	= 9
τ_b	=	18.6 \pm 3.20	N	= 12
e	=	0.64 \pm 0.08	N	= 12

W	=	63.2% HH101		
E	=	3.04 \pm 0.08	N	= 12
τ_b	=	35.5 \pm 3.80	N	= 11
e	=	0.98 \pm 0.06	N	= 11

W	=	83.8% HH101		
E	=	3.28 \pm 0.13	N	= 12
τ_b	=	43.8 \pm 1.40	N	= 9
e	=	1.11 \pm 0.06	N	= 10

TABLE A.12SUMMARY OF TENSILE PROPERTIES FOR
AMORPHOUS iPS/PPO BLENDS

W	=	100% amorphous iPS		
E	=	3.15 ± 0.17	N	= 9
τ_b	=	49.4 ± 2.3	N	= 9
e	=	1.20 ± 0.05	N	= 9
W	=	25% PPO		
E	=	3.28 ± 0.10	N	= 16
τ_b	=	59.5 ± 2.10	N	= 16
e	=	1.42 ± 0.05	N	= 16
W	=	50% PPO		
E	=	3.42 ± 0.06	N	= 15
τ_b	=	73.7 ± 2.10	N	= 14
e	=	1.81 ± 0.08	N	= 15
W	=	75% PPO		
E	=	3.17 ± 0.10	N	= 16
τ_b	=	79.4 ± 1.80	N	= 16
e	=	2.35 ± 0.13	N	= 16

TABLE A.13

GLASS TRANSITION TEMPERATURES

<u>Composition</u>	<u>Tg (°C) *</u>
HH101	103
iPS	101
16.2% α -PS/83.8% HH101	109
36.8% α -PS/63.2% HH101	116.5
63.6% α -PS/36.4% HH101	129.5
100% α -PS	154.5
PPO	220
83.9% PPO/16.1% α -PS	203
61.7% PPO/38.3% α -PS	184
35% PPO/65% α -PS	170

*See Chapter III. for experimental details.

